



## Durham E-Theses

---

### *Compositional and shear strength characteristics of a spoil heap at Littleton colliery, Staffordshire*

McWilliam, D. J.

#### How to cite:

---

McWilliam, D. J. (1975) *Compositional and shear strength characteristics of a spoil heap at Littleton colliery, Staffordshire*, Durham theses, Durham University. Available at Durham E-Theses Online: <http://etheses.dur.ac.uk/8963/>

#### Use policy

---

The full-text may be used and/or reproduced, and given to third parties in any format or medium, without prior permission or charge, for personal research or study, educational, or not-for-profit purposes provided that:

- a full bibliographic reference is made to the original source
- a [link](#) is made to the metadata record in Durham E-Theses
- the full-text is not changed in any way

The full-text must not be sold in any format or medium without the formal permission of the copyright holders.

Please consult the [full Durham E-Theses policy](#) for further details.

---

Academic Support Office, Durham University, University Office, Old Elvet, Durham DH1 3HP  
e-mail: [e-theses.admin@dur.ac.uk](mailto:e-theses.admin@dur.ac.uk) Tel: +44 0191 334 6107  
<http://etheses.dur.ac.uk>

COMPOSITIONAL AND SHEAR STRENGTH  
CHARACTERISTICS OF A SPOIL HEAP  
AT LITTLETON COLLIERY, STAFFORDSHIRE.

- by -

D. J. McWILLIAM

Thesis submitted for the Degree of Master  
of Science in the University of Durham.



September, 1975

## ABSTRACT

Since the Aberfan colliery spoil heap disaster the National Coal Board has sponsored a research programme on existing British spoil heaps. This thesis is part of that programme and considers an unburnt, unwashed, conical spoil heap at Littleton Colliery, Staffordshire. Tipping took place from about 1900 to about 1940 and records relating to discard constituents are very sparse. A slope failure in 1970 instigated this research project which is aimed at elucidating the compositional and shear strength characteristics affecting the stability of spoils in the Littleton area.

Mineralogical, chemical and shear strength analyses were carried out on samples from the spoil heap and contributing underground measures. The absence of an underground measure from the original list of contributors was detected during the mineralogical and chemical analyses. This measure was identified, showing the value of such analyses in clarifying the history of such ancient tips. Mineralogy was found to correlate well with the chemical analyses of the samples, and the analyses of the spoil heap materials correlated well with those of the underground materials. No evidence of leaching or weathering was found in the tip. The shear strengths of the materials tested correlated well with the mineralogical and chemical analyses, the unusually low shear strengths of Littleton Spoil Heap No. 1 being reflected by high clay mineral contents.

The slope stability problems occurring in the spoil heap are believed to be related to the Maclane Tippler method of spoil placement which has resulted in the spoil heap material approaching or achieving residual shear strength. A perched water-table within the spoil heap has initiated instability, giving rise to a deep-seated, circular slip.

## ACKNOWLEDGMENTS

The writer is indebted to the National Coal Board who provided a grant in aid of this research project, and especially to Mr. W. J. Bygott (Area Civil Engineer, N. C. B.), Mr. K. Whitworth (Geologist, Littleton Colliery) and the late Mr. F. Phillips (Civil Engineer, Littleton Colliery) who provided help during the fieldwork.

The writer would also extend very warm thanks to Dr. R. K. Taylor (Durham University) who supervised the research project and whose help and encouragement enabled this thesis to be completed. Mr. R. G. Hardy helped with both the mineralogical and chemical X-ray analyses at Durham University, and Mr. A. Swann carried out the structural improvements on the 12-inch direct shear-box. Dr. G. Armstrong helped with the computer program for shear-box data processing. The writer would like to express his appreciation of the help given by these and other members of Durham University.

# CONTENTS

	<u>Page</u>
ABSTRACT.....	i
ACKNOWLEDGMENTS.....	ii
CONTENTS, FIGURES, PLATES.....	iii
Chapter I. INTRODUCTION.....	1
Chapter II. MINERALOGY.....	8
II. 1. Sampling and sample location .....	10
II. 1. a. Sampling technique .....	10
II. 1. b. Sample location .....	11
II. 2. Mineralogical techniques .....	12
II. 2. a. Sample preparation .....	12
II. 2. b. X-ray diffraction technique .....	13
II. 3. Mineralogical results .....	14
II. 3. a. Mixed-layer clay mineral .....	14
II. 3. b. Crystallinity .....	16
II. 4. Conclusions .....	18
II. 4. a. Quartz .....	20
II. 4. b. Carbonates .....	20
II. 4. c. Rutile and Apatite .....	21
II. 4. d. Clay minerals .....	21
II. 4. e. Carbon .....	22
II. 4. f. Comparison of underground and tip samples .....	22
Chapter III. SHEAR STRENGTH INVESTIGATION.....	26
III. 1. 12-inch direct shear-box technique .....	26
III. 1. a. Box reversal .....	26
III. 1. b. Shearing in reverse .....	28
III. 1. c. Sample conservation .....	28
III. 1. d. Rate of shearing .....	33
III. 1. e. Automation of test results.....	40
III. 1. f. Integration of triaxial compression and shear-box tests .....	42

	<u>Page</u>
III. 2. 4-inch triaxial compression test technique .....	45
III. 2. a. Sample preparation .....	45
III. 2. b. Volume change measurement .....	46
III. 3. 12-inch shear-box results .....	46
III. 3. a. Presentation of shear-box results .....	46
III. 3. b. Allowance for area reduction in direct shear tests .....	48
III. 3. c. Residual shear strength determination .....	48
III. 3. d. Volume change .....	60
III. 3. e. Choice of samples tested .....	61
III. 4. Compatibility of shear-box and triaxial tests .....	61
III. 5. Shear strength results .....	66
III. 5. a. Results from underground measures .....	66
III. 5. b. Results from spoil heap material .....	67
III. 6. Comparison of underground and spoil heap materials .....	69
III. 6. a. Conclusions .....	70
III. 7. Particle size analysis .....	71
III. 7. a. Coulter Counter technique .....	71
III. 7. b. Coulter Counter results .....	72
III. 7. c. Wet sieving technique and results .....	75
III. 7. d. Conclusions .....	75
III. 8. Shear strength analysis conclusions .....	76
Chapter IV CHEMISTRY .....	80
IV. 1. Chemical techniques .....	80
IV. 1. a. X-ray fluorescence techniques .....	80
IV. 1. b. Wet chemical techniques .....	81
IV. 2. Chemical results .....	81
IV. 2. a. Chemical analyses: Table IV. 1. and Table IV. 2. ....	85
IV. 2. b. Combined silica/Al <sub>2</sub> O <sub>3</sub> ratio: Table IV. 3. ....	86

	<u>Page</u>
IV.2. c. Free silica/combined silica ratio.....	87
IV.2. d. $K_2O/Al_2O_3$ ratio .....	87
IV.2. e. Comparison of chemistry and mineralogy of spoil heap samples .....	88
IV.2. f. Comparison of chemistry and mineralogy of underground samples .....	89
IV.3. Statistical comparison of chemical results .....	89
IV.3. a. Comparison of Yorkshire Main and Littleton .....	93
IV.3. b. Comparison of underground material and spoil heap at Littleton .....	94
IV.4. Chemistry conclusions .....	94
Chapter V. SLOPE STABILITY ANALYSIS .....	96
V.1. Taylor and Hardy (1971) slope stability analysis .....	96
V.2. Effect of water-table on stability .....	97
V.3. Effect of subgrade data alteration .....	99
V.4. Effect of spoil heap data alteration .....	101
V.5. Shallow slip analysis .....	105
V.6. Janbu Method.....	107
V.7. Conclusions.....	109
Chapter VI. CONCLUSIONS .....	110
VI.1. The spoil heap as a mixture of the underground materials .....	110
VI.2. Shear strength relationships.....	111
VI.3. Weathering and leaching.....	113
VI.4. Slope stability.....	113
VI.5. Genesis of the 1970 failure.....	113
BIBLIOGRAPHY.....	115
APPENDIX A Computer print-out of shear-box results .....	118
APPENDIX B Shear strength test results .....	123



## FIGURES

		<u>Page</u>
Fig. I. 1.	Map of the West Midlands .....	2
Fig. I. 2.	Map of the Cannock area .....	3
Fig. I. 3.	Geological section of the Coal Measures in Littleton Colliery .....	5
Fig. II. 1.	Littleton Spoil Heap No. 1 .....	9
Fig. II. 2.	(Quartz/Total Clay) v (10- $\text{\AA}$ /7- $\text{\AA}$ Clay) graph for Littleton samples .....	19
Fig. III. 1.	Non-fastening thrust bearing on the shear- box, rigid only in forward travel .....	27
Fig. III. 2.	Fastening of thrust bearing for rigidity in forward and reverse travel .....	27
Fig. III. 3.	Vertical view of shear-box .....	29
Fig. III. 4.	Packing inserted in the shear-box .....	30
Fig. III. 5.	Movement of material within the specimen during shearing .....	30
Fig. III. 6.	Wedging apart of the shear-box halves by displaced material .....	32
Fig. III. 7.	Framework to prevent vertical movement of the upper shear-box during shearing .....	32
Fig. III. 8.	Vertical movement of the framework during shearing .....	34
Fig. III. 9.	Coulomb's Law .....	36
Fig. III. 10.	Pore-pressure monitoring system .....	36
Fig. III. 11.	Digital voltmeter calibration curve .....	38
Fig. III. 12.	Composite shear strength diagram for underground and spoil heap samples tested .....	49
Fig. III. 13.	Shear strength diagram for spoil heap samples tested .....	50
Fig. III. 14.	Shear strength diagram for underground samples tested and the 1970 slip plane .....	51
Fig. III. 15.	Shear stress v displacement curves .....	52
Fig. III. 16.	Shear stress v displacement curve showing the origin of the small peak .....	55
Fig. III. 17.	Shear plane undulations .....	59
Fig. III. 18.	Isabella Heap material, 12-inch direct shear-box results .....	63

	<u>Page</u>
Fig. III. 19. Isabella Heap material, 4-inch drained triaxial compression tests results .....	64
Fig. III. 20. Isabella Heap material high pressure 4-inch triaxial compression tests results .....	65
Fig. III. 21. Mohr circle "top point" construction .....	68
Fig. III. 22. Coulter Counter particle size results for the spoil heap material .....	73
Fig. III. 23. Coulter Counter particle size results for the underground material .....	74
Fig. III. 24. Wet sieving particle size results for the 1970 failure .....	77
Fig. V. 1. Slip circle analysed for the 1970 failure (Taylor and Hardy, 1971) .....	98
Fig. V. 2. Slip circle and water-table used in the calculation of Table V. 1 .....	100
Fig. V. 3. Safety factor v $\phi'_r$ graph for the circle shown in Fig. V. 4. ....	102
Fig. V. 4. Slip circle analysed for the results shown in Fig. V. 3. ....	103
Fig. V. 5. Safety factor v $\phi'_r$ graph to find $\phi'_r$ for safety factor = 1. ....	104
Fig. V. 6. Shallow-seated slip circles analysed. ....	106
Fig. V. 7. Planar slip analysed by the Janbu Method. ....	108

## PLATES

	<u>Page</u>
Plate I. 1. Aerial photograph of Littleton Colliery .....	4
Plate III. 1. Retaining bracket attached to the rear of the shear-box .....	29
Plate III. 2. 12-inch direct shear-box .....	41
Plate III. 3. Original thrust ram .....	43
Plate III. 4. 12-inch direct shear-box equipment.....	47
Plate III. 5. Lower half of sample TTO3.....	57
Plate III. 6. Upper half of sample TTO3 .....	58

# CHAPTER I

## INTRODUCTION

The National Coal Board's mining activities are producing about 55 million tonnes of coarse discard per year. This material is disposed of by tipping onto some of the two thousand spoil heaps owned by the National Coal Board (Taylor, 1975). The Aberfan disaster (Bishop et al., 1969) focused public and National Coal Board attention on stability problems in spoil heaps, resulting in a protracted research programme concerning existing spoil heaps in Britain. The main aim of the programme has been to identify possible mineralogical controls on the physical and mechanical properties of colliery spoils.

This research project concerns Littleton Colliery near Cannock, Staffordshire, Grid Reference SJ 969131 (Fig. I. 1), and the work was carried out with the intention of elucidating the compositional and shear strength factors affecting the instability of spoils from the Cannock Chase area. Spoil Heap No. 1 at Littleton (Fig. I. 2 and Plate I. 1) has long shown signs of instability and this research project was instigated by a slip on the west face of the spoil heap (Fig. II. 1). A preliminary report served as a starting point for the investigation (Taylor and Hardy, 1971).

Spoil Heap No. 1 is an unwashed, largely unburnt conical tip which was placed by Maclane Tippler, tipping having ceased in about 1940 (Phillips, personal communication). The spoil had been processed before tipping by "picking" of the coal contained in the discard. The original height of the tip was 52.7m (173 ft) but after the last slope failure this was reduced to 40.5m (133 ft). The average angle of repose was  $22^{\circ}$ , and the maximum was  $38^{\circ}$ . The coal seams whose extraction had given rise to the discard contained in the spoil heap were the Brooch, Benches, Eight Feet, Park and Deep (Fig. I. 3). It was proposed to examine the roof and floor horizons of these seams and compare their physical and chemical properties with those of spoil heap samples. In this way it was hoped to

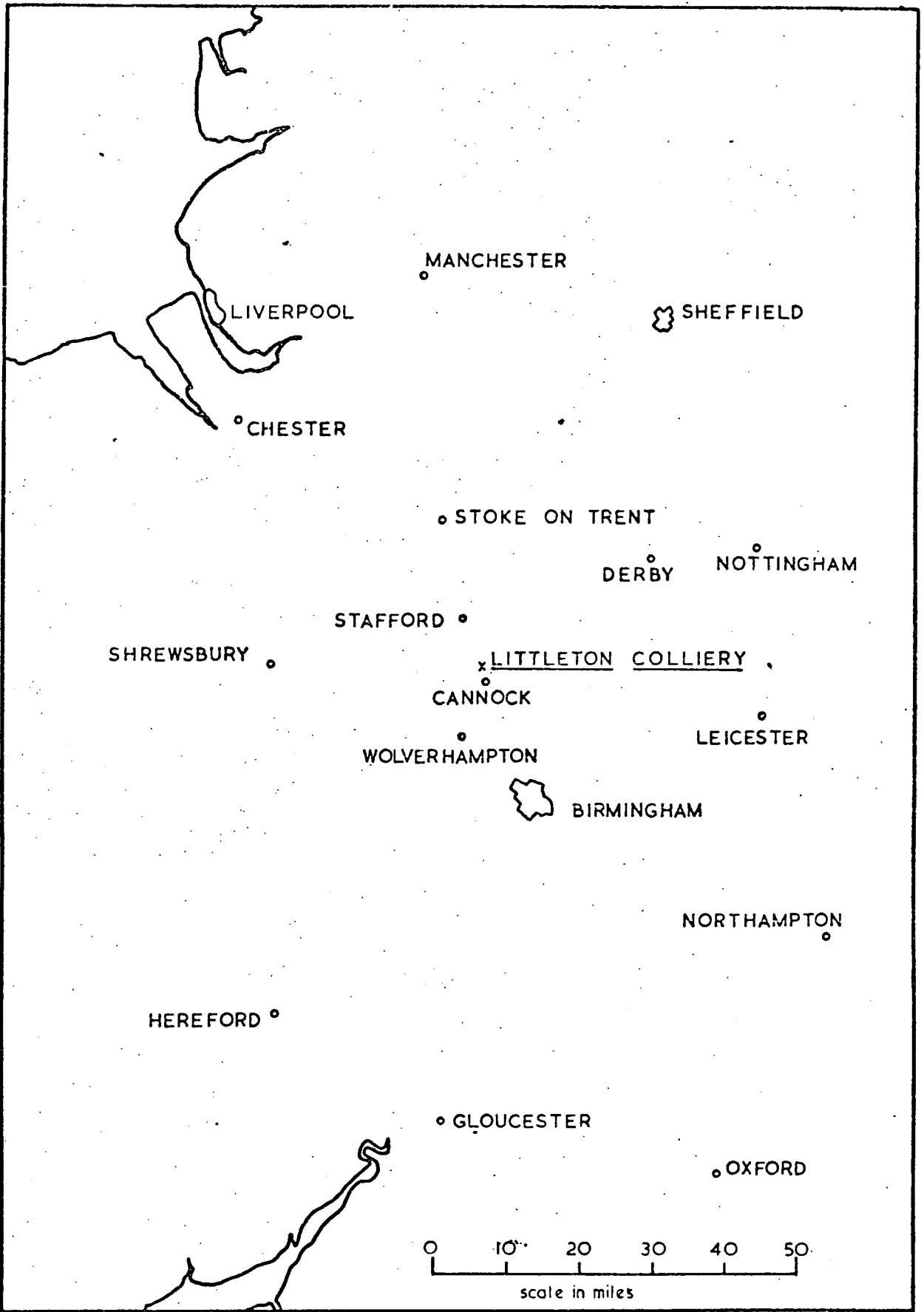


Fig. 1.1. Map of the West-Midlands and Welsh Borders showing the location of Littleton Colliery.

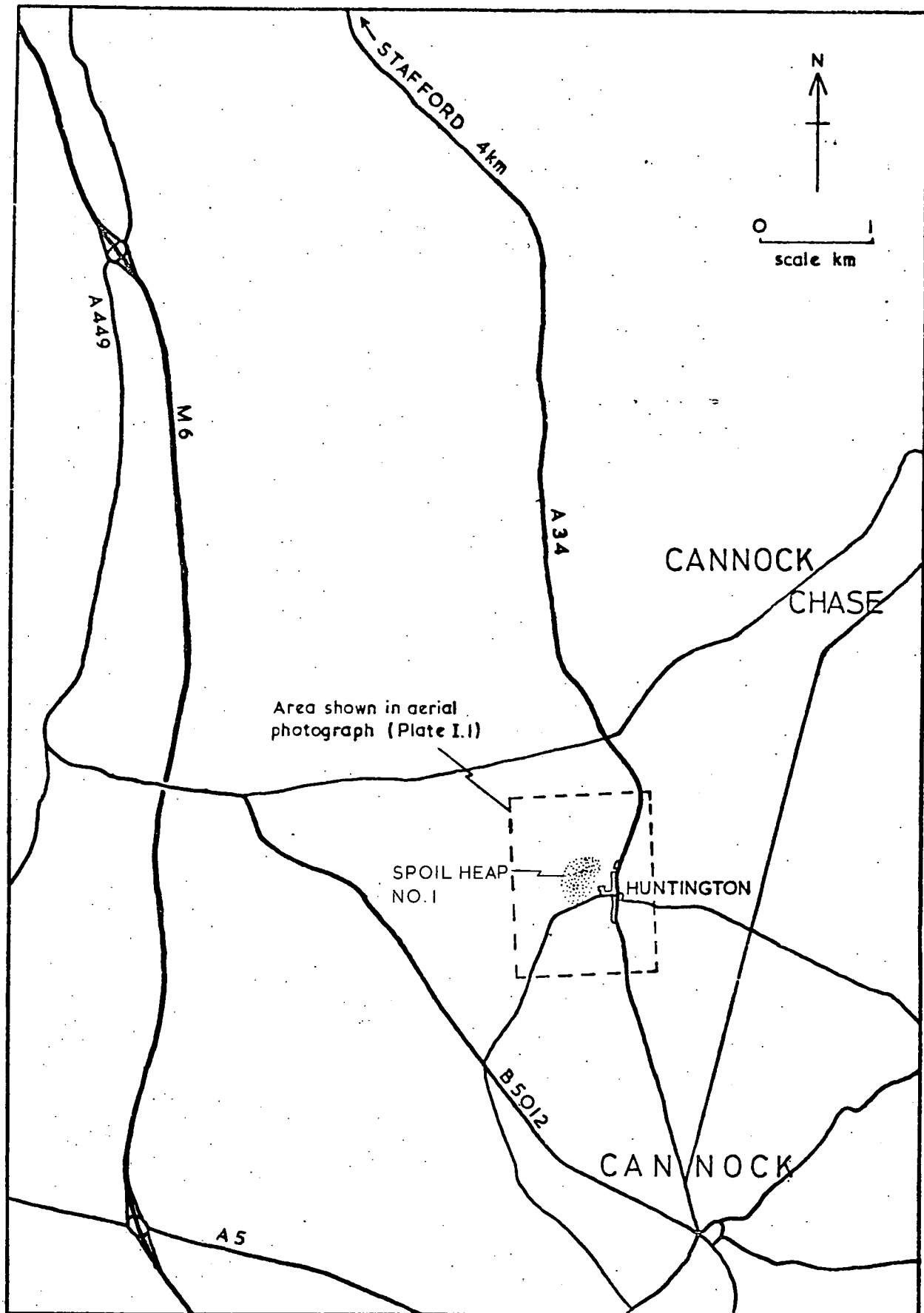


Fig. 1.2. Map of the Cannock area showing the location of Littleton Colliery.



Plate I. 1. Aerial photograph of Littleton Colliery and Huntington Village. Area shown on Fig. I. 2.

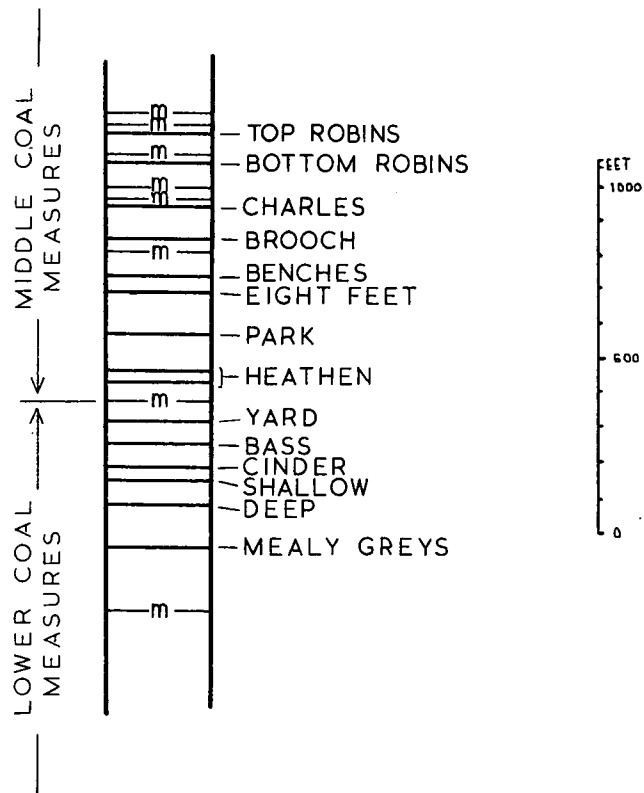


Fig. 1. 3. Generalized geological section of the Coal Measures rocks mined at Littleton Colliery.



find whether weathering of the tip material was an important factor in the instability of the tip.

For this purpose it was necessary to ascertain the percentages of the tip which were contributed by the various underground materials. Unfortunately the age of the tip made accurate quantification difficult. However, a survey of old records allowed the Area Civil Engineer of the National Coal Board to supply the following estimated figures (Bygott, personal communication):

Brooch	60% floor 40% roof
Benches	60% floor 40% roof
Park	60% floor 40% roof
Deep	100% floor
Eight Feet	100% floor

Of these, the Brooch and Benches were minor constituents when compared with the Eight Feet, Park and Deep. Subsequent mineralogical and chemical research showed that these materials were unlikely to be the only materials contained in the spoil heap (Chap. II. 3. b). Consequently, the Civil Engineer at Littleton Colliery was asked to pursue the question of the spoil heap constituents. He produced the following figures (Phillips, personal communication):

Deep Floor	< 50%
Eight Feet Roof	c. 30%
Park Floor and Roof	c. 15%
Benches Roof	c. 5%
Brooch Roof	c. 2%

Shear strength tests were carried out to investigate any correlations between shear strength and chemical and mineralogical properties (Taylor, 1975). The relationships between these properties and particle size distributions were also studied.

Slope stability analyses were used in conjunction with shear strength results to investigate the nature of the 1970 failure, and the factors which may have lead to it occurrence.

The following chapters of this thesis are: Mineralogy, Shear Strength Investigation, Chemistry, and Slope Stability. Mineralogy and chemistry are separated in the text to facilitate the continual reference to mineralogy which is necessary on reading the chapter on shear strength investigation. It is recognized that mineralogy and chemistry are intimately related, but a main purpose of this research project has been to relate mineralogy to shear strength. In consideration of this mineralogy and shear strength are considered in adjacent chapters.

## CHAPTER II

### MINERALOGY

The samples collected from Spoil Heap No. 1 and from the underground Coal Measures at Littleton Colliery were subjected to mineralogical and chemical investigation.

The location of the sample sites on the tip are shown in Fig. II. 1, the underground material being collected from the relevant horizons in Littleton Colliery.

The nomenclature of the samples collected is:

#### SPOIL HEAP

TTO	-	Tip Top Outer
TTC	-	Tip Top Centre
TSL	-	Tip Surface Layer
TFB	-	Tip Flank Bottom
TIP 1	-	From a berm at half height on tip
U 4	-	Driven U 4's from the saddle between the two mounds comprising the tip

#### UNDERGROUND

##### ROOF MEASURES:

BNCH	-	Benches Roof
BR	-	Brooch Roof

##### FLOOR MEASURES:

PF	-	Park Floor
8FF	-	Eight Feet Floor
DF	-	Deep Floor

The samples collected each weighed c. 50kg , which was enough material for three 12-inch direct shear-box tests, as well as chemical and mineralogical determinations.

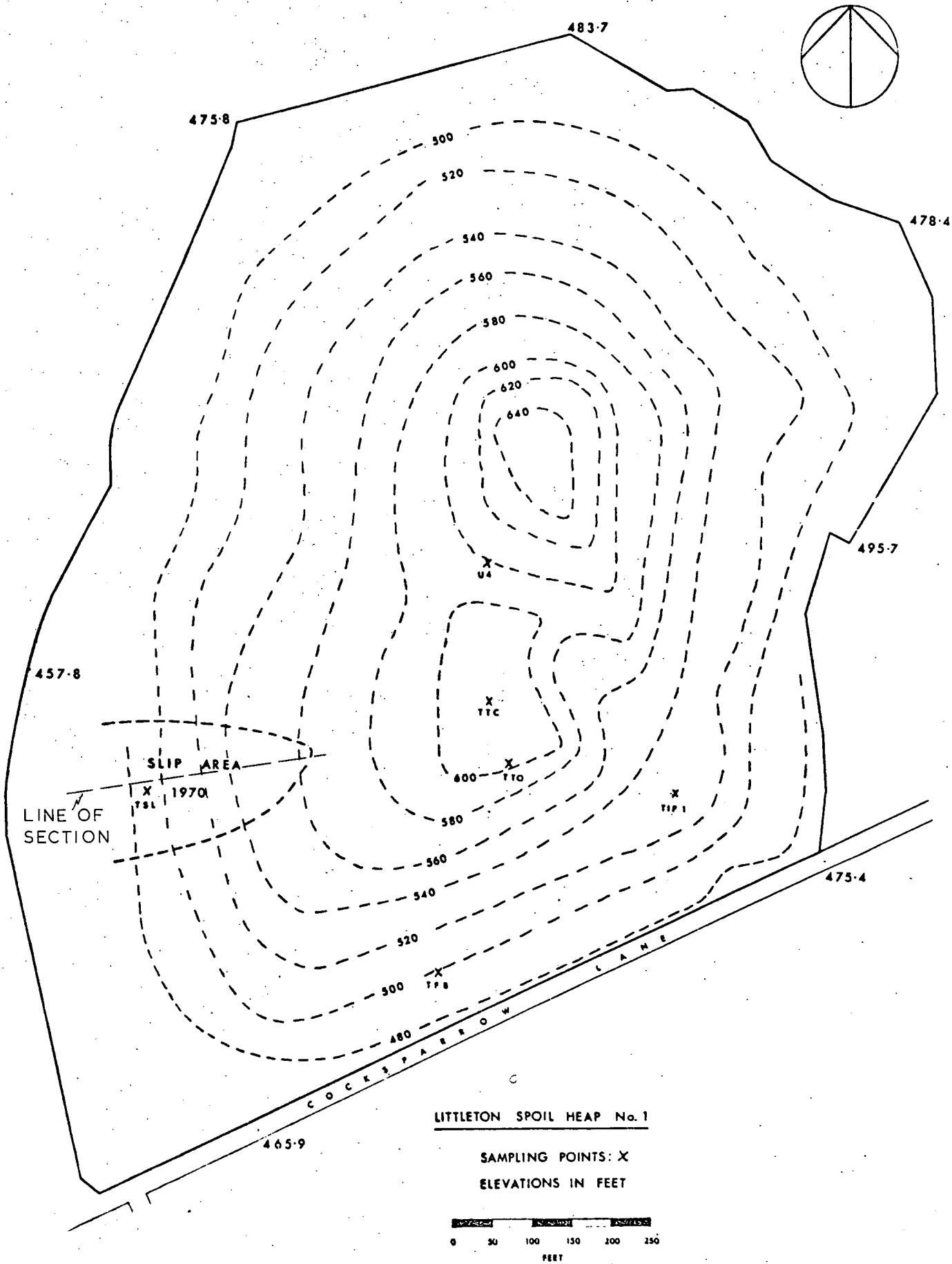


Fig.II. 1. Littleton Spoil Heap No. 1.

The choice of sample locations, both underground and on the tip, was limited by the need to obtain heavy samples and by the consequent need for easy access. However, this problem was partially overcome by using N. C. B. transport facilities underground.

(II.1.a) SAMPLING TECHNIQUE The boxes containing the samples were specially made of aluminium, for lightness and to prevent sparking against rock underground. They were of sufficient size to carry the block specimens for the 12-inch direct shear-box (0.82m long x 0.36m wide x 0.21m deep). In fact, bulk specimens were collected since block samples were found to be impracticable and unnecessary in the normally consolidated tip material.

The samples were wrapped in aluminium foil, and an air-tight seal was effected by pouring paraffin wax around the foil lining. Thus the natural moisture content of the material was preserved until the samples were needed for testing. This prevented desiccation and the consequent anomalous breakdown of the material when it was flooded with water in the shear-box.

It was difficult to obtain representative samples from the underground measures because lateral changes of chemistry and mineralogy can be quite pronounced in a sedimentary sequence (Spears *et al.*, 1971). So the siting of sample positions was important. Even within Littleton Colliery variations are marked, as are age relationships within the tip. This raises doubts about the prevailing type of spoil produced at any one time. This type of problem obviously makes representative sampling difficult.

The sample sites were selected after discussions with N. C. B. officials, one priority being that the samples should come from freshly exposed faces. This condition could not be met in the Deep Floor since mining of this seam has been discontinued. Therefore this sample was

collected from an old exposure in an existing roadway.

(II.1.b) SAMPLE LOCATION The underground samples were collected from current workings, except that of the Deep Floor, as indicated above.

The tip samples were collected from points on the heap as shown in Fig. II.1.

During sampling the tip was being regraded to decrease the slope angle in the 1970 Slip Area. The top of the southern mound was removed, revealing buried material which was collected at TTC and TTO. These samples, then, represent the body of the southern mound.

The sample U4 consisted of four driven 100 mm tubes taken from the saddle between the north and south mounds. Their level is c. 0.3m below ground level (b. g. l.) and they represent the portion of the tip probably weathered to the greatest depth, since they contain material lying on level ground affected by run-off from two slopes.

TIP 1 was taken from a berm half-way up the tip slope. Material from 0.2m b. g. l. to 0.5m b. g. l. is included.

TFB was taken from an excavation in the lower flank of the tip, 3m b. g. l.

TSL represents the skin material of the tip. This sample was scraped off the tip surface, to a depth of 0.02m. This material should show the maximum effect of surface weathering and leaching on the tip, when TSL is compared with buried samples, such as TFB and TTC.

Three samples (M1, 2 and 3) were taken from the area directly affected by the 1970 failure (Taylor and Hardy, 1971).

M1 is material from the slip plane,

M2 is material from the toe of the slip,

M3 is material from the top of the tip.

Sub-samples obtained from the boxed samples were used for quantitative X-ray diffraction analysis. The results were correlated with the physical properties (Chap. III) and the chemistry (Chap. IV) of the material.

(II.2. a) SAMPLE PREPARATION All the samples were dried at 60°C to remove excess water, and were fed into a tungsten carbide disc mill, which reduced them to a fine powder of approximately 20 μm size.

This powder was then used for X-ray diffraction determinations. To obtain quantitative data, an internal standard of synthetic boehmite was added, in a modified version of the method described by Griffin (1954). Using an accurate chemical balance, 0.9000 gm<sub>0</sub> of sample was weighed out, then 0.1000 gm<sub>0</sub> of synthetic boehmite weighed out and mixed thoroughly with the sample. This gave a mixture of 10% boehmite and 90% natural material.

The intensity of an X-ray diffraction peak is directly proportional to the concentration of the component mineral producing it, when allowance is made for absorption effects (Klug and Alexander, 1954). Hence it has been possible to develop quantitative analytical methods based on peak intensities.

Curves from existing standards whose compositions were comparable to those of the samples tested enabled quantitative estimates to be made for the percentages of quartz, illite, kaolinite, chlorite, ankerite, calcite and siderite contained in the samples. Curves of this type have been used in all previous work on tips carried out in Durham, and are referred to by Taylor (1971b).

The material was analysed in smear mounts, using acetone as the liquid medium. The advantage of acetone over water is that its high volatility reduces preferred orientation in the particles, because the liquid evaporates quickly.

(II.2. b) X-RAY DIFFRACTION TECHNIQUE The X-ray equipment used

was a 3kW Philips PW 1130 X-ray diffractometer using iron-filtered cobalt  $K\alpha$  radiation at 60 kV and 30 mA, with divergent, scatter, and receiving slits of  $1^\circ$ ,  $1^\circ$  and  $0.1^\circ$  respectively.

All the specimens were run at a scanning speed of  $1^\circ$  of  $2\theta$  per minute over a range of  $4^\circ$  to  $40^\circ$  of  $2\theta$ . Previous work on colliery spoils used 1kW and 2kW machines with Cu nickel-filtered radiation.

A sealed proportional counter in conjunction with a pulse height selector circuit, to improve background peak discrimination, was used to monitor peak intensities. This counter was connected to a linear response chart recorder which produces a visual trace of the diffraction peaks.

The peak intensities were taken as the area of the graph lying under the peak after subtraction of the background interference. The area of the peak is a better approximation to mineral concentration than peak height (Griffin, 1954).

The areas relating to different minerals were measured with an "Allbrit" polar planimeter.

The peaks relating to different minerals were identified by the Bragg angle ( $2\theta$ ) at which they occurred. This angle depends upon the characteristic lattice spacing of individual minerals (Table II.1).

New working curves have been constructed in Durham (Taylor, 1971b), plotting (peak area for mineral X)/(peak area 10% boehmite) versus the concentration of mineral X. Using these curves, the area of the peak will give the percentage of mineral X present in the multi-component mineral suite.



MINERAL	2θ (cobalt)
Chlorite	7.22 <sup>o</sup>
Illite	10.27 <sup>o</sup>
Kaolinite	14.38 <sup>o</sup>
Boehmite	16.85 <sup>o</sup>
Quartz	24.25 <sup>o</sup>
Calcite	34.25 <sup>o</sup>
Ankerite	35.95 <sup>o</sup>
Siderite	37.42 <sup>o</sup>

TABLE II. 1. PRINCIPAL 2θ IDENTIFIERS  
USED FOR MINERALS IN  
COLLIERY SPOILS

(II. 3)

MINERALOGICAL RESULTS

The mineralogical compositions determined for the specimens from Littleton Colliery are shown in Table II. 2. Kaolinite, illite, chlorite, quartz, ankerite, siderite, and calcite were all determined by X-ray diffraction. Rutile and apatite concentrations were calculated from the X-ray fluorescence percentages for titanium and phosphorous respectively (Chap. IV and Table IV. 1). Organic carbon determinations were obtained by the carbon train method (Groves, 1951) (Chap. IV. 1. b).

Before considering variations in mineralogy, some points which arose during the interpretation of X-ray diffractions will be discussed.

(II. 3. a) MIXED-LAYER CLAY MINERAL Although not determined, some samples showed the presence of a mixed-layer clay mineral. This manifested itself by a "tail" on the high-angstrom side of the 10-Å illite X-ray diffraction peak, caused by slight variations in the d-spacing of the mineral. This was strongest - indicating a larger proportion of expanding clay to illite - in PF, BR and 8FF. The tip specimens showed a wide

Sample	Kaolinite	Illite	Chlorite	Quartz	Ankerite	Siderite	Calcite	Rutile (TiO <sub>2</sub> )	Apatite	Carbon	Total %
ROOF											
Benches	8.2	39.0	4.7	34.3	2.0	0.4	0.0	1.0	0.2	0.4	90.2
Brooch	7.8	58.0	6.0	21.9	0.0	1.0	1.2	1.0	0.2	0.9	98.0
FLOOR											
Eight Feet	13.2	54.4	0.2	18.5	0.0	4.6	0.1	0.8	0.1	4.5	96.4
Park	12.9	79.0	0.1	3.0	0.0	0.0	0.0	1.1	0.2	3.4	99.7
Deep	9.1	29.0	0.1	51.4	0.0	0.0	0.0	1.3	0.0	1.3	92.2
TIP											
TTO	10.3	56.5	5.9	29.4	0.0	2.6	0.0	0.9	0.3	4.0	109.9
TTC	13.4	57.5	4.4	26.3	0.0	1.5	0.0	0.9	0.2	3.5	107.7
TSL	11.0	39.0	3.6	25.0	0.0	3.9	0.0	0.9	0.3	5.0	88.7
TFB	7.6	45.1	3.6	34.6	0.0	0.7	0.0	1.0	0.3	3.8	96.7
TIP 1	14.9	59.0	3.8	31.6	0.0	1.1	0.0	0.9	0.3	5.0	116.6
U <sub>3</sub> 4	8.4	43.0	3.1	30.9	0.0	0.7	0.0	0.9	0.3	1.9	89.2
M <sub>1</sub>	12.0	59.0	6.5	20.2	3.5	1.0	0.0	1.0	0.2	1.8	103.4
M <sub>2</sub>	9.0	51.5	5.6	22.0	0.0	0.0	0.0	0.9	0.5	6.8	89.5
M <sub>3</sub>	10.0	55.2	4.8	22.5	0.0	1.5	0.0	0.9	0.4	4.2	95.3

MINERALOGICAL ANALYSES

TABLE II.2.

\* Taylor and Hardy (1971)

variation from quite strong (in TFB, TIP 1 and U 4), through weak (TSL and TTO), to absent (TTC). Sample BNCH showed little "tail", and in DF the "tail" was absent. Previous work on Littleton tip material (Taylor and Hardy, 1971) showed that mixed-layer clay accounts for some 10 to 19% of the total tip constituents. Moreover, Taylor and Spears (1970) concluded that in the Park Floor and the Brooch seat-earth mixed-layer clay accounts for 21% and 23% respectively, of the total clay mineral components (oriented disc technique).

(II.3.b) CRYSTALLINITY The diffracting ability of a mineral depends upon the order of the structural arrangement. By substitution of atoms, the structure of a mineral may be varied. Hence the diffraction trace of a mineral gives an indication of its crystallinity (Griffin, 1954 and Gibbs, 1967). A measure of the crystallinity may be made by obtaining shape factors from the diffraction trace. The shape factor is the ratio of peak width at half peak height to peak height (Taylor, 1971a). For muscovite a factor of 0.001 was obtained; Morris illite with mixed-layer clay gave 0.134 and Mansfield Marine Band shales with mixed-layer clay gave 0.213 to 0.215. Shape factors for the 10-Å illite peak are shown in Table II.3.

Since shape factor = (width of peak at half peak height) divided by (peak height), an increase in shape factor denotes a decrease in degree of crystallinity. Table II.3 shows that crystallinity was higher in the tip samples than in those from underground, which is paradoxical since expansion of the mixed-layer clay, in response to any degradation processes, ought to decrease crystallinity. Furthermore, the Deep Floor constitutes about 50% of the tip material (Phillips, personal communication), and the Deep Floor illite has a shape factor of 1.000, yet all the tip samples show lower shape factors than any of the parent rocks.

In view of this, the original information concerning the proportions of underground materials contained in the tip (Bygott, personal communication) was questioned.

	SAMPLE	ILLITE SHAPE FACTOR
ROOF	BENCHES	0.221
	BROOCH	0.402
FLOOR	EIGHT FEET	0.257
	PARK	0.311
	DEEP	1.000
TIP	TTO	0.151
	TTC	0.114
	TSL	0.165
	TFB	0.185
	TIP 1	0.218
	U 4	0.174

TABLE II. 3. ILLITE SHAPE FACTORS FOR LITTLETON MATERIAL

Phillips (personal communication) believed that 30% of the tip was made up of Eight Feet Roof material, which had not appeared in Bygott's estimate of the tip constituents. Consequently, samples of the Eight Feet Roof material were collected, at a later date in the research.

The Eight Feet Roof immediately above the coal seam proved to be a canneloid shale, and a sample 0.45m above the coal seam contained abundant mica (hydromuscovite) with a shape factor of 0.065, together with kaolinite, quartz and minor chlorite. A further sample 0.6m above the coal seam showed essentially the same mineralogy with a little more quartz. The mica component was now a mica and mixed-layer clay suite i. e. it had become more illitic, and it had a shape factor of 0.171. A sample from a height of 1.0m above the coal seam contained illite and mixed-layer clay with a shape factor of 0.267.

From this information it is concluded that the tip does, in fact, contain a substantial proportion of the Eight Feet Roof, and that the material is probably from the first 0.45m above the coal seam, so supporting Phillips' estimate.

This is a particularly striking example of the use of mineralogy as a tool in the elucidation of tip history.

(II.4)

#### CONCLUSIONS

Variations in the mineralogical compositions of the samples (Table II.2, Fig II.2) are most pronounced in the group of underground specimens. The tip material shows a certain constancy of composition, bearing out its formation as a mixture of the underground measures. Considering individual minerals and their distribution, it is possible to gain an appreciation of the major points found during the investigation.

The compositions of individual samples are referred to in later chapters, where they may affect physical and chemical characteristics. These compositions are listed in Table II.2.

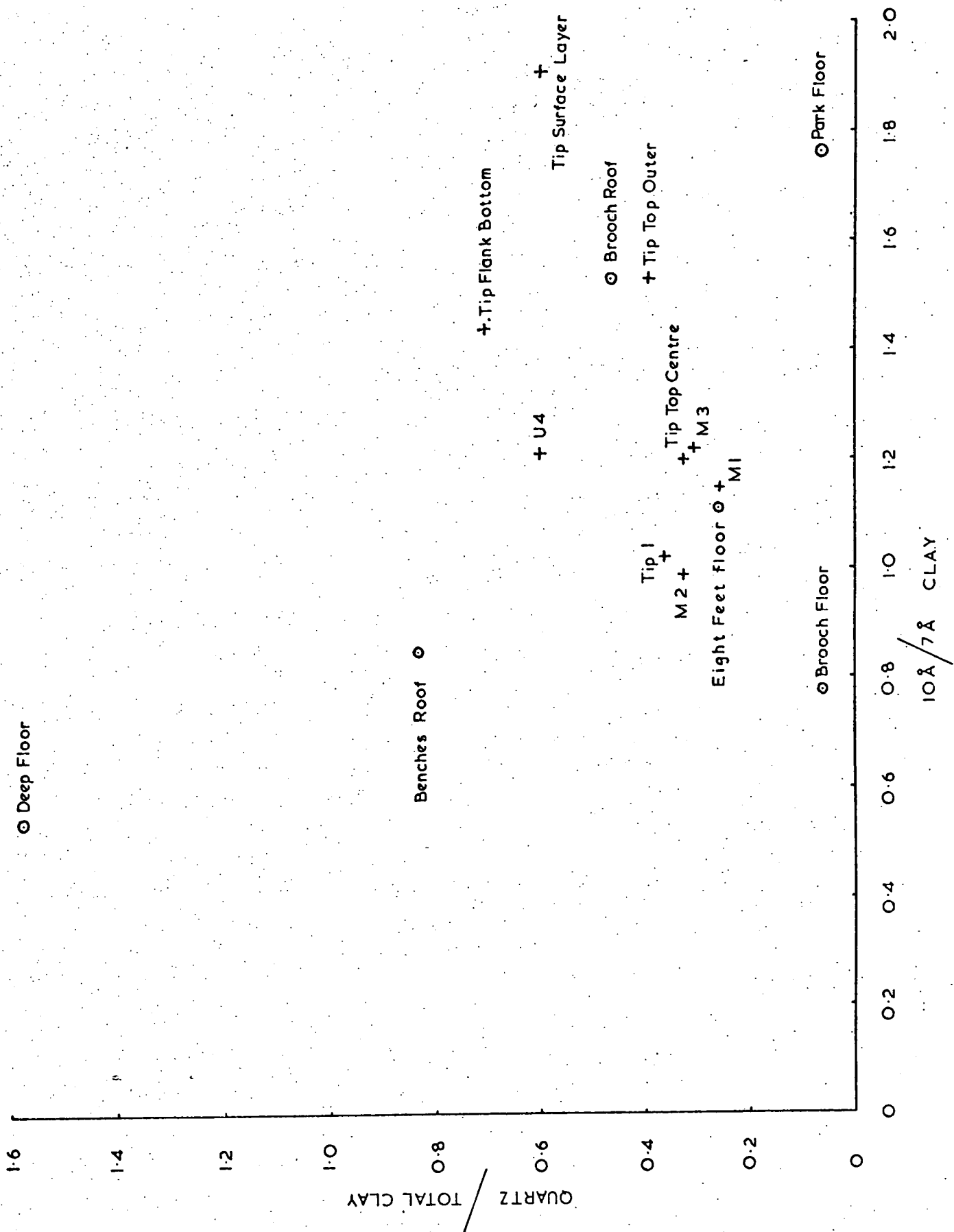


Fig. II. 2. (Quartz/Total Clay) versus (10-Å / 7-Å Clay) graph for Littleton samples.

(II. 4. a) QUARTZ The quartz determinations show an overall range of 3.0% (PF) to 51.4% (DF); the tip material range being 20.0% (M<sub>1</sub>) to 34.6% (TFB).

There seems no distinction between roof and floor measures, i. e. that one set shows a greater quartz concentration than the other. However, the roof measures show a more constant value than the floor samples, which contain the extreme concentrations of quartz.

The tip material shows a low variation compared to its parent materials. This indicates a good degree of mixing of the measures in the tip. The average percentage of quartz in the tip (28.0%) is higher than that in the underground measures (25.8%). This indicates that the Deep Floor (51.4% quartz) forms a large proportion of the tip material. Phillips (personal communication) has indicated that the Deep Floor may constitute 50% of the tip material, which bears out this contention.

(II. 4. b) CARBONATES The non-detrital carbonate minerals identified in the underground measures were ankerite, siderite, and calcite. The tip material contained siderite, with very little ankerite or calcite. The concentration of siderite varied from 0.0% (PF; DF; M<sub>2</sub>) to 4.6% (8FF). Calcite occurred in only two samples: 1.2% in BR, and 0.1% in 8FF. Ankerite was also rare, again occurring in only two samples: 2.0% in BNCH, and 3.5% in M<sub>1</sub>.

The high values for siderite in the tip material may be explained by the mineral's long-term stability (Taylor and Spears, 1970). The calcite and ankerite are more susceptible to chemical weathering, and this explains their almost complete absence in the tip material. In the Yorkshire Main tip it was found that ankerite and calcite originated as secondary minerals which infilled the cleat of the coal (Spears *et al.*, 1971). In other words, carbonates found in tips are not all necessarily derived from associated roof and floor measures. Furthermore, some of the tip carbonate will have been derived from the fossil debris in the canneloid shale of the Eight Feet Roof (Chap. II. 3. b).

(II.4.c) RUTILE and APATITE The concentrations of rutile and apatite are low, as in most non-marine Coal Measures rocks, but only the DF sample shows an absence of apatite. The determination of these low concentrations is a result of the more refined analytical technique used for these oxides (X-ray fluorescence, Chap. IV).

On an X-ray diffraction trace, the rutile and apatite peaks would certainly be overlooked in concentrations of less than about 1%.

The rutile in the samples is probably present as needles in the clay minerals (Taylor, 1971a; Reeves, 1971).

Little can be inferred from the concentrations present in tip and underground samples, except that the generally higher concentrations of apatite in the tip indicate incomplete sampling, and may be due to the presence of material from excavation of roadways through Carboniferous Limestone.

(II.4.d) CLAY MINERALS It is obvious from Table II.2<sub>0</sub> that the bulk of the material investigated is made up of the clay minerals: illite, kaolinite, and minor chlorite.

Illite is the main contributor of these three. As mentioned above, this is sometimes associated with a mixed-layer clay, which has been included in the illite concentration percentages. Overall, the percentage of illite varies from 29.0% (DF) to 79% (PF). The tip samples lie between these extremes, as is to be expected. The lowest tip concentration is 39.0% (TSL), and the highest is 59.0% (M<sub>0</sub>1 and TIP 1).

Kaolinite also occurs in all the samples analysed, ranging from a concentration of 7.8% (BR) to 14.9% (TIP 1). This distribution, like that of apatite, is anomalous in that the highest concentration is in tip material, whereas the maximum value ought to occur in one of the parent samples. This apparent paradox will be mentioned again with respect to chlorite.

Chlorite is the rarest of the clay minerals, ranging from 0.1% (PF and DF) to 6.5% (M<sub>0</sub>1). Taylor and Hardy (1971) identified the



chlorite (14.26-Å peak) as magnesium-rich, non-swelling penninite.

The presence of the maximum concentration of chlorite and kaolinite in the tip material led to the conclusion that some roof measure material may have been unaccounted for in the tip. Records relating to measures contributing to older tips are often incomplete and indeed may at times be a matter of personal recollections. With Littleton the mineralogy of the tip indicates the omission of some material from the initial samplings: possibly roof measures. This has subsequently been shown to be the case (Chap. II.3.b).

(II.4.e) CARBON The carbon concentrations show a definite increase in the tip samples (average 4.0%) when compared with those from underground (average 2.1%).

This may be adequately accounted for by the mining process. Coal removed with the associated roof and floor measures during extraction invariably finds its way into a tip in greater or lesser amounts, thus increasing the amount of carbon present.

Hence the large discrepancy between the tip material and underground measures may be explained by means other than sampling error. Quantitative mineralogical analyses are by their nature somewhat imprecise (e.g. total mineralogical ranges - 88.7% to 116.6%; Table II.2). Previous work on tip materials has shown that such variations are due to variations in crystallinity not reflected by the calibration curves. With fresh roof and floor materials the error is greatly reduced (about 95% to 105%; Reeves, 1971). However, they do provide a useful comparative guide as mentioned below.

(II.4.f) COMPARISON OF UNDERGROUND AND TIP SAMPLES Despite failings in quantitative mineralogical precision, the main points shown in this investigation are plain. The most important feature is the constancy of composition of the tip samples. Fig. II.2 shows a plot of quartz/total clay versus 10-Å diffraction peak area (Illite)/7-Å diffraction peak area (Kaolinite and minor chlorite) (Taylor and Spears, 1970). Ignoring

minor constituents such as carbon (<6.8%), carbonates (<4.7%), rutile (<1.3%), and apatite (<0.5%), this graph gives a representation of the main mineralogies of the samples analysed. The tip samples fall in a distinct group, indicating a consistency of composition which is clearly not demonstrated by the wide scatter of the underground samples.

Of the underground samples, the most important is the Deep Floor since it forms up to 50% of the tip material. The extremely high quartz content (51.4%) and low illite (29.0%) of the Deep Floor are reflected in its position on Fig. II. 2.

In the same way, the Park Floor is shown to be outside the normal compositional limits. Its position on Fig. II. 2 reflects a very high illite content (79.0%) and a very low quartz concentration (3.0%).

The illite concentration in the tip material is high when compared with that of the Deep Floor. However, the very high concentration of illite in the Park Floor (< 15% of the tip) can account for this.

The tip shows a higher quartz concentration than might be expected, but that is readily explained by the high percentage of quartz in the Deep Floor, which may contribute 50% of the spoil heap.

The absence of pyrite in all the samples analysed from Littleton (an unburnt tip) is an important feature and tends to reflect the low organic carbon (coal) content of the tip.

The mineralogies of the underground and tip samples were compared statistically, using the "Student's *t*" method (Moroney, 1970). This is a method of comparing means of populations. The significance of the differences (the probability that they are different) is assigned three confidence levels: 95% (probably significant), 99% (significant), and 99.9% (highly significant). The results of this test are shown in Table II. 4.

Only chlorite and apatite are significantly different in the two sets of data with organic carbon (coal) falling very close to the lower boundary; all are significantly higher in the tip material than in the underground samples. As mentioned above, all these three components

Mineral	Underground <sup>†</sup> Mean	Spoil Heap <sup>*</sup> Mean	'Student's' <sup>†</sup> Test	Confidence Level
Kaolinite	9.70	9.92	not significantly different	
Illite	48.52	50.27	not significantly different	
Chlorite	1.04	4.07	significantly different	98% confidence level
Quartz	25.80	29.63	not significantly different	
Ankerite	0.40	0.00	not significantly different	
Siderite	1.20	1.75	not significantly different	
Calcite	0.26	0.00	not significantly different	
Rutile	1.04	0.92	not significantly different	
Apatite	0.14	0.28	definitely significantly different	99% confidence level
Carbon	2.10	3.87	probably significantly different	95% confidence level

<sup>†</sup> Average of 5 samples

<sup>\*</sup> Average of 9 samples

TABLE II.4. STATISTICAL COMPARISON OF UNDERGROUND AND SPOIL HEAP MINERALOGY AT LITTLETON COLLIERY

are represented as minor constituents and the deficiency in chlorite in the underground materials can very reasonably be accounted for by the absence of the Eight Feet Roof from the statistical analysis. The coal content of the tip is low in comparison with other tips (13%) and obviously marginal from a statistical viewpoint. It should also be mentioned that  $P_2O_5$  (hence apatite) is also found in organic matter.

Generally, however, the "Student's"t test demonstrates the similarity between the underground material mineralogy and that of Spoil Heap No. 1 at Littleton Colliery.

## CHAPTER III

### SHEAR STRENGTH INVESTIGATION

The bulk samples from the tip and underground measures were subjected to direct shear tests in a 12-inch shear-box (modified Farnell 305) and consolidated-drained triaxial tests in a conventional 4-inch cell, using a 5-ton Wykeham Farrance compression machine. These tests were used together for evaluation of peak shear strength parameters. The nature of the materials tested, and the need for residual shear strength evaluation, necessitated the development of new testing techniques and the modification of the standard shear-box equipment.

#### (III.1) 12-INCH SHEAR-BOX TECHNIQUE

The Farnell Model 305 12-inch shear-box was originally designed to find the peak shear strength of construction aggregates. Difficulties arose when attempting to use it for multiple reversal evaluation of residual shear strength.

Modifications were made, and they are described below.

(III.1. a) BOX REVERSAL As delivered, the drive-motor of the shear-box was reversible. However, the thrust ram connecting the gear-box to the lower half of the shear-box was not rigidly attached to the box (Fig. III. 1). Therefore, when the motor was reversed the thrust ram retracted, but the box was not drawn backwards. This left the box in a sheared position on reversal.

A new thrust ram was fabricated, with a flange at the end in contact with the box. High-tensile steel bolts were tapped into the shear-box through the flange, fastening the box securely onto the ram (Fig. III. 2).

On reversing the motor, the thrust ram retracted, now drawing the box with it.

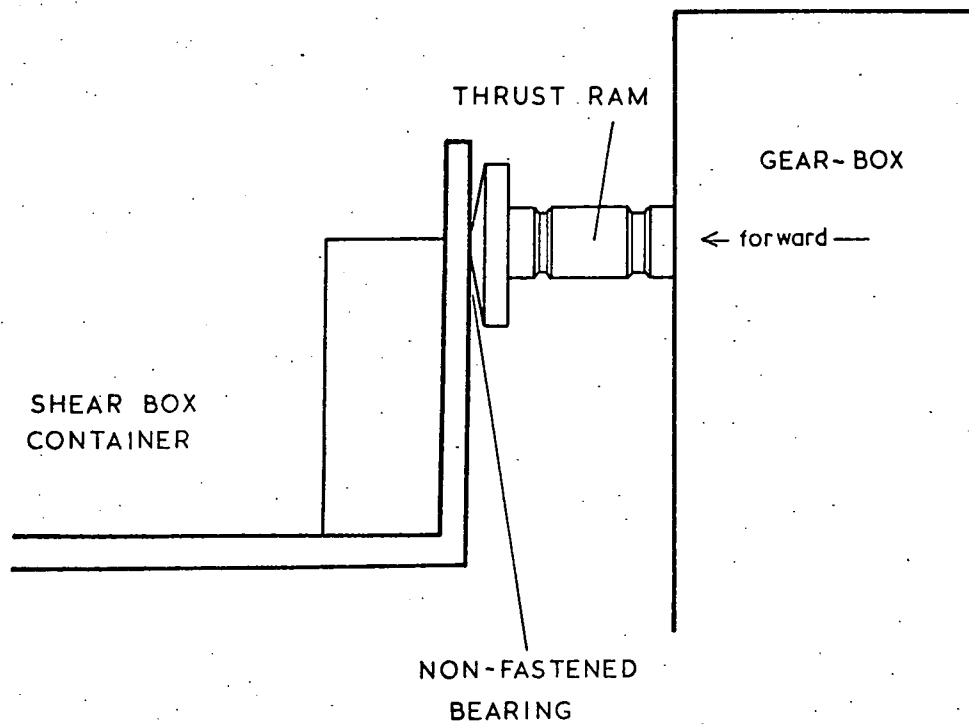


Fig. III. 1. Non-fastened thrust bearing on the shear-box, rigid only in forward travel.

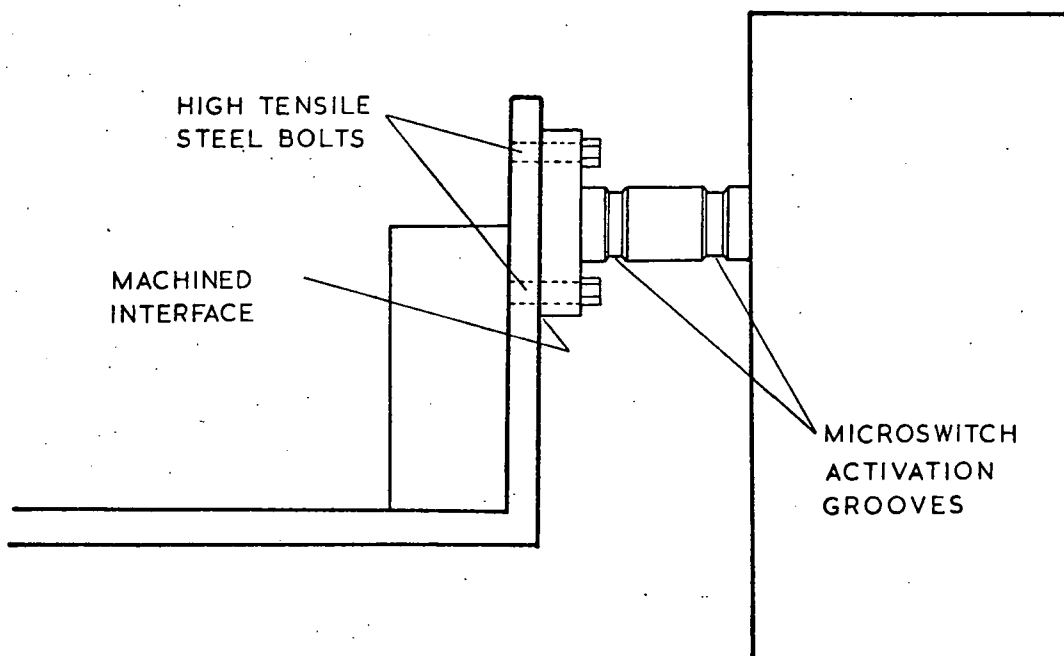


Fig. III. 2. Fastening of thrust bearing for rigidity in forward and reverse travel.

(III. 1. b) SHEARING IN REVERSE Having achieved reversal of the box it was found that the sample did not shear on reversal. The frame connecting the upper half of the box to the proving ring constrained the movement of the box only in the forward direction (Fig. III. 3). On reversal, the lower half of the box drew the upper half of the box backwards in a sheared position. Hence it was necessary to prevent the upper half of the box from moving backwards, in such a way that the upper frame was still removable, to facilitate loading and unloading the box.

It was therefore decided to bolt a heavy bracket onto the structural framework at the rear of the machine, which held the upper half of the box rigid while the lower half was displaced during reversal.

It was necessary to place this in the line of force producing the shear, so that no overturning moments were created.

A 25.4 mm diameter bolt was tapped through the bracket, parallel to, and concentric with, the drive-ram of the gear-box (Plate III. 1). This acted upon the rear of the framework which activated the proving ring. By adjusting the bolt, a zero position on the proving ring dial gauge was matched to a minimum dead-time between forward and reverse shears.

In the water reservoir, which contains the two halves of the shear-box, packing had to be inserted between the bottom half of the box and the forward wall of the reservoir. This prevented the lower half of the box sliding during reverse runs, with consequent non-shearing of the sample (Fig. III. 4).

(III. 1. c) SAMPLE CONSERVATION During the shearing experiment, migration of the sample occurs. This involves movement of sample material in response to the horizontal stresses set up during shearing (Fig. III. 5). The upward movement of the sample tends to lift the upper half of the box away from the lower half. This exposes sample on, and above, the shear plane. Some of the sample is then forced out through the gap between the box halves by the vertical load and the shear displacement.

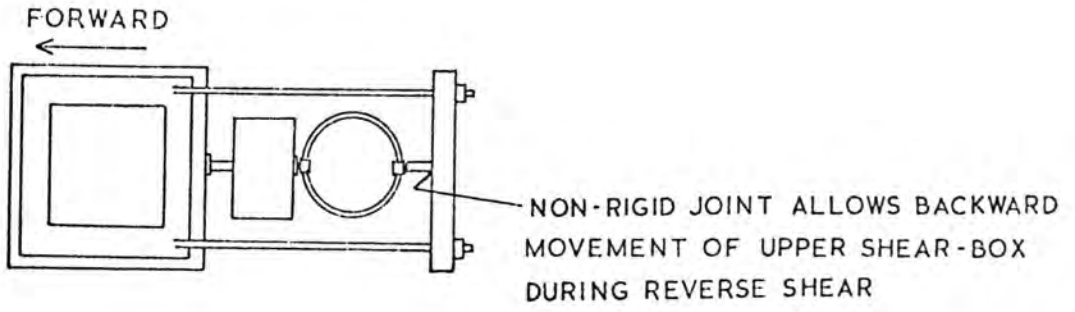


Fig. III. 3. Vertical view of shear-box showing non-constraint of the upper half of the shear-box during reverse shear.

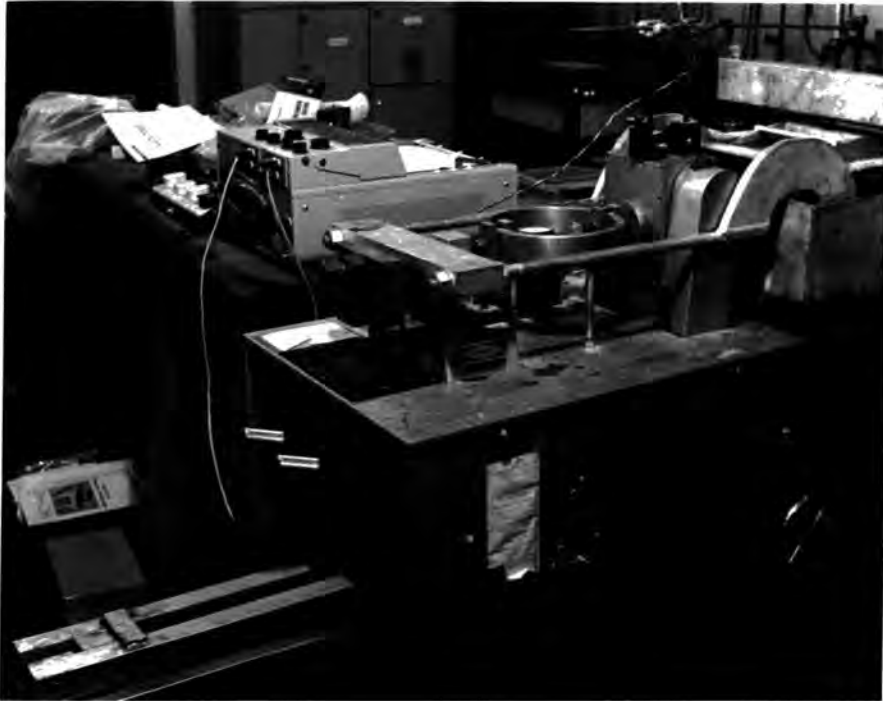


Plate III. 1. Retaining bracket attached to the rear of the shear-box to prevent movement of the upper half of the shear-box during reverse shear.



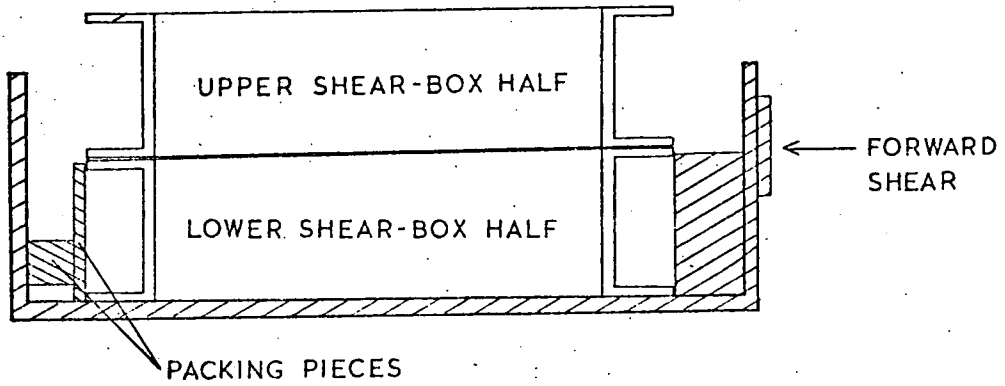


Fig. III. 4. Packing inserted in the shear-box container to prevent movement of the lower half of the shear-box during reverse shearing.

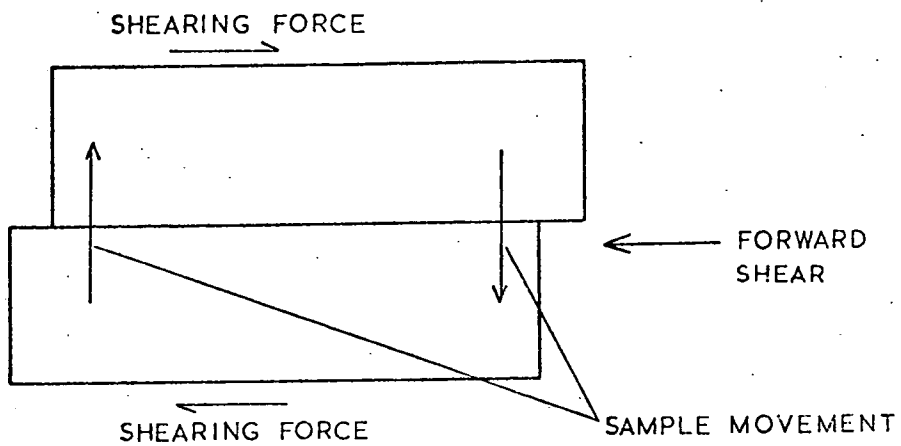


Fig. III. 5. Movement of material within the specimen during shearing.

Furthermore, each shearing movement carries material out of the box, into the space between the "lips". As this material is added to on alternate shears, it wedges the box halves apart (Fig. III.6).

This was rectified by preventing vertical movement of the upper box as much as possible. Means of effecting this were restricted since any inhibition of movement of the upper box must affect the internal friction of the machine and the vertical load on the sample. This in turn must affect the stress readings and subsequent calculations of shear strength.

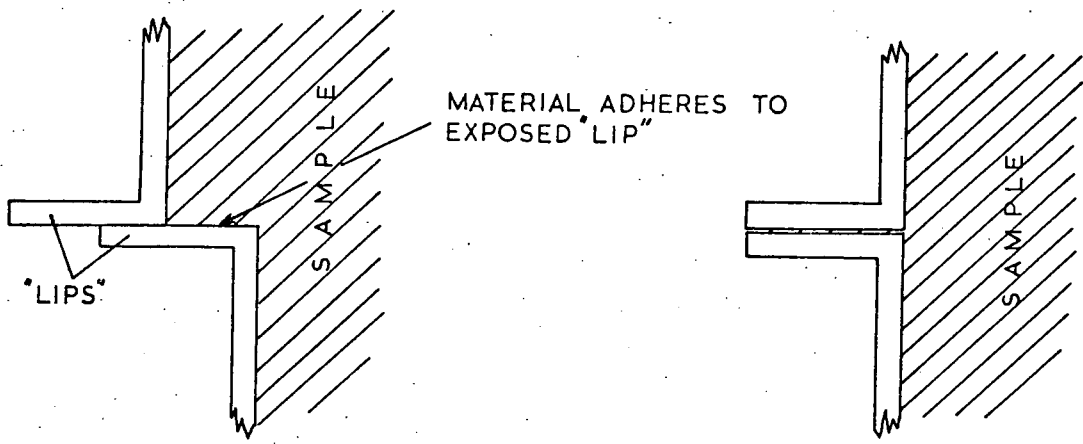
The restraining mechanism must obviously be self-supporting. Merely weighting down the upper box would affect the stress readings by altering the vertical load on the specimen.

A rectangular framework was eventually used, which fitted across the box-end of the machine, being anchored to plates welded onto the legs of the shear-box (Fig. III.7 and Plate III.2).

A top bar, with recesses on the underside to take ball-bearings, was screwed down onto the top of the upper half of the shear-box, using nuts on the threaded side arms. Shear stress readings could only be taken during a forward shear, since the proving ring deflection mechanism only operated in compression (Fig. III.3). Therefore, the bar was screwed down tightly on the backward run, when no readings were taken. This modification subsequently helped to reduce sample loss to a minimum.

During the forward run, the two halves of the box could not be brought together, because of the resulting friction between them, so the bar was loosened to give a 1 mm clearance between the ball-bearings and the bar. This clearance was gradually taken up as the test progressed.

Until the clearance was taken up, all readings were obviously accurate, since no restraint was being applied. After the upper half of the box began to stress the top bar, it was necessary to ensure that there was a minimal effect on the stress readings, and the restraining bar structure was designed with this in mind.



(a) DURING FORWARD SHEAR

(b) AFTER FORWARD & REVERSE SHEAR

Fig. III. 6. Wedging apart of the shear-box halves by displaced material.

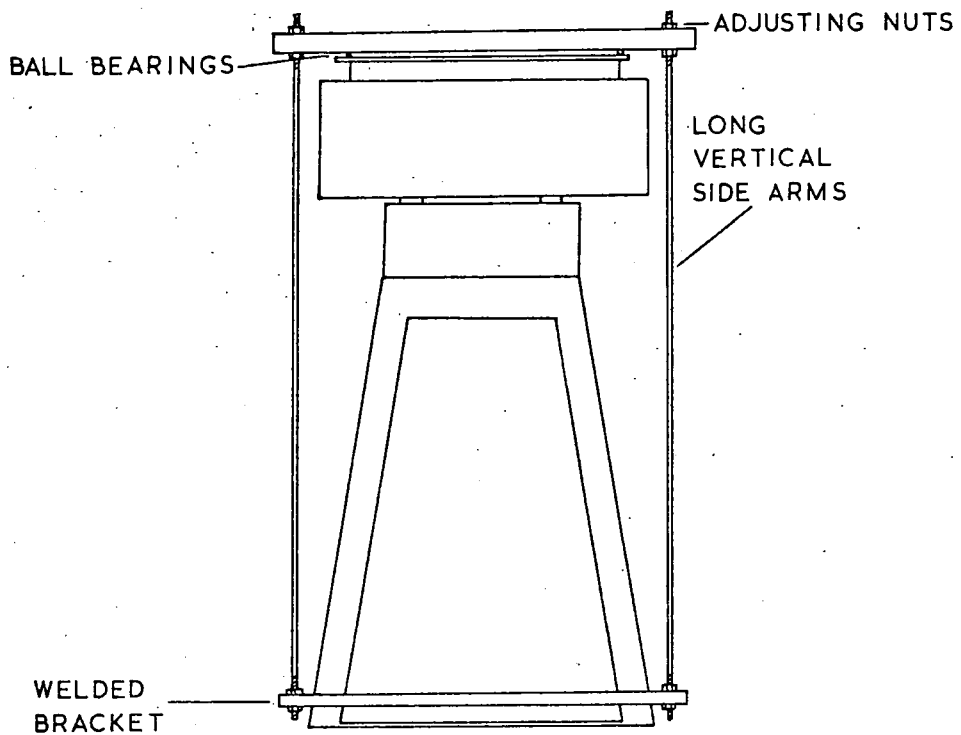


Fig. III. 7. Framework to prevent vertical movement of the upper shear-box half during shearing.

To minimize the horizontal stress induced by the bar, the side arms of the frame were made as long as possible, and ball bearings were inserted below it.

In lengthening the side arms, the downward movement of the bar was kept to a minimum (Fig. III. 8). Considering OA as the side arm of the frame, during movement of the upper half of the box, the point A moves to A<sup>1</sup>, tracing AA<sup>1</sup>: an arc of a circle, centre O (the lower fixing point of the side arm). This movement induces a vertical movement of length CD. For equal lengths of AA<sup>1</sup> (equal strains of a sample), CD will decrease as AO increases.

Hence, even assuming that the ball-bearings do not rotate, and consequently that the bar does not move relative to the box, the vertical movement of the upper box will decrease with an increase in the length of the side arms.

The volume of sample used for each test in the 12-inch shear-box depends on the depth of the material, since the area is constant. Originally, the Farnell 305 was built to take a sample 153 mm deep, but this was reduced by placing the bottom platen, on which the sample lies, on top of two 25.4 mm bars on the bottom of the box container. This reduced the volume of sample used in each test, giving a sample thickness of 50.8 mm below the shear plane. Skempton (1964) has shown that shear planes, in material not unlike a fine-grained spoil, comprise a family of shear planes up to 20 mm thick, lying in a band about 24 mm across. Hence, reducing the thickness of the sample does not affect the shear planes developed.

The void created below the bottom platen was filled with water when saturating the sample before tests were begun.

(III.1.d) RATE OF SHEARING The shear strength of a soil can be said to depend upon: (a) the apparent internal friction of the soil, and (b) the apparent cohesion of the particles.

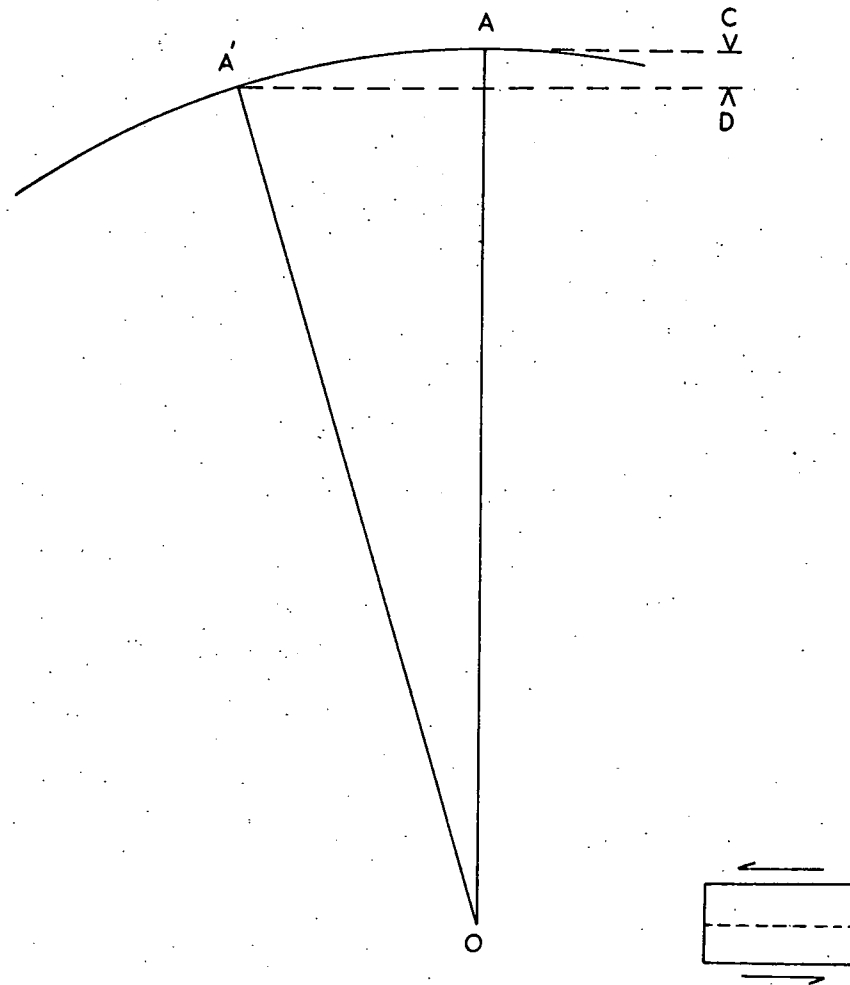


Fig. III. 8. Vertical movement of the framework during horizontal shearing.

These three are related by Coulomb's law:

$$\tau_f = c + \sigma \tan \phi \dots\dots\dots (III.1)$$

where the angle " $\phi$ " is the angle of shearing resistance, " $c$ " is the apparent cohesion, " $\tau_f$ " is the shear stress at failure, and " $\sigma$ " is the total normal stress (Fig. III.9). The constants " $c$ " and " $\phi$ " in equation (III.1) refer to the total applied stresses.

In the shear-box, much of the pore space between grains is filled with water, since the sample is immersed at least to the shear plane. This simulates sub-water-table conditions in a tip, allowing strength parameters to be evaluated for that condition. When the sample is loaded, part of the applied stress " $\sigma$ " is transmitted by interparticulate contact: the "effective stress", " $\sigma'$ ". The remainder of the applied stress is transmitted by the fluid pressure " $u$ " developed in the pore-water.

Therefore, the external stress is balanced by the sum of opposing internal stresses:

$$\sigma = (\sigma' + u) \dots\dots\dots (III.2)$$

and consequently, the effective stress is:

$$\sigma' = (\sigma - u) \dots\dots\dots (III.3)$$

giving a modified Coulomb equation:

$$\tau_f = c + (\sigma - u) \tan \phi \dots\dots\dots (III.4)$$

in terms of effective stresses.

The drainage of a specimen in the large shear-box depends upon the soil's permeability. Should the drainage be poor - as in the case of this type of tip material which has a high clay content - the rate of shear is critical. This pertains because with a rapid rate of shear, pore-water pressure will be built up rapidly, and dissipation will be impeded by the low permeability. Consequently, in equation (III.4) " $u$ " will increase to give a lower value of  $(\sigma - u)$ , and the shear stress at failure is reduced.

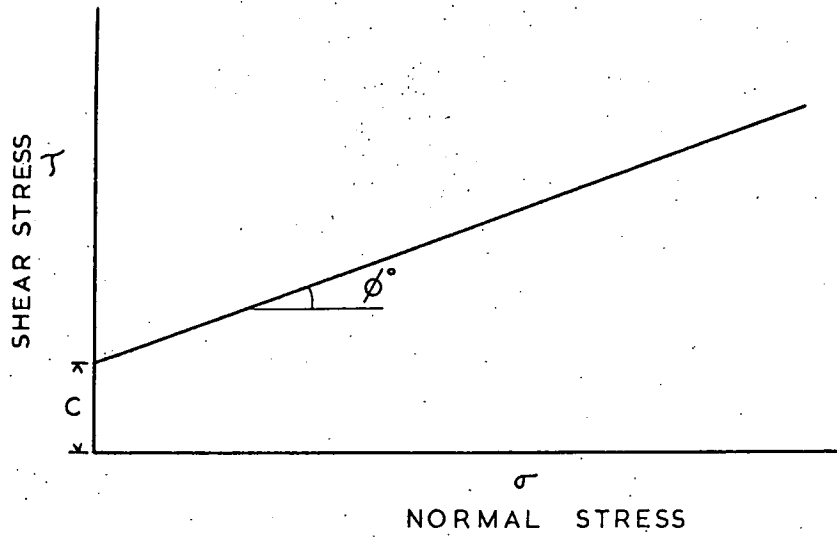


Fig. III. 9. Coulomb's law.

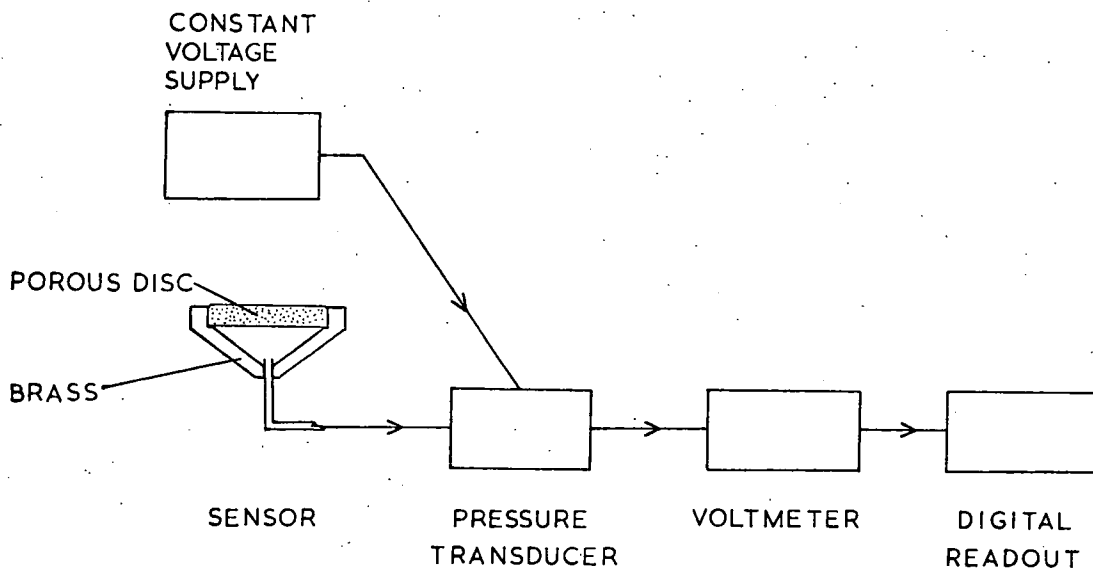


Fig. III. 10. Pore-pressure monitoring system.

Two methods are available to estimate acceptable shear rates (Bishop and Henkel, 1972). Both were designed for the triaxial compression test, giving strain rates which keep pore pressure within the accepted level of 95% dissipation.

The first method involves the direct measurement of pore-water pressure, checking that it does not rise above 5% of the vertical stress. The second method involves calculation based upon consolidation parameters. This is partly based on the geometry and drainage possibilities in a triaxial specimen, hindering application to shear-box tests.

For the direct method, a pressure sensor was placed in the specimen during emplacement of the sample. Considering the probable thickness of the shearing zone, the sensor was placed so that it lay not more than 5 mm below the shear plane of the shear-box halves after consolidation. This gave acceptable values for pore-pressure readings on the shear plane.

A brass inlet, masked by a porous disc, formed the sensor inlet (Fig III. 10).

From the inlet, a plastic tube passed down through a drainhole in the bottom platen, into the void below the sample. The tube was led through a hole in the side of the lower shear-box to a  $689.5 \text{ kN/m}^2$  ( $100 \text{ lbf/in}^2$ ) pressure transducer (Electro Mechanisms Ltd., Type P. S. G.). Before sealing, water was passed through the pipe, and all air evacuated.

The output from the pressure transducer was monitored on a digital voltmeter (Solartron Type LM 1420.2).

The system was calibrated, against a Budenburg test gauge, in  $10 \text{ kN/m}^2$  steps. From Fig. III. 11 it can be seen that a range from 0 to  $100 \text{ kN/m}^2$  is linear against the voltmeter readings.

During shearing of the Deep Floor sample, at a normal stress of  $80.3 \text{ kN/m}^2$ , a maximum pore pressure of  $3.0 \text{ kN/m}^2$  resulted. This represents a pore-water pressure component of only 3.7%. The rate of



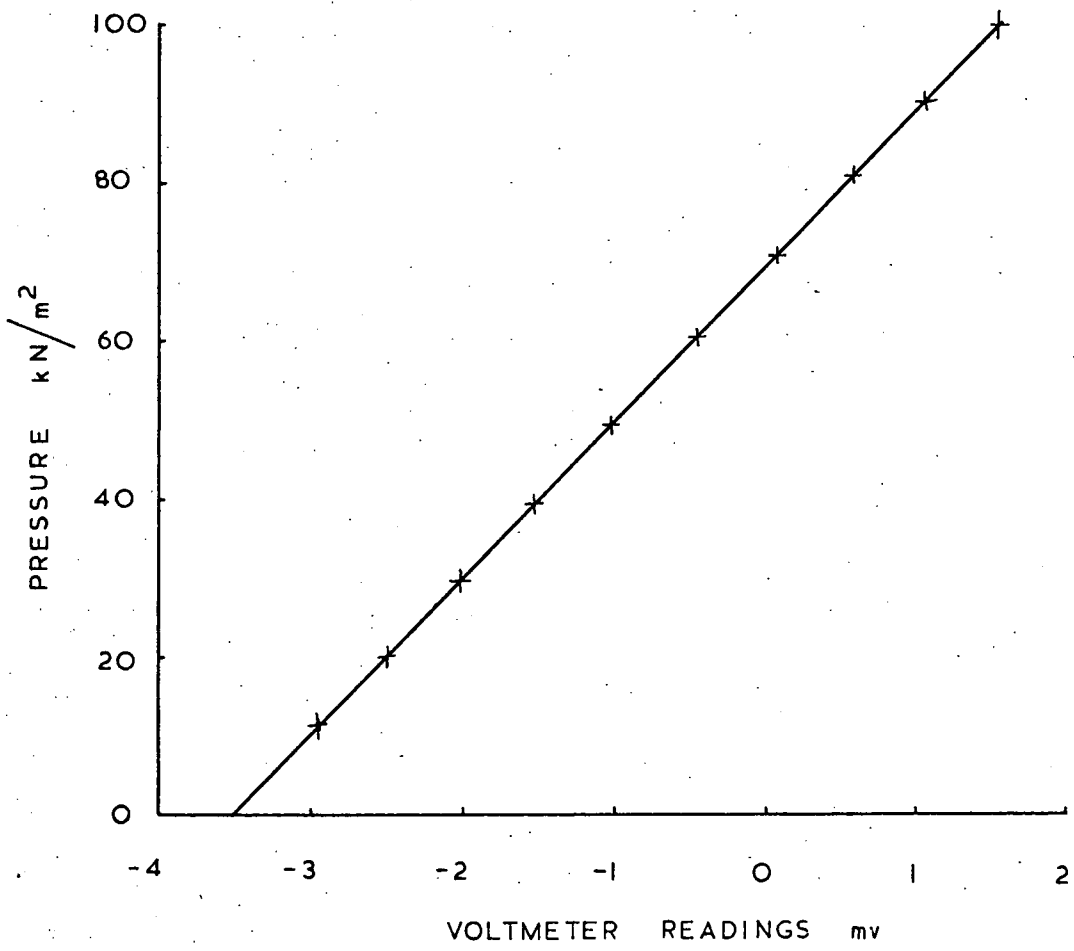


Fig III. 11. Digital voltmeter calibration curve for pore pressure measurement.

shear was 0.076 mm/min (E8 on the machine gear-box). This is acceptable within the terms of 95% pore-water pressure dissipation and E8 is the rate used in the current work.

The second method is theoretical, the required time to failure of a specimen " $t_f$ ", being:

$$t_f = \frac{20 h^2}{\eta C_v} \text{ min} \dots \dots \dots (III.5)$$

where  $h$  is the height of the specimen,  $C_v$  is the coefficient of consolidation and  $\eta$  is "a factor pending upon drainage conditions at the sample boundaries" (Bishop and Henkel, 1972, p.125).

This formula is based upon Terzaghi's Theory of One-Dimensional Consolidation, and it ought to be possible to allow for the geometry of the shear-box specimen, as opposed to that of the triaxial specimen for which the formula was developed. However, the drainage factor " $\eta$ " is difficult to determine in the case of the shear-box. In the triaxial test, the factor varies in value from 3.0 for the case of drainage from both ends of the specimen, to 40.4 for the case of drainage from both ends and a radial boundary. The difference between these two values is very large, and since  $t_f$  varies inversely with  $\eta$  it is most important to determine an accurate value of  $\eta$ .

Considering the shear-box sample as a modified triaxial sample, it is obvious that drainage occurs at both ends. Less obvious is the part played by the shear plane between the shear boxes. Pore-water pressure must be drained at the perimeter of the sample, but it is difficult to estimate how far into the sample this effect penetrates. Therefore the shear plane cannot be considered as a true radial boundary in the shear-box specimen, where specimen thickness is a fraction of specimen length.

In view of the difficulties involved in applying this method, the empirical test was taken as sufficient evidence that 95% pore-water pressure dissipation was achieved at the rate of shear used during testing, which was 0.076 mm/min.

(III.1.e) AUTOMATION OF TEST RESULTS The shear-box was already

fitted with a microswitch to limit both forward and reverse travel.

This operated on the drive ram of the machine, breaking contact at the limits of travel when the switch plunger dropped into grooves on the ram (Plate III.3).

This allowed the tests to be run without constant supervision, since possible overrun of the machine and consequent damage of the gear-box was prevented.

At the rate of shear shown to be acceptable by the experiment outlined above, the duration of each shear was  $6\frac{1}{2}$ -hours. This allowed only one forward recording run each day, with a reverse run overnight at a lower speed, giving a 24-hour cycle. To accommodate two recording runs per day, one reverse run would have had to have been inserted, necessitating tripling the rate of shear to obtain three separate shears.

On average the length of shear taken to reach residual was 0.6-0.7m, hence 12 days were required to obtain a residual value. Furthermore, at least 3 days were taken to consolidate the sample fully.

Manual readings over a total of 15 days would have been extremely wasteful, and so the shear stress and vertical strain readings were automated.

Linear Variable Differential Transducers (L.V.D. T.s) were attached to the shafts of the dial gauges already fitted to the machine (Electro Mechanisms Ltd. Types 500 SS-L and 100 MS-L). The shear stress L.V.D. T. measured the deflection of the proving ring, and the vertical strain L.V.D. T. measured vertical displacement of the upper platen of the sample (Plate III.2 and Plate III.4). By attaching the L.V.D. T.s directly to the shafts of the dial gauges it was possible to calibrate their output easily: essential after disturbing the equipment when unloading and loading samples.

The outputs of the L.V.D. Ts were registered on a twin-pen pen recorder (Rikadenki Type B-261).



Plate III. 2. 12-inch direct shear-box with framework (A) attached to prevent vertical movement of the upper shear-box half.

Automation of the strain dial gauge was not undertaken because movement of the shear-box was assumed to be linear with respect to time. Therefore the stress v time curve produced by the pen recorder is effectively a stress v strain curve. This assumption is viable only when the proving ring is not flexed, or is flexed at a constant rate. Over the last 90% of a test flexure of the proving ring is low, and so the assumption is valid for that portion of the test. For the first 10%, however, the inadequacy of the system has to be overcome by frequent manual readings.

### (III.1.f) INTEGRATION OF TRIAXIAL COMPRESSION AND SHEAR-BOX TESTS

In order to determine  $c'$ ,  $\phi'$  and hence  $\tau_f$  in the Coulomb equation (Chap. III.1.d), the graph shown in Fig. III.9 is drawn. To draw this straight-line graph, at least 3 points on it must be ascertained, therefore 3 tests are performed at different values of  $\sigma_1$ .

Originally, 3 samples were sheared at different values of  $\sigma_1$  in the shear-box. However, at least 10 days of shearing and 3 days of consolidation were required for each specimen, giving a total time of some 6 weeks for each set of results to be obtained. Furthermore, some 9 kgs of sample were used. To avoid this wastage of time and material, it was decided to modify the standard technique.

Instead of using three separate shear-box specimens to obtain results, one shear-box and two or three triaxial compression samples were tested.

Starting at the lowest required vertical stress, the shear-box sample was consolidated and sheared to residual. This gave the peak and residual shear strength parameters at that vertical stress. Having reached residual shear strength, the vertical load on the specimen was increased to the next required stress, and the sample left to consolidate.

After consolidation, the sample was again sheared to residual shear strength, and the cycle repeated for the third, and highest, vertical load.

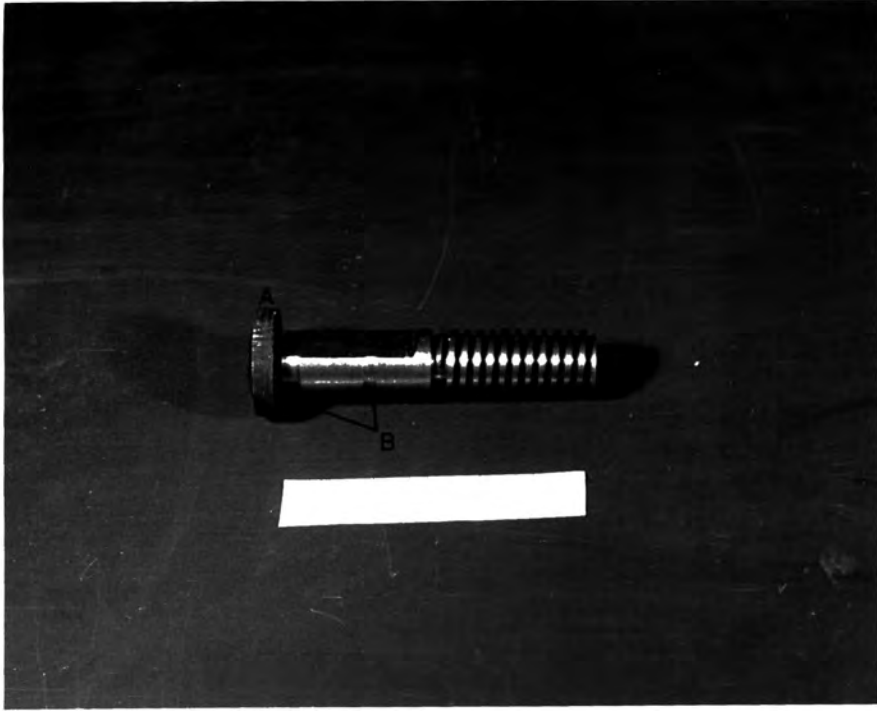


Plate III. 3. Original thrust ram with non-rigid bearing (A) and microswitch activation grooves (B).

This produced three residual strength values and one peak strength value. The two peak strengths corresponding to the higher residual strengths were evaluated in the triaxial compression machine, at confining pressures corresponding to the vertical stresses in the shear-box. It will be shown that triaxial and shear-box results are compatible.

Hence a complete set of six results was obtained. Time was saved because having reached residual shear strength at one vertical stress, the time to residual at the higher loads was much reduced, due to reactivation of an existing shear plane. The amount of sample used was also reduced, since the two 4-inch triaxial samples were smaller than the two shear-box samples which they replaced.

On completion of the test at the highest vertical load, the equipment was adjusted and a single recorded shear performed at both of the lower vertical loads. The values gained from these showed a slightly lower shear strength than first obtained. This is partly due to the comminution of the shear-plane material at higher loads, and the extended length of shear. Though the reductions were less than 5% of the first results gained, they indicated that shear strength continues to fall after long shear displacements of normally consolidated material, though to a lesser extent than that achieved just after peak shear strength has been passed. Rotary shear tests over very extended shear displacements bear out this conclusion (Bishop *et al.*, 1971). For stability calculations, the residual shear strength values obtained from shear-boxes should be adequate. However, it should be borne in mind that the Maclane Tippler method of spoil tipping can produce shear planes at the time of emplacement which will be extensive and may well be of sufficient length after subsequent tipping and slumping to produce a significant fall in their shear strength.

In fact, an actual segment of a shear plane from Littleton Spoil Heap No. 1 was tested by Taylor and Hardy (1971), but did not show any serious deviation from the results obtained from bulk specimens sheared during this study. (Chap. III. 5. b).

### (III.2) 4-INCH TRIAXIAL COMPRESSION TEST TECHNIQUE

The consolidated-drained triaxial tests were undertaken to obtain peak shear strength parameters, as outlined above. Deviation from normal technique and equipment was only necessary in sample preparation and volume change measurement.

(III.2. a) SAMPLE PREPARATION The samples from the tip and underground were originally intended for testing in the 12-inch direct shear-box. Hence they were all bulk samples, and so triaxial specimens were fabricated using the available material.

The required density of the samples was calculated as 95% of the maximum dry density of the tip material. This is the conventional civil engineering standard that may well be applied to all colliery tips (Bishop *et al.*, 1969). Using the standard compaction test (B.S. 1377: 1967), the maximum dry density was found to be  $1.682 \text{ Mg/m}^3$  ( $105 \text{ lb/ft}^3$ ) at a moisture content of 15%, giving a required density of  $1.604 \text{ Mg/m}^3$  ( $99.7 \text{ lb/ft}^3$ ).

The required dimensions of each triaxial sample were 203.2 mm (8 in) height, by 101.6 mm (4 in) diameter. Using the resultant volume and the calculated density, the mass of material required for each specimen was found. This amount was weighed out, and placed in a stainless steel U4 tube. A 4-inch ram was placed in the tube, and the material compacted to the required volume in a Dennison 100-ton compression machine.

Both tip and underground materials were compacted to the same density, since the performance of the material under tip conditions was under investigation.

The sample produced was measured accurately with a vernier caliper, to ensure uniformity, and prepared in the normal way, with filter-paper drains and rubber sheaths, for triaxial compression testing.

The tests performed were triaxial, consolidated-drained tests, necessitating at least 24 hours of consolidation, and the identical rate of shear to that used in the direct shear-box tests.



(III.2. b) VOLUME CHANGE MEASUREMENT During consolidation, volume change varied in different materials, but a general value of over 100 ml loss was recorded (c. 6.5%). This is a higher value than usual, and this is due to the laboratory compaction of the specimens with an attendant increase in the roughness of the specimen's surface over that encountered in a driven tube-sample. The volume changes encountered rendered normal measuring apparatus inadequate, and so a 250 ml burette was adapted in a U-tube arrangement. The lower limb of the U-tube was rubber, allowing the burette water-level to be equalized with the water-level in the other arm, ensuring a direct measurement of volume change.

(III.3) 12-INCH SHEAR-BOX RESULTS

The results determined during direct shear tests were used in the calculation of peak and residual shear strength parameters. Tests were carried out on tip and underground materials, showing the relationship between the tip shear strength characteristics, and those of the underground measures. Furthermore, a relationship between mineralogy and shear strength was observed.

Difficulties were encountered during interpretation of the results, especially those concerned with residual shear strength parameters. However, standardization of technique - both practical and assessive - allows comparison to be made between materials tested.

(III.3. a) PRESENTATION OF SHEAR-BOX RESULTS The results gained from multiple-reversal direct shear tests were reduced using a computer program. This program processed the raw data, ultimately plotting the results for a given normal (or vertical) stress as a normalized shear stress/vertical stress versus displacement graph (Appendix A).

The continuous monitoring during the test produced by the chart recorder (Chap. III.1. e) indicated the form of the graph to be produced by the computer. The points shown on the computer graphs were not taken from the pen recorder, but were manual readings taken during the test. The purpose of the pen recorder was to illustrate any short-term effects during shear which may be overlooked through intermittent manual

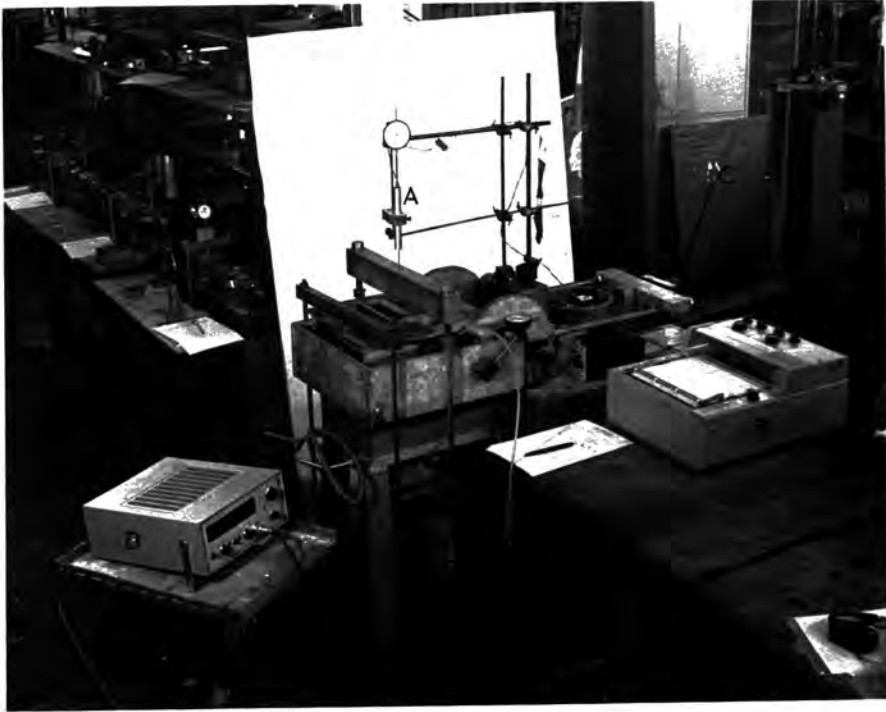


Plate III. 4. 12-inch direct shear-box equipment; showing vertical movement L.V.D. T. (A), pen recorder (B), reverse-shearing movement restraining bracket for the upper box (C) and the pore-pressure monitoring digital voltmeter (D).

reading. A phenomenon found by this method was a small peak in shear strength at the start of runs nearing residual (Chap. III. 3. c).

The chief purpose of the computer program was to produce a manageable representation of the results of the tests carried out, though it was also useful in giving a listing of values of strain and shear strength parameters for the tests.

### (III. 3. b) ALLOWANCE FOR AREA REDUCTION IN DIRECT SHEAR TESTS

During direct shear tests, the relative movement of the box halves produces a reduction in the area of the sample, which has a straight-line relationship with displacement (change in area = displacement x width of shear-box). Hence the vertical stress and shear stress must be recalculated from the shear-box readings and the appropriate value of displacement.

However, the vertical stress and shear stress are recalculated using the same factor produced from the change in area, therefore the value of (shear stress)/(vertical stress) is not affected by change in area, since the factors above and below the line cancel out. This was one of the considerations which led to the adoption of (shear stress)/(vertical stress) as the y-axis of the computer-produced stress-displacement graphs. The other consideration was that the ratio very rarely exceeds a value of 1.0, so that the axis construction instructions to the computer did not vary, and all the graphs are immediately comparable.

In producing composite shear strength graphs, plotting shear stress against vertical stress (Figs. III. 12-14), reduction in area has been allowed for in recalculation of shear and vertical stress.

(III. 3. c) RESIDUAL SHEAR STRENGTH DETERMINATION Difficulties in assigning a value to residual shear strength are apparent from the form of the graphs produced from experimental results (Fig. III. 15 and Appendix A). The curve which theoretically can be designated as the locus of failure may be drawn in such a manner that it coincides with the final point on the individual shear strength/displacement plots, and is concurrent with their later portions (Fig. III. 15).

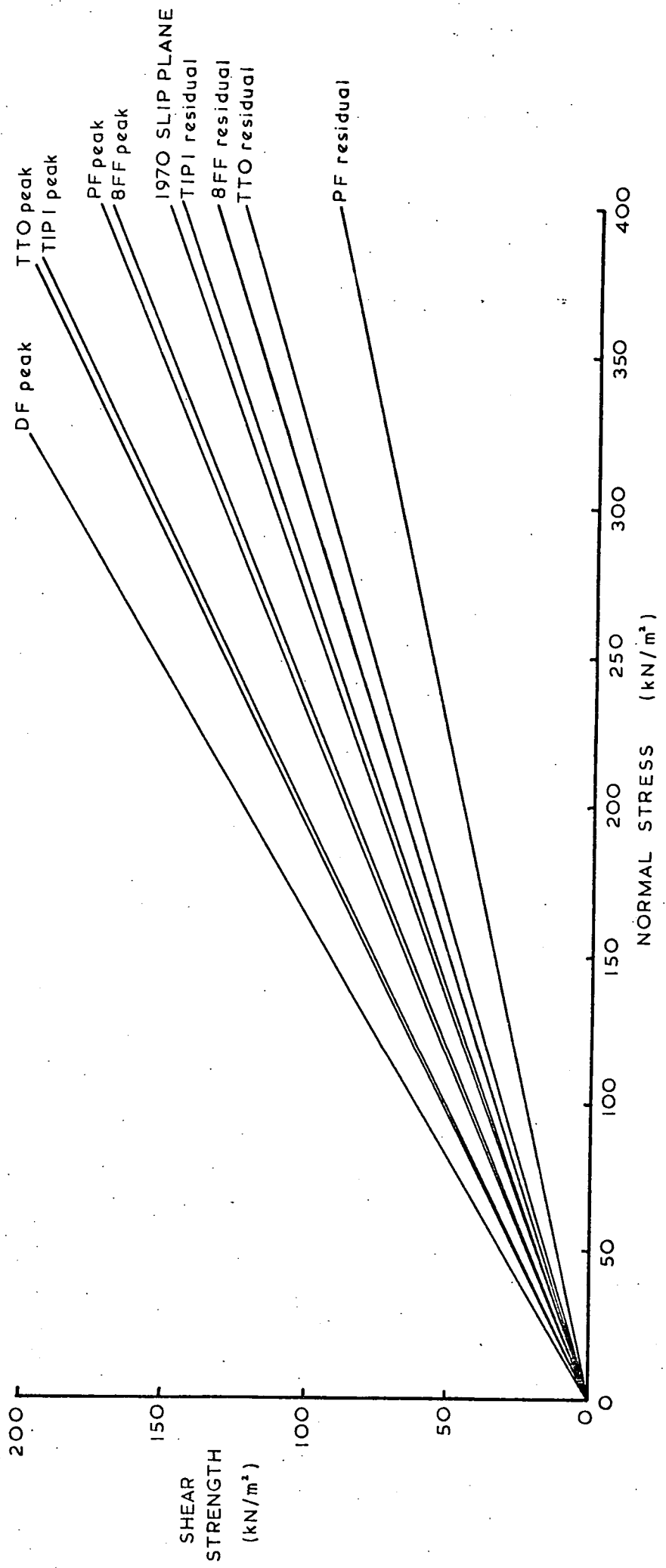


Fig. III. 12. Composite shear strength diagram for underground and spoil heap samples tested. The angles plotted are  $\phi'_e$  and  $\phi'_{er}$  (Appendix B).

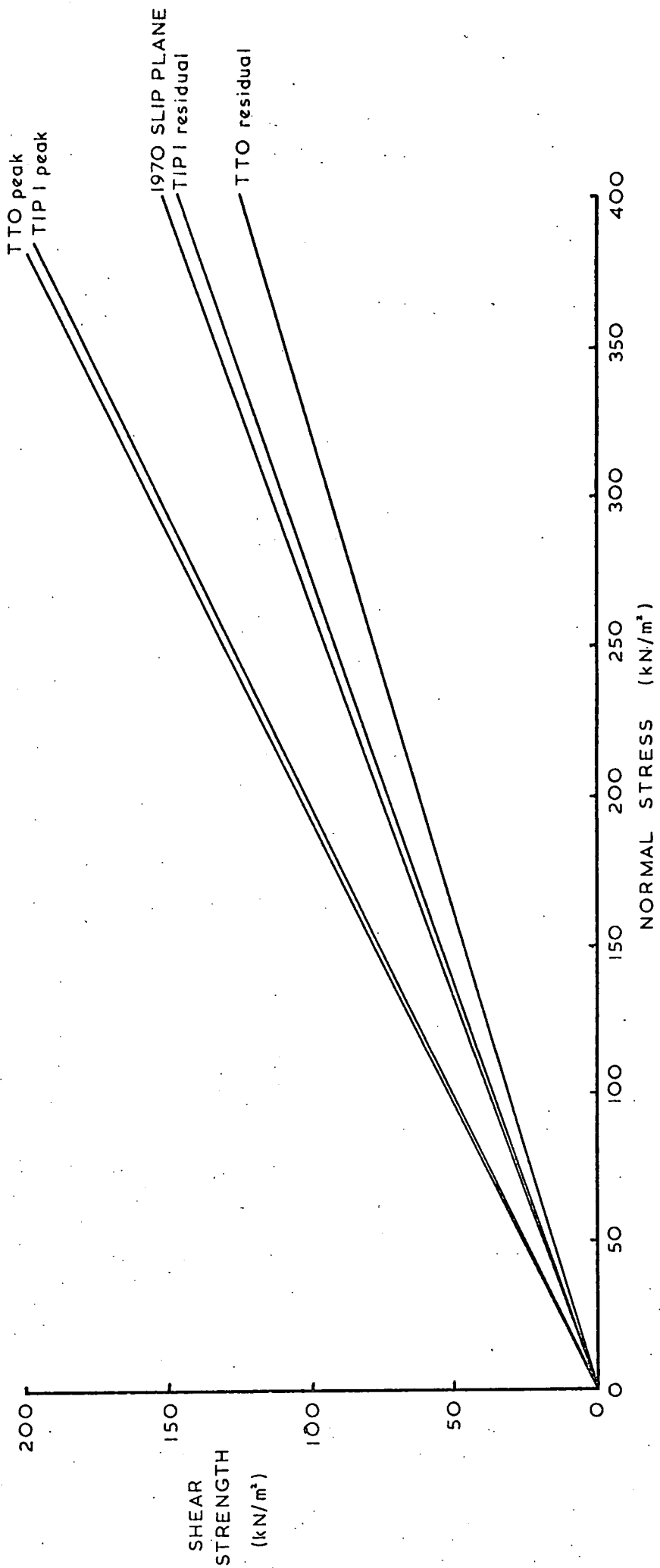


Fig. III. 13. Shear strength diagram for the spoil heap samples tested. The angles plotted are  $\phi'_e$  and  $\phi'_{er}$  (Appendix B).

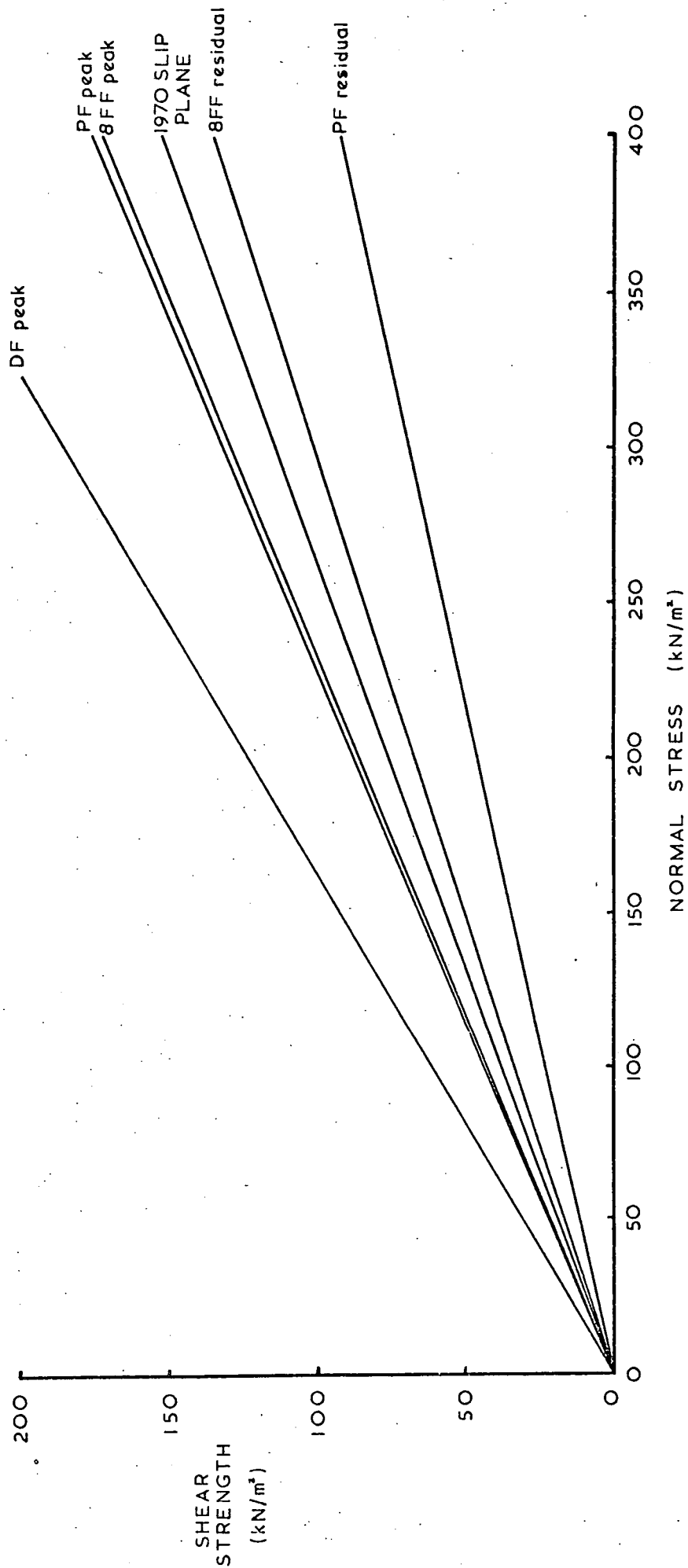


Fig. III. 14. Shear strength diagram for the underground samples tested and the 1970 Slip Plane. The angles plotted are  $\phi'_e$  and  $\phi'_{er}$  (Appendix B).

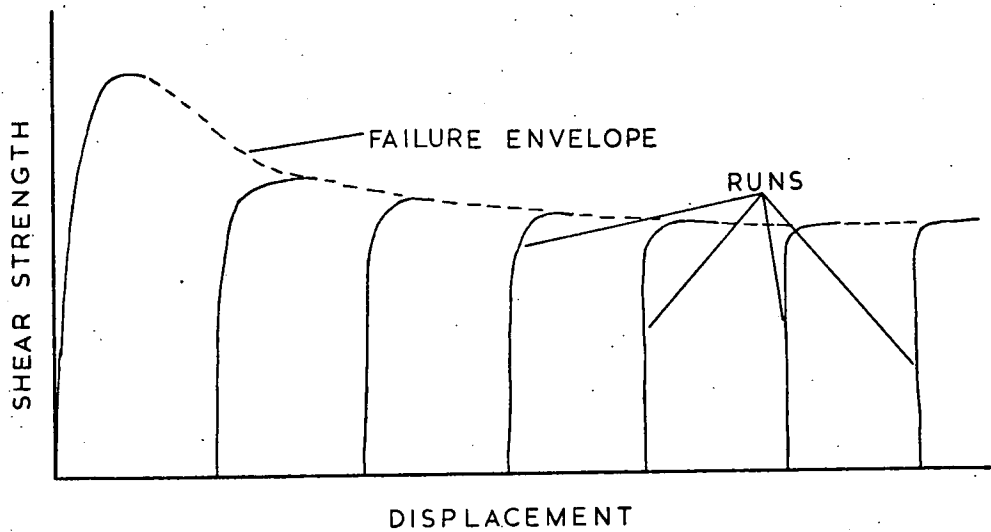


Fig. III. 15(a). Ideal residual shear strength/displacement curves.

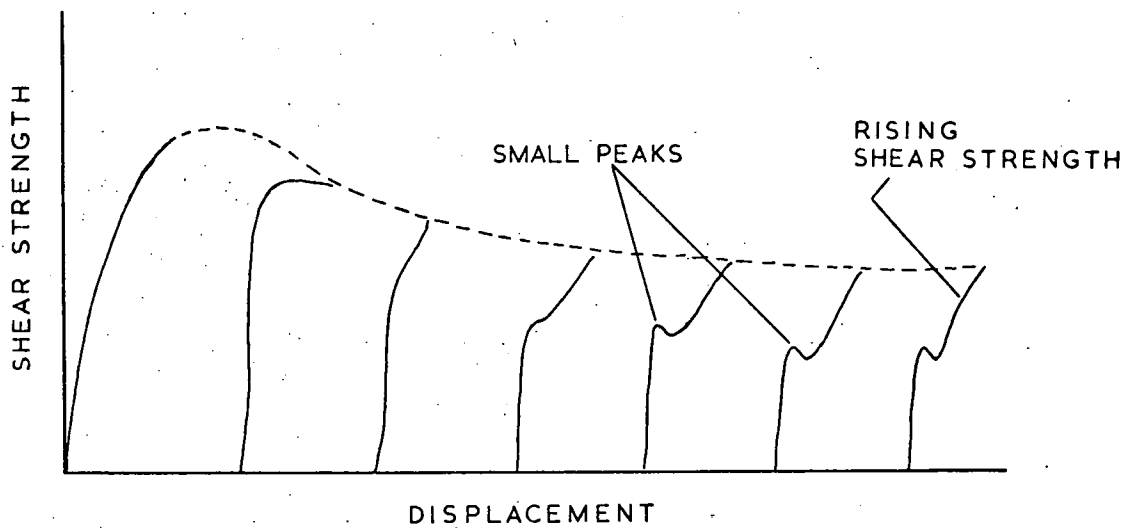


Fig. III. 15(b). Actual family of curves produced experimentally.

Fig. III. 15. Shear stress/displacement curves.

Here the values of the residual shear strength parameters are indisputable. However, the individual shear graphs' strength/displacement curves produced by experiment using the 12-inch direct shear-box show two main features of diversion which must be considered. These are : (a) a small peak at the start of later runs (those nearing residual shear strength); and, (b) a rise in shear strength towards the end of such runs (Fig. III. 15(b)). These are discussed below.

(a) Small Peaks at start of Shear The small peaks at the start of individual shear tests (as shown by samples PF 1 and PF 3 in Appendix A) have been interpreted by other workers as orientation effects (Agarwal, 1968; Bishop et al., 1971), who used 60-mm x 60-mm shear-boxes. This was verified by a set of tests on sample PF 1.

The sample was sheared normally, until the small peak was passed and shear stress had fallen again (Fig. III. 16). The machine was then reversed until the stress dial reading was zero, without displacement of the sample. The machine was then run forward until the same shear stress was reached as that recorded before reversal, but no peak was recorded. This ruled out the possibility that the peak was produced by internal friction of the shear-box. The shear test was continued to the limit of travel and then reversed. Forward travel was then initiated again at the lowest rate of strain possible (1.02 mm/hour). The peak then reappeared, showing that pore pressure is not involved in its production, so long as the rate of shear is below that calculated as in Chapter III. 1. d.

Hence the peak is produced by an effect within the material being sheared, and reorientation of particles on the shear plane after reversal is most likely.

In order to check this theory the sample was sheared in the forward direction to the end of the travel, and the small peak was produced. Prior to reversal the vertical load was removed, and the two halves of the box separated, so that the sample halves were not in contact. Ball bearings were then inserted between the metal flanges on the shear-box halves, and the machine was reversed to the limit of displacement.



The ball bearings were then removed and the sample halves brought together. The normal load was reapplied and the sample allowed to reconsolidate.

On forward travel, no peak was produced by the sample (Fig. III. 16).

These experiments demonstrated that the peak is a reorientation effect due to material on the shear plane; the movement of particles being produced by the multiple changes in direction of travel.

It could be suggested that the true residual shear strength of a sample will be the lowest point on the graph following the small orientation peak. However, it has already been shown that this point is more likely to be symptomatic of the behaviour of larger particles within and close to the shear plane (sensu stricto). It is merely the point where orientation effects are decreasing and are therefore masked by the main shear characteristics of the specimen. During the tests on the specimen PF 1, to determine the origin of the orientation peak, it was noted that the curve produced by shearing the "non-reversed" specimen could be superimposed on the "reversed" specimen curve after the peak. This indicates that the "unreversed" curve up to the small peak is the real stress/displacement curve for the specimen. Therefore the lowest point after the peak is no more unique than any other point on the real stress/displacement curve.

Not all the samples tested exhibit the orientation peak. Attempts to correlate its occurrence with particle size, mineralogy and vertical stress are not conclusive, though it does appear to be most pronounced at low vertical loads in specimens rich in illite plus kaolinite (PF 1 and PF 3), and with larger average particle size (Table III. 1).

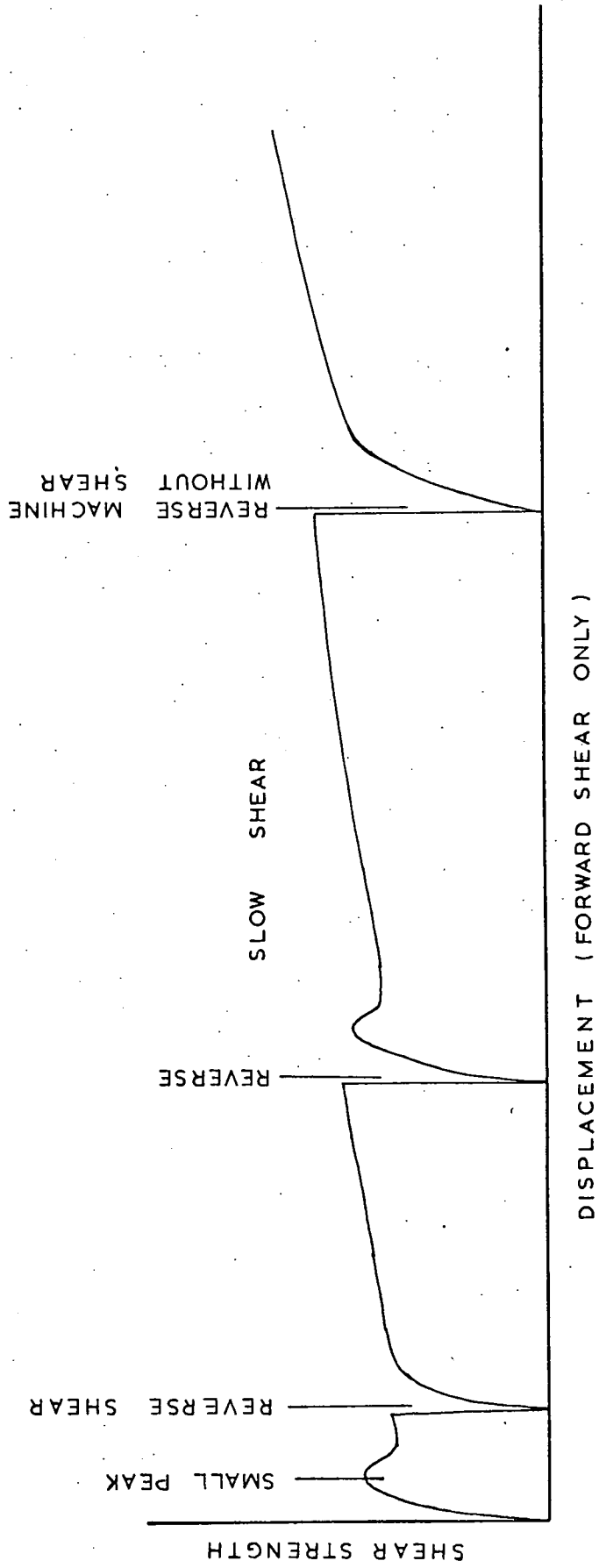


Fig. III.16. Shear stress/displacement curve to show origin of the small peak at the start of shearing runs approaching residual shear strength.

PEAKS OCCUR				PEAKS DO NOT OCCUR			
Sample	Vert.	Stress	% Clay	Sample	Vert.	Stress	% Clay
PF1	80	kN/m <sup>2</sup>	91.9	PF2	214	kN/m <sup>2</sup>	91.9
PF3	134	"	91.9	TTO4	134	"	66.5
TTO3	214	"	66.5	TTO2	80	"	66.5
				TTC	80;134;214	"	70.9
				TIP1	80;134;214	"	73.0

TABLE III. 1. CORRELATION OF ORIENTATION PEAK OCCURRENCE WITH PHYSICAL AND CHEMICAL DATA

As can be seen from Table III. 1, the general rules for orientation peak occurrence are broken by the high vertical stress of TTO3 with peak occurrence, and low (illite + kaolinite) content of TTO3. However, TTO3 does have a slightly larger average particle size than the others (Fig. III. 22).

(b) Rising Shear Strength at end of Shear This effect has also been demonstrated in 60-mm x 60-mm direct shear tests (Agarwal, 1968; Bishop et al., 1971). The rise could again be due to material effects which necessarily must be more pronounced in the later stages of shearing, especially as the rise in shear strength is of non-linear form with respect to displacement (Fig. III. 15(b)).

The major shear plane produced in the samples is very irregular (Plate III. 5 and Plate III. 6), the contours being dictated by local conditions within the sample. The general pattern is of ridges and grooves up to 20 mm in height, which run parallel to the direction of shear (induced slickensides). On shearing, these undulations are truncated by the horizontal edges of the shear-box (Fig. III. 17) which cut into the sample beyond the shear plane generated across these undulations. Having cut into the body of the sample, the shear stress increases as larger,



Plate III. 5. Lower half of sample TTO3 after being sheared in a 12-inch shear-box with multiple reversal.

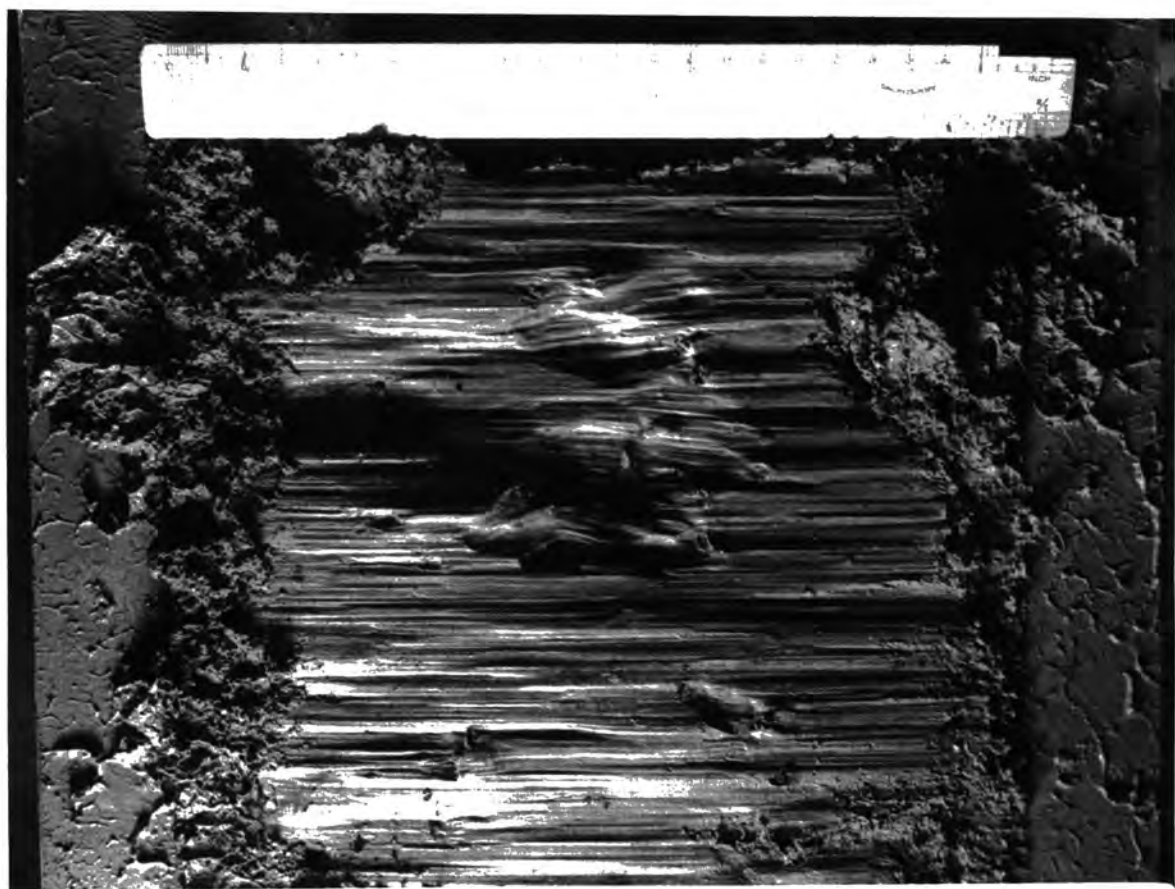


Plate III. 6. Upper half of sample TTO3 after being sheared in a 12-inch shear-box with multiple reversal.

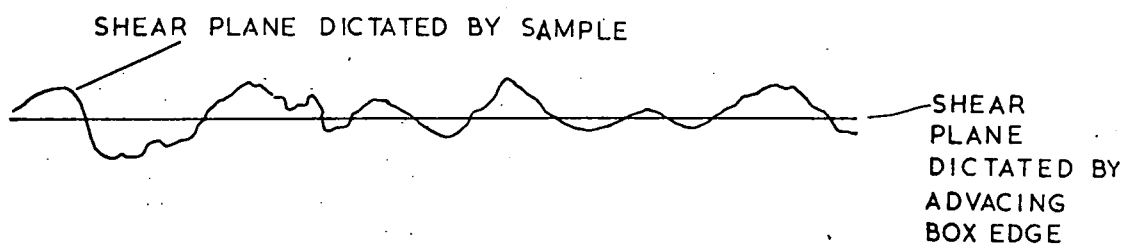


Fig. III. 17. Shear plane undulations cut through by the advancing horizontal edge of the shear-box. Maximum height of undulation 20 mm.

unsheared particles are disturbed away from the defined shear plane. As the test progresses, the area affected by the cutting of the undulations increases, giving an increase in the apparent shear stress.

The residual shear strength values plotted for calculation of  $c'_f$  and  $\phi'_f$  were taken from the computer-drawn graphs of the test results (Appendix A). It was felt that the end of the individual D/E (stress ratio) v strain graph gave an inflated value of residual shear strength due to the truncation of the induced slickensides. An extension of the lower, concave downwards, portion of the D/E v strain graph would give a more accurate value of residual shear strength. Consequently, the point of maximum curvature above the point of inflexion on the D/E v strain graph was used in the calculation of residual shear strength parameters.

(III. 3. d) VOLUME CHANGE During tests in the 12-inch direct shear-box volume change was monitored by a pen recorder attached to an L. V. D. T. which measured vertical displacement of the top platen of the shear-box (Plate III. 4).

This showed the consolidation curve for the sample prepared for shear tests, and the volume changes resulting from shearing. Samples were generally consolidated for 3 to 4 days. On commencement of shearing the volume reduced dramatically during the first run. This is due to reorientation of particles in response to the shear stresses which allowed closer packing of the normally consolidated material. On later runs where residual shear strength was approached, the reduction in volume was not as marked, and from a point roughly half-way through the run the volume increased again (dilation) to virtually regain its original value at the start of that run.

Generally, the total reduction in volume was about 7% of the original volume, although this is not strictly accurate because constant loss of sample during shearing and through drain holes in the lower platen contributed to the volume change. However, the general trends of initial constant reduction in volume and a later cycling in volume are noteworthy.

(III. 3. e) CHOICE OF SAMPLES TESTED Due to the length of time required to reach residual shear strength conditions in the 12-inch shear-box, and because of the on-going modifications listed in Chapter III. 1, it was not possible to test completely all the bulk samples collected at Littleton Colliery. However, by careful selection of the materials tested on the basis of mineralogy, it was possible to gain a representation of the shear strength characteristics of the spoil heap, their derivations and consequences.

It was obvious that a complete set of data on the spoil heap shear strength was needed, and so two samples (TTO and TIP 1) were tested to their residual shear strength.

Of the underground material, two samples (8FF and PF) were tested to residual; one sample (DF) had only peak shear strength determined.

The major criterion used as a guide to representativeness was mineralogy. Kenney (1967) and Taylor (1974) have observed a correlation between mineralogy and shear strength; obviously factors such as particle size will also affect shear strength, but these factors in turn depend upon mineralogy. The mineralogical compositions of the samples tested are shown graphically on Fig. II. 2. The underground samples tested (DF and PF) represented the end-members of the spoil heap's parent-series, and a member plotting within the group of spoil heap samples (8FF). Thus the extreme and "average" conditions possible in the spoil heap were investigated.

(III. 4) COMPATIBILITY OF SHEAR-BOX  
AND TRIAXIAL TESTS

In an effort to shorten the length of time required for a set of tests on each sample, the 4-inch triaxial compression machine was used in conjunction with the 12-inch shear-box, as described in Chapter III. 1. f. The validity of this technique was tested by the comparison of results obtained using the 12-inch shear-box and 4-inch triaxial machine during investigation of a single-type material.

The samples used were from the Isabella Spoil Heap in Northumberland. These gave a high value of the internal friction angle  $\phi$  ( $37^{\circ}$ - $38^{\circ}$ ); thus any deviation between the two types of test would be



readily discernible. The material from Littleton Colliery was regarded as having too low a  $\phi'$  value for useful comparison.

Figure III. 18 shows the results obtained from a set of 12-inch direct shear-box tests on the Isabella Heap material. The peak angle of friction ( $\phi'$ ) is  $37^\circ$ ; cohesion is  $10.5 \text{ kN/m}^2$ . Figure III. 19 shows the results obtained from drained triaxial tests on the same type of material. Here  $\phi'$  is  $38^\circ$ ; cohesion is  $16.5 \text{ kN/m}^2$ . The maximum normal pressure during the shear-box tests was  $213.7 \text{ kN/m}^2$ , and the maximum cell pressure during the triaxial tests was  $70 \text{ kN/m}^2$ . This shows compatibility at low confining pressures.

	12-inch Shear-Box Tests		4-inch Triaxial Tests
Confining Pressure ( $\text{kN/m}^2$ )	$< 214.7 (\sigma'_h)$	$< 70 (\sigma'_3)$	$< 500 (\sigma'_3)$
Peak Angle of Friction ( $\phi'$ )	$37^\circ$	$38^\circ$	$30.5^\circ$
Cohesion ( $\text{kN/m}^2$ )	10.5	16.5	44.2

TABLE III. 2. COMPARISON OF SHEAR-BOX AND TRIAXIAL RESULTS

On testing in the triaxial compression machine at higher confining pressures ( $< 500 \text{ kN/m}^2$ ), a fall-off in  $\phi'$  was observed (Fig. III. 20; Table III. 2). This phenomenon has been observed by other workers (National Coal Board, 1972; Chandler, 1969), and is ascribed to the breakdown of particle junctions (comminution), which increases in response to increased confining pressure. As a result of work on colliery spoil, McKechnie Thompson and Rodin (1972) conclude that the cohesion intercept ( $c'$ ) is zero and that in some cases the failure envelope may be curved (National Coal Board, 1972). Description of the shear strength characteristics of materials which produce curved failure envelopes cannot be adequately described in terms of  $c'$  and  $\phi'$  since  $\phi'$  varies at different stress ranges. Consequently, an arbitrary equivalent angle of shearing resistance,  $\phi'_e$  was introduced. The angle  $\phi'_e$  is taken as the  $\phi'$  angle drawn to the origin on a failure envelope graph from the point on the failure envelope at which the effective normal stress is  $350 \text{ kN/m}^2$ .

$\phi = 37^\circ$   
 $c = 10.5 \text{ kN/m}^2$

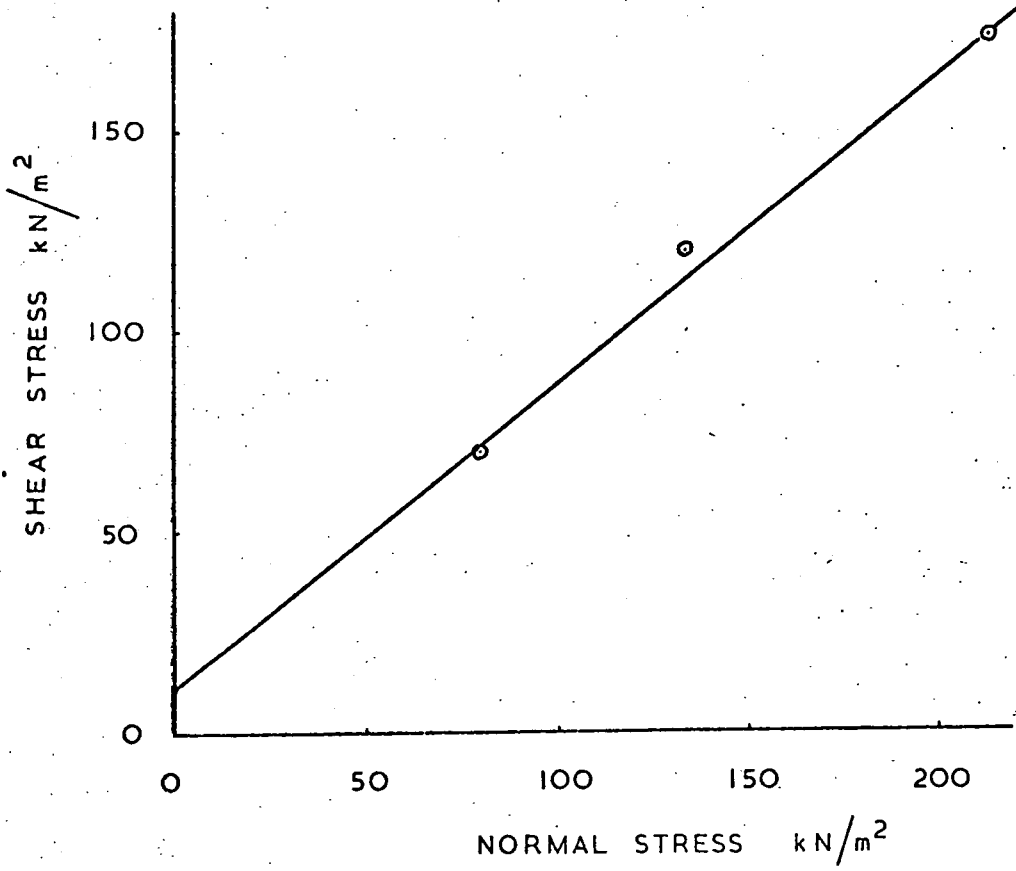


Fig III. 18. Isabella Heap material, 12-inch direct shear-box results.

$\phi \cdot 38^\circ$   
 $c \cdot 16.5 \text{ kN/m}^2$

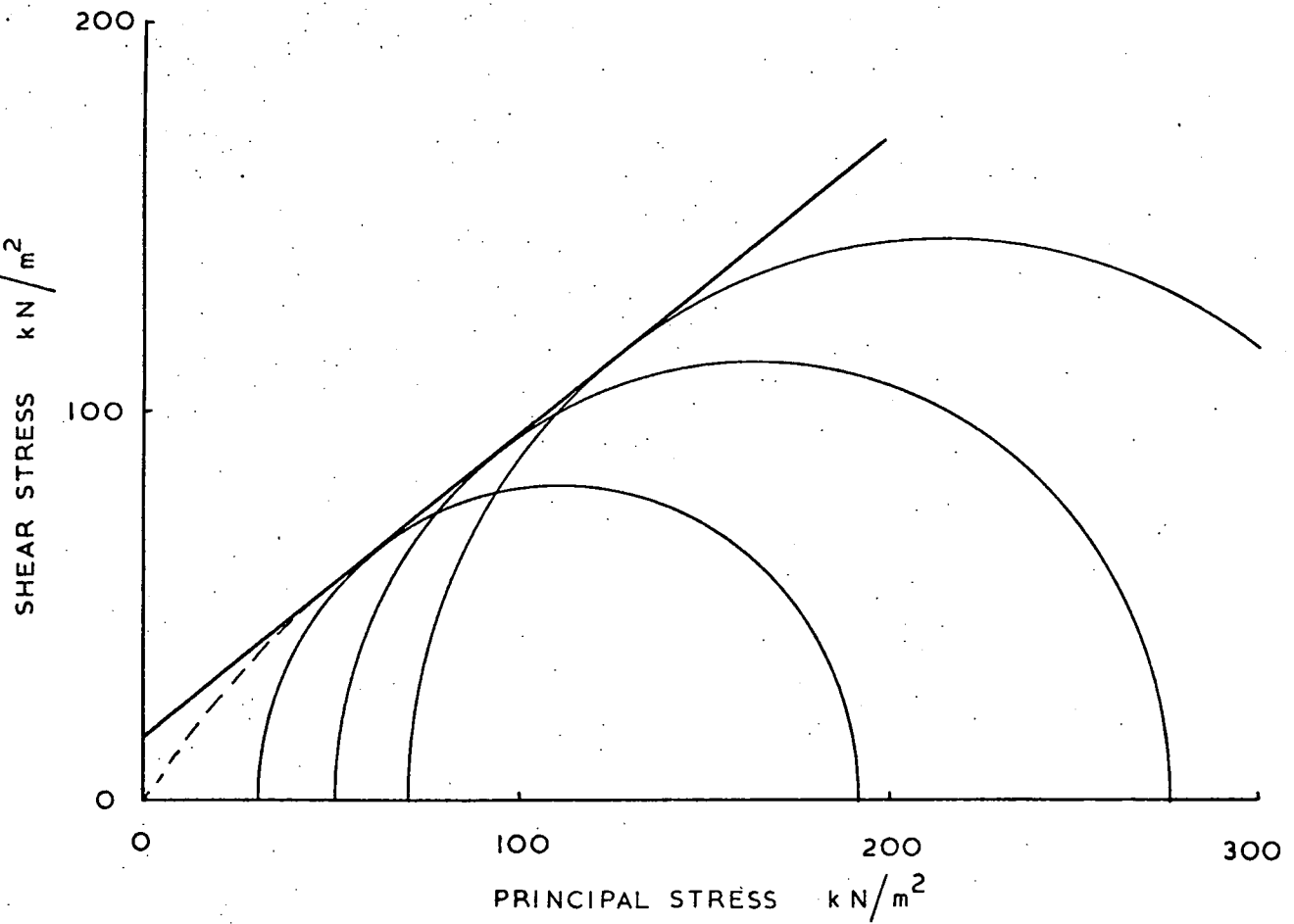


Fig. III. 19. Isabella Heap material 4-inch drained triaxial compression tests results.

$\phi = 30.5^\circ$   
 $c = 44.2 \text{ kN/m}^2$

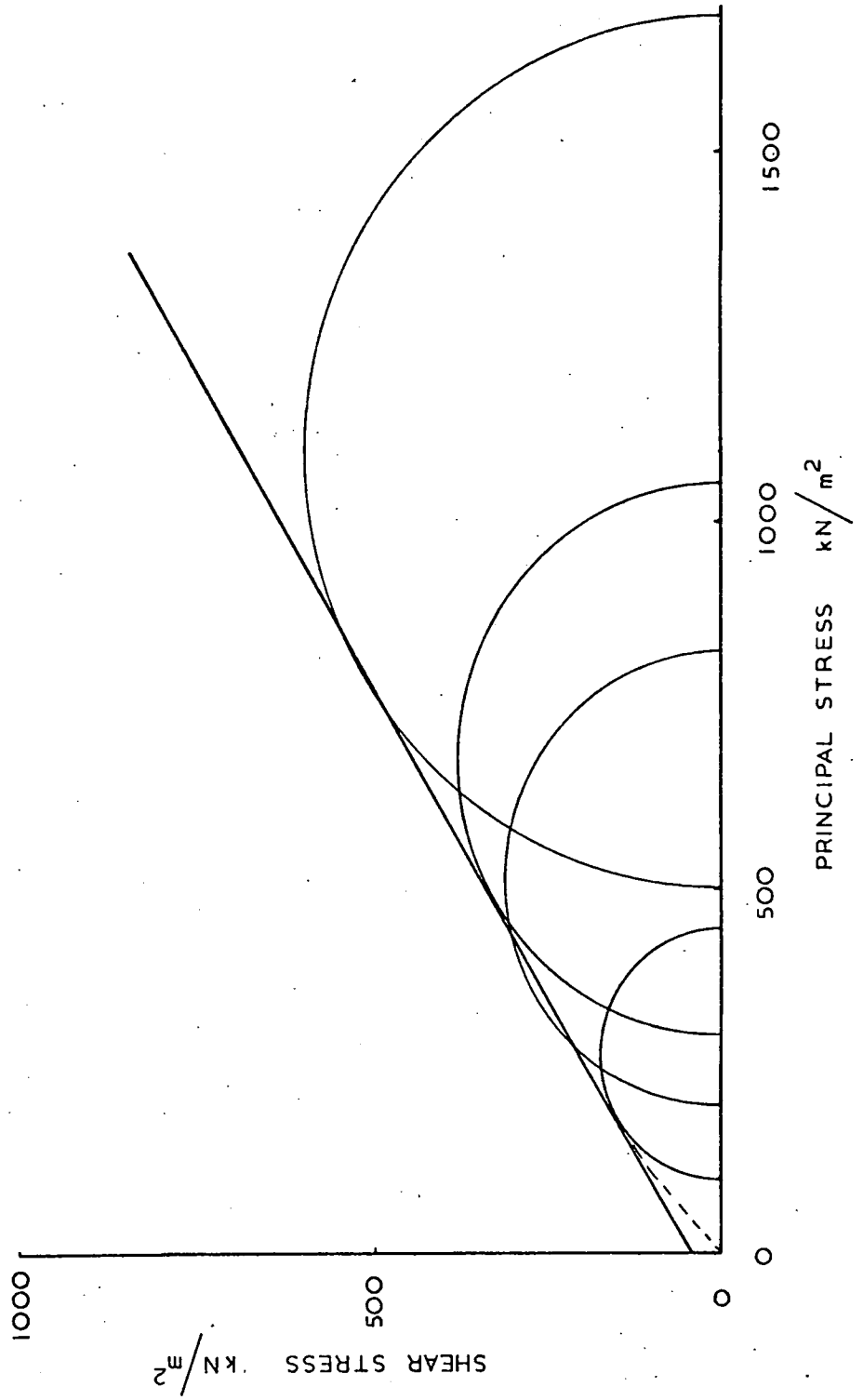


Fig. III.20. Isabella Heap material high pressure 4-inch triaxial compression tests results.

The angle  $\phi'_e$  is used to compare the results of shear strength tests on the Littleton materials. A full list of the shear strength results is contained in Appendix B.

In order to plot the triaxial and shear-box results on the same graphs (Figs. III. 12-14) it was first necessary to plot the triaxial results separately, using the  $K_f$ -line construction (Mohr circle "top point") (Fig. III. 21). A "least squares" regression line can then be fitted to the top points, giving the modified failure envelope. The parameters  $c'$  and  $\phi'$  are then produced from the slope of the regression line ( $\alpha'$ ) and the intercept on the y-axis ( $a'$ ) (Craig, 1974):

$$\phi' = \sin^{-1} (\tan \alpha')$$

$$c' = \frac{a'}{\cos \phi'}$$

The values of  $c'$  and  $\phi'$  were then corrected to give  $\phi'_e$  by linear production of the regression line (plotted on a shear strength v normal stress graph) to its intercept with the normal stress = 350 kN/m<sup>2</sup> line. The slope of the line drawn from the origin to the intercept produced is  $\tan \phi'_e$ . A parabolic construction would have been more correct in view of the curved envelope proposed by McKechnie Thompson and Rodin (1972), but the spread of points produced during testing often made the resulting parabola unreasonable, even impossible.

The values of  $\phi'_e$  produced for the triaxial tests allowed the results to be plotted directly with the shear-box results onto a shear strength v normal stress graph, as a fan of lines.

(III. 5)

### SHEAR STRENGTH RESULTS

The results from the 12-inch shear-box and 4-inch triaxial tests were examined together to provide a complete representation of peak and residual shear strength characteristics. The most useful way to consider these results is to observe the relationship of the underground samples to those from the spoil heap. A complete table of the shear strength results is contained in Appendix B.

(III. 5. a) RESULTS FROM UNDERGROUND MEASURES Having decided to

choose the samples to be tested on the basis of Kenney's (1967) investigation, it was necessary to determine whether his findings applied to the Littleton Colliery material.

Figure III. 14 shows the results obtained from the underground material. From this it is obvious that the peak shear strength values for the Deep Floor show the highest value of  $\phi'_e$ . The mineralogy of the Deep Floor shows 51.4% quartz (Table II.2) showing that high shear strength is reflected by a high quartz percentage in these bulk samples. The bulk samples of the underground material are, of course, a much better indication of that material's performance in normally consolidated spoil heap conditions than a block sample would be.

The lowest shear strengths on Fig. III. 14 are shown by the Park Floor residuals. Table II.2 shows that the Park Floor contains only 3.0% quartz, showing that low shear strength reflects a low concentration of quartz.

The Eight Feet Floor sample lies between these extremes on Fig. III. 14, and its quartz concentration is 18.5% (Table II.2), which again shows a relationship between shear strength and quartz content.

The values of  $\phi'_e$  and  $\phi'_{er}$  found for the underground materials are shown in Table III.3. The residual value for the Deep Floor was not determined, but the peak shear strength shown by it is important in the correlation of shear strength and mineralogy.

SAMPLE	$\phi'_e$	$\phi'_{er}$	% QUARTZ
Park Floor	23.8°	13.0°	3.0
Eight Feet Floor	23.3°	18.7°	18.5
Deep Floor	31.7°	-	51.4

TABLE III.3. COMPARISON OF SHEAR STRENGTH CHARACTERISTICS AND MINERALOGY FOR UNDERGROUND MATERIAL

(III.5.b) RESULTS FROM SPOIL HEAP MATERIAL The results obtained from

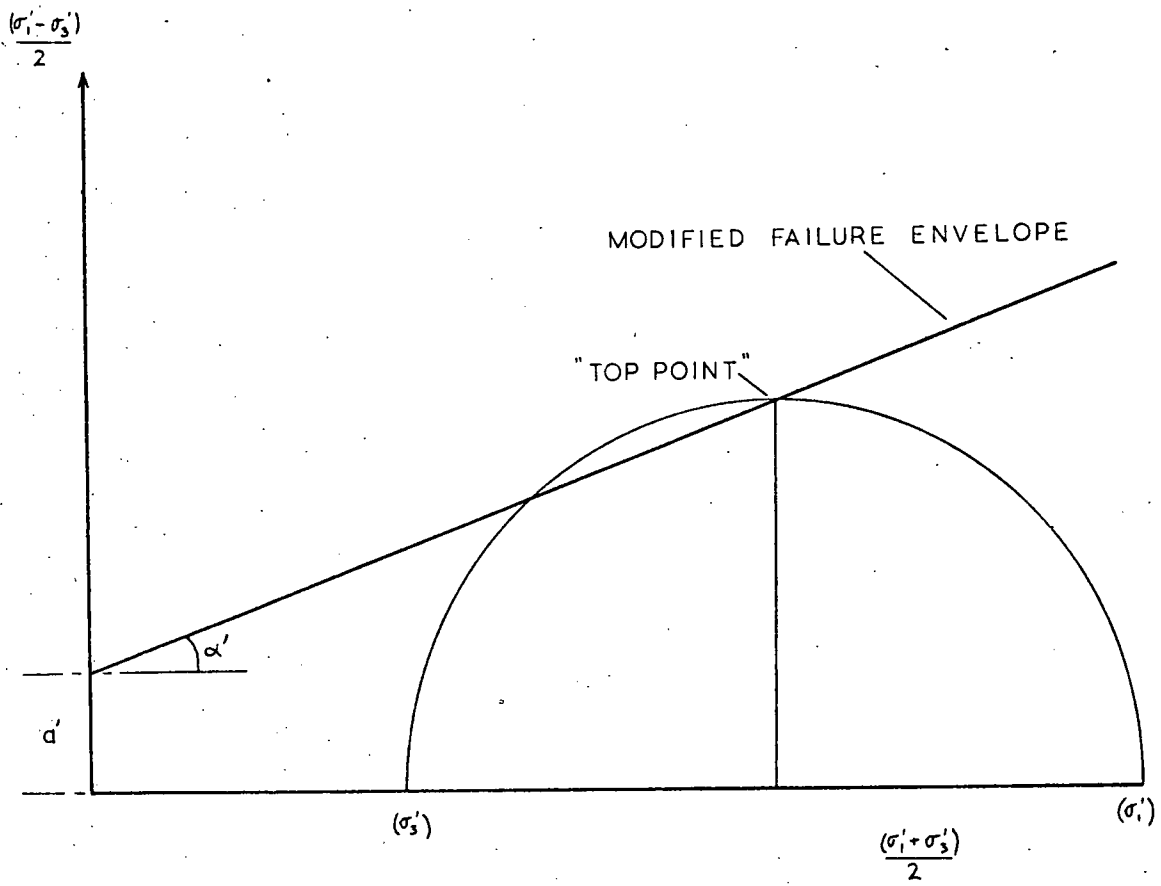


Fig. III. 21.

Mohr circle "top point" construction  
(after Craig, 1974, p. 85).

tests on the spoil heap material are shown in Fig. III. 13. Two samples were tested in the 12-inch shear-box and triaxial compression machine to yield complete data on peak and residual shear strengths. The samples tested were Tip Top Outer and Tip 1. A specimen from the shear plane of the 1970 slip at Littleton was tested in a 60-mm x 60-mm shear-box (Taylor and Hardy, 1971) and the results of this test are included on the diagram for comparison.

The mineralogy of the specimens shows no great dissimilarities; Tip Top Outer contains 29.4% quartz, Tip 1 contains 31.6% quartz, and the 1970 slip plane sample contained 20.2% quartz.

On the basis of Kenney's work (1967) this leads one to expect a similarity in shear strength characteristics. Table III. 4 and Fig. III. 13 show that there is a similarity in shear strength properties.

SAMPLE	$\phi'_e$	$\phi'_{er}$	% QUARTZ
Tip Top Outer	27.5°	20.0°	29.4
Tip 1	27.2°	17.5°	31.6
1970 Slip Plane*	-	20.9°	20.2

\* Taylor and Hardy, 1971

TABLE III. 4. COMPARISON OF SHEAR STRENGTH CHARACTERISTICS AND MINERALOGY FOR SPOIL HEAP MATERIALS

(III. 6) COMPARISON OF UNDERGROUND AND SPOIL HEAP MATERIALS

Figure III. 12 is a composite diagram showing the shear strength characteristics of all the samples tested. From this diagram one can observe the characteristics of the spoil heap materials compared with those of the underground samples.

The most important point is that the spoil heap discard lies between the extremes of the underground measures in terms of shear strength. This is as expected from mineralogical analyses (Table II. 2) and the postulated correlation of mineralogy and shear strength. The maximum



shear strength is given by the Deep Floor (Table III.5), the minimum is shown by the Park Floor. The spoil heap lies between these, and the slip plane of the 1970 failure may be taken as characteristic, by virtue of its natural origin.

SAMPLE	$\phi'_{e}$	$\phi'_{er}$
Park Floor		13.0°
1970 Slip Plane		20.9°
Deep Floor	31.7°	

TABLE III.5. COMPARISON OF SHEAR STRENGTH CHARACTERISTICS OF SPOIL HEAP AND UNDERGROUND MATERIALS

The other spoil heap samples (Tip Top Outer and Tip 1) also lie between the limits set by the underground material. Tip Top Outer is closest to the upper limit of the Deep Floor; their peak strengths differ by 4.2° of  $\phi'_{e}$ . Tip 1 has a peak  $\phi'_{e}$  of 27.2°, which is 4.5° lower than the Deep Floor, the residual  $\phi'_{er}$  is 20°. The Tip Top Outer residual  $\phi'_{er}$  is 17.5°, which is 4.5° higher than that of the Park Floor. Therefore, the shear strengths of the spoil heap samples are bracketed by the underground samples. There is a spread of values for the spoil heap with reference to shear strength, especially residual, as there was with reference to mineralogy.

(III.6.a) CONCLUSIONS The shear strength tests carried out on samples from Littleton Colliery demonstrate two main points. These are: (1) that the spoil heap reflects the mixture of the underground materials and has an average shear strength which is equivalent to the "average" of the roofs and floors of former materials; and, (2) the shear strength of the materials tested was dependent upon mineralogy.

The relationship between the shear strength characteristics of the spoil heap and underground materials may appear obvious, but the effects of weathering, chemical and mechanical, might have been strong enough to reduce the strength of the spoil heap to below that of the weakest

underground contributor. From the shear strength analysis, then, it appears that weathering has not played a large part in reducing the strength of the spoil heap so as to constitute a failure mechanism.

The relationship between shear strength and mineralogy is also plain. Considering the material to be quartz/clay mixture (as plotted on Fig. II.2), it is seen that the spoil heap samples form a discrete group bracketed by the underground materials. In the same way, the shear strengths of the spoil heap materials are bracketed by those from underground samples (Fig. III.12). Taylor (1975) has shown that there are mineralogical controls on spoil heap physical and mechanical properties. He concludes that coal has a major effect on peak shear strength and fundamental properties since it acts as the principal diluent, being introduced during the extraction processes. No such trend can be discerned in the few samples tested from Littleton alone.

(III.7)

#### PARTICLE SIZE ANALYSIS

The spoil heap and underground materials were subjected to particle size distribution tests. All the samples were tested in a Coulter Counter (Coulter Electronics Ltd.) over a size range  $1.48\mu\text{m}$  to  $60\mu\text{m}$ . This gave comparative results for use in correlation with mineralogy and shear strength characteristics. The spoil heap material was also analysed by pipette and wet sieving methods to show the effects of large shear displacements on coarse particle size distributions. Because of the massive nature of the Deep Floor and Eight Feet Floor, pipette and wet sieving analyses were not carried out on underground material.

(III.7. a) COULTER COUNTER TECHNIQUE The material to be tested in the Coulter Counter should not be of larger size than the sampling orifice on the apparatus. Therefore, all the samples were passed through a  $53\mu\text{m}$  sieve before testing with a  $100\mu\text{m}$  orifice.

The samples were dispersed in Isoton saline solution, using Nonidet P42 as a wetting agent to aid ultrasonic disaggregation.

It should be noted that the results from the Coulter Counter were necessarily only comparative. The method was internally accurate,

but the interpretation of the readings before results are produced was rather subjective. Other methods (pipette analysis and hydrometer) were attempted, but the errors within these methods were considered too great and it is believed that the Coulter Counter provides a better comparative assessment of particle size distributions.

(III.7. b) COULTER COUNTER RESULTS The results from the tests are recorded on Fig. III.22 and Fig. III.23, for spoil heap and underground materials respectively.

From the results for the spoil heap material it is plain that the curves follow the same form, and are closely grouped. This indicates good sorting in the spoil heap, and probably reflects a fairly constant mineralogy.

The inter-relationship between mineralogy and fine fraction particle distribution is best seen in the curves for the underground material. It is apparent (Fig. III.23) that the Deep Floor deviates from the other group of samples. This is well reflected in the mineralogy of the samples, where the Deep Floor shows an abnormally high quartz content. Quartz is an equant habit massive mineral, and a high percentage will tend to move the particle size distribution curve towards the coarser sizes.

The group of curves for the spoil heap material lies between the main group for the underground material and the Deep Floor curve. This is a reflection of the composition of the spoil heap material. The Deep Floor must be present in a large proportion in the spoil heap to produce a deviation away from the trend of the other constituents. In fact, Phillips (personal communication) has indicated that the Deep Floor may constitute up to 50% of the spoil heap material.

Two samples from the shear-box tests were also analysed to investigate possible comminution effects during shearing. These were the Park Floor (PF) and Tip Top Outer (TTO). On removal of the sample after shearing, material was scraped off the shear plane. This was then analysed in the Coulter Counter against a bulk sample specimen (Fig. III.22, TTO shear plane; Fig. III.23, PF shear plane).

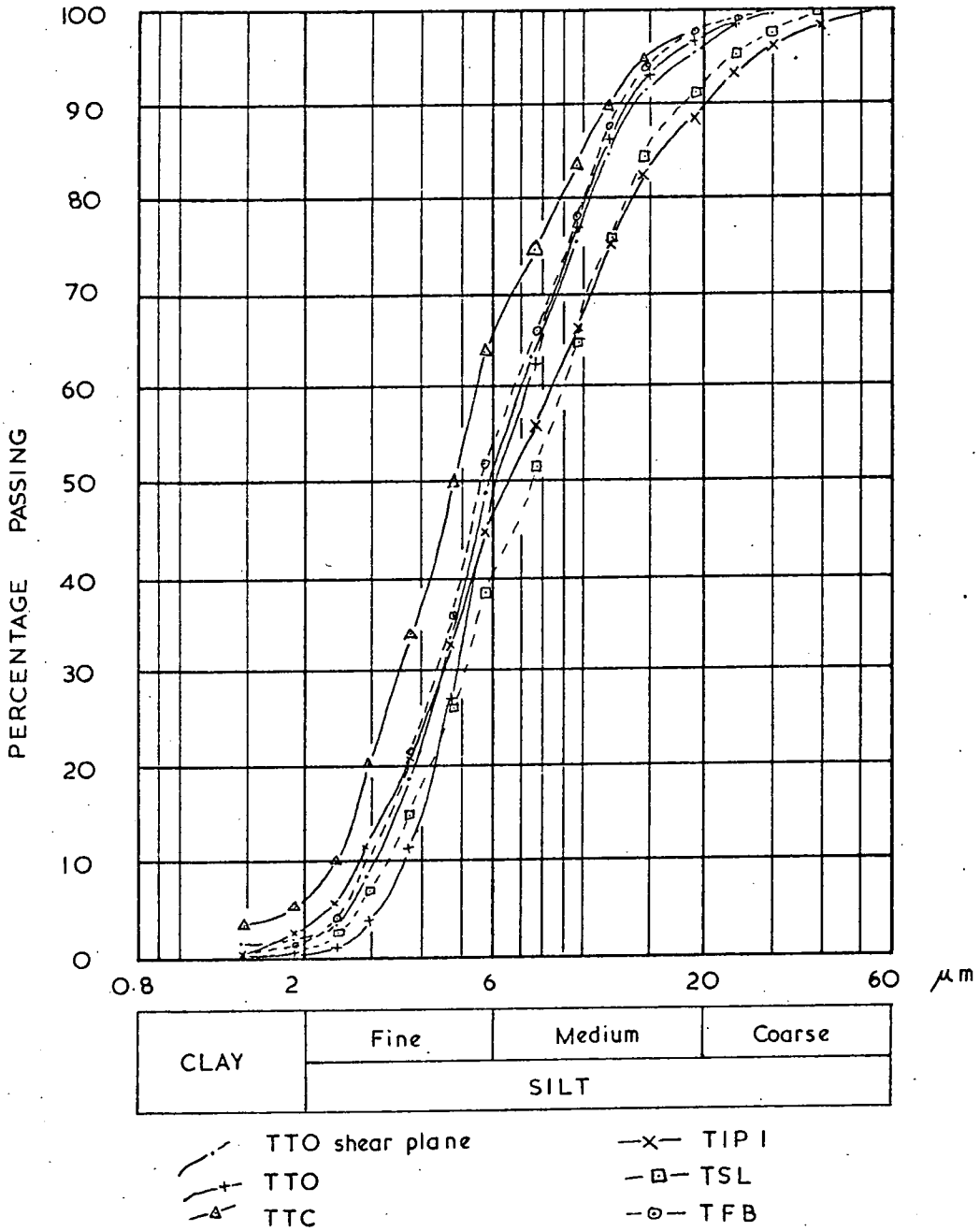


Fig. III.22. Coulter Counter particle size results for the spoil heap material.

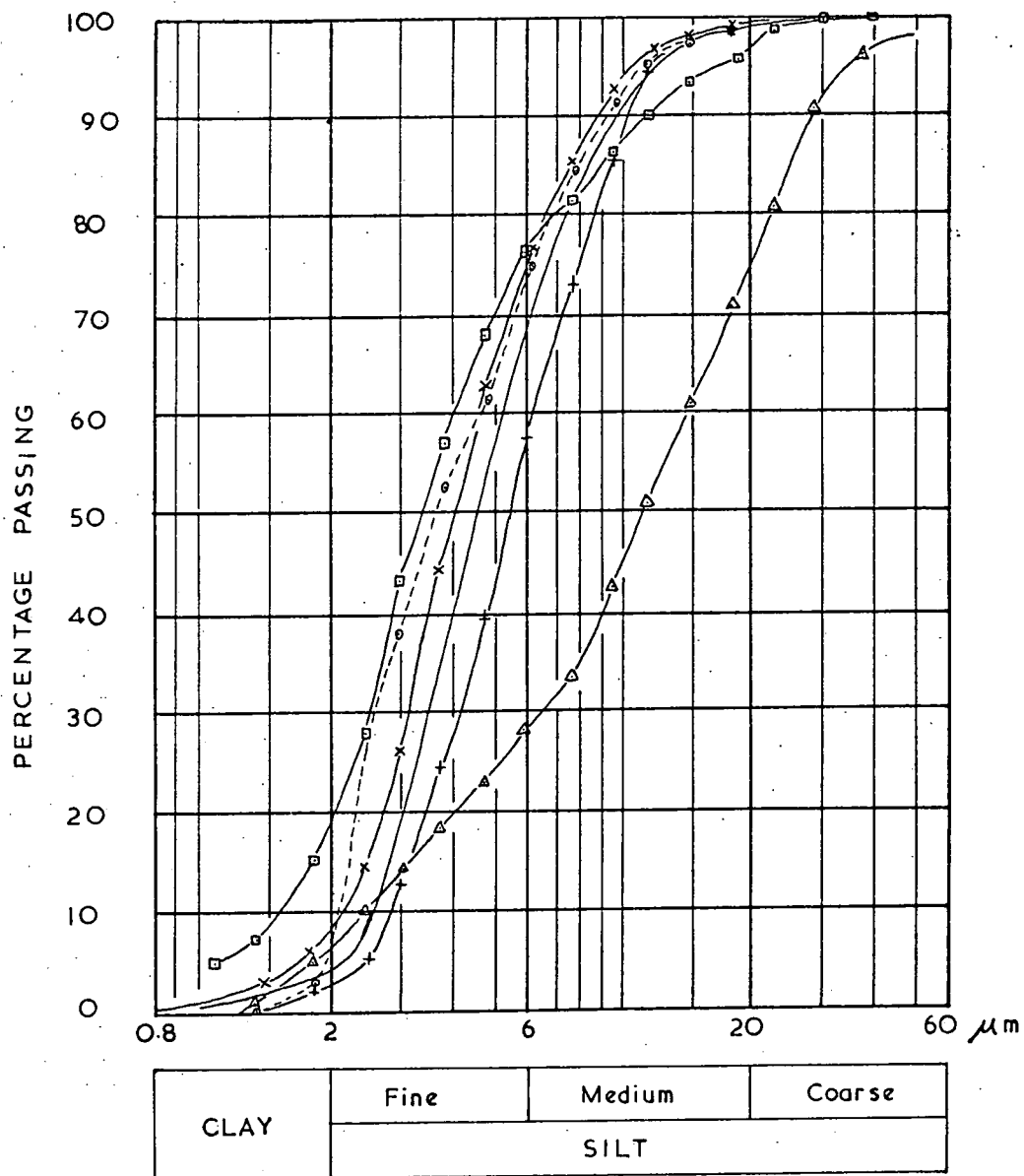


Fig. III. 23. Coulter Counter particle size results for the underground material.

In the Tip Top Outer specimens, little change in particle size was found (Fig. III.22). However, the Park Floor showed a distinct reduction in particle size (Fig. III.23). The difference in behaviour may be explained by the mineralogy of the specimens. The Park Floor has 79.0% illite with a high proportion of mixed layer clay; (Taylor and Spears, 1970), 12.9% kaolinite and 3.0% quartz, whilst the Tip Top Outer has 56.5% illite, 10.3% kaolinite and 29.4% quartz. During shearing over large displacements, the clay-rich materials are more likely to comminute than well slaked spoils containing a higher proportion of quartz. Therefore, materials with a higher quartz/clay ratio, such as the Tip Top Outer, will show a lower fall-off in particle size than those with a lower quartz/clay ratio, such as the Park Floor, which in any case has not been subject to slaking (desiccation and saturation) during its immediate history.

The behaviour of the Park Floor does lend credence to the theory that comminution of fine shear plane material is one of the phenomena leading to attainment of residual strength (Bishop et al., 1969; Taylor, 1971b).

(III.7.c) WET SIEVING TECHNIQUE AND RESULTS The techniques used in the wet sieving and pipette analyses were those outlined by Akroyd (1964). Wet sieving and pipette analyses were carried out on material from the tip, and from the shear plane of the 1970 failure (Taylor and Hardy, 1971), to find the effect of shearing on larger particles.

The results (Fig. III.24) show that the shear plane is of a much finer particle size than bulk samples of tip materials. The difference in grain size between the curves is much greater than that shown by the Coulter Counter tests on fine particles from the shear-box.

(III.7.d) CONCLUSIONS The comparative results from the Coulter Counter show that there is a relationship between particle size distribution and mineralogy. This has the form that a high quartz/clay ratio gives a generally coarser particle size distribution. It is also concluded that where the quartz/clay ratio is low, then comminution processes may be

more active in the attainment of residual shear strength.

The wet analyses results (using conventional methods, not the Coulter Counter) show that breakdown in the larger particles is important during the formation of shear planes. This is consistent with the theory of "progressive failure" (where stresses are built up around strong points in a material, until they shear and failure occurs in the whole structure).

The sample from the 25-mm skin of the tip (Tip Surface Layer; Fig. III.22) does not indicate any apparent breakdown of particles which would be attributable to weathering processes. In other words, it has not reached a smaller fundamental size level. The amount of expanding clay minerals is low (Chap. II), and the quartz/clay minerals ratio is high; therefore this distribution is to be expected. The displacement of the Tip Surface Layer curve towards the coarser end of the M. I. T. Classification (Fig. III.22) may be due to washing off of fine particles, but since the material was collected at the base of the tip slope, this is unlikely.

### (III.8) SHEAR STRENGTH ANALYSIS CONCLUSIONS

The samples from Littleton Colliery exhibited major features which were shown during shear strength and associated tests. These features concern shear strength and take into account the origin and mineralogy of the spoil heap. Characteristics observed during particle size analyses and other tests serve to bear out these main points.

As outlined above (Chap. III.6) the spoil heap shows that it has been derived from underground measures not unlike the samples tested in Durham. This is demonstrated by the bracketing of the spoil heap shear strength parameters by those of the underground samples. The same effect has been observed during mineralogical investigations (Chap. II), and indicates a relationship between mineralogy and shear strength. As pointed out (Chap. III.5. a), it was observed that an increase in quartz concentration leads to an increase in shear strength in these normally-consolidated bulk samples. While the particle size analysis of the coarse spoil heap material (Fig. III.24) shows a distinct breakdown to finer particles, the Coulter Counter analyses of the  $2\mu\text{m}$  to  $60\mu\text{m}$  size fraction

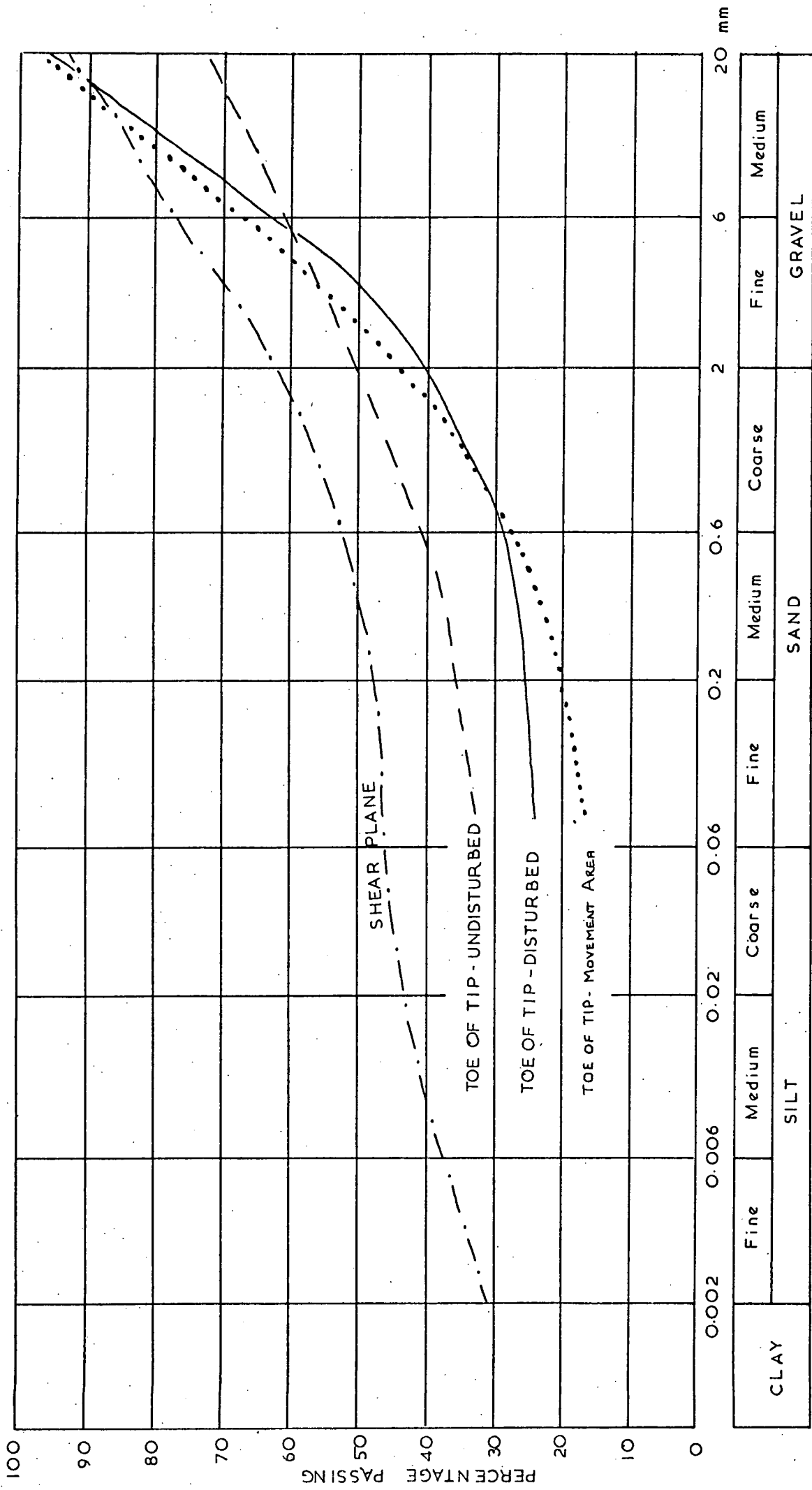


Fig. III.24. Wet sieving particle size results for the 1970 failure (Taylor and Hardy, 1971).



(Fig. III.22) show a less distinct breakdown, in shear-box material, but a comminution nonetheless. Possible weathering or degradation should be shown by comparing the particle size distribution of Tip Surface Layer (TSL) with those of the other spoil heap samples. Little variation is noted, suggesting that weathering is of small importance. Confirmation of this will be given in the chapter on chemistry (Chap. IV.2. d).

The behaviour of clay minerals as a function of preferred orientation along an established shear plane, and the effect of equant habit minerals, was investigated by Skempton (1964), Kenney (1967), Taylor and Spears (1972). The Littleton results have clearly confirmed that with increasing quartz (decreasing clay mineral content)  $\phi'_e$  does, in fact, increase.

The attainment of residual shear strength was investigated during the testing sequence. Displacements of up to 0.7m were required before residual was reached - rather more than anticipated. It has also been postulated that comminution of particles on the shear plane is partly responsible for residual shear strength attainment. Particle analyses show that major breakdown does, in fact, occur within the zone containing a continuous shear plane.

The accuracy of the testing methods is, of course, open to criticism. The only means of appraising results from colliery discard materials is to point out that they are comparative if standard testing techniques are used. New techniques, such as the integration of the consolidated drained triaxial test and shear-box, were attempted during this research and found to be largely successful.

In comparison with spoil heaps in other parts of the country, Littleton shows a low  $\phi'_r$ .

SPOIL HEAP LOCATION	$\phi'_r$	REFERENCE
Littleton	16°	
Aberfan	17.5°	N. C. B., 1972
Brancepeth	22°	Taylor, 1971

TABLE III.6. COMPARISON OF  $\phi'_r$  FOR SPOIL HEAPS

Taylor and Spears (1970) and Perrin (1971) have shown that there is a geographical variation in the clay mineralogy in British coalfields, and Taylor and Spears have also shown that instability of certain West-Midlands rocks is a function of the mixed-layer mica-montmorillonite component. The spoil heap at Littleton contains a mean of 50.3% illite, with a mixed-layer component averaging 14.6% (Taylor and Hardy, 1971). Undoubtedly this mixed-layer component is instrumental in lowering the shear strength of Littleton spoil heap. This reasoning is based on the fact that authors such as Kenney (1967) have shown that  $\phi_r^1$  is exceedingly low ( $< 10^\circ$ ) for montmorillonite itself and clay-shales with a known free montmorillonite content. It is not unreasonable therefore to infer that montmorillonite as a mixed-layer component (particularly in the Park Floor) will help in reducing  $\phi_r^1$ .

This conclusion is borne out by a  $\phi_{er}^1$  of  $13^\circ$  for the Park Floor, and must point to the fact that spoil heaps in this area, with similar mineralogy, have low residual angle values. In view of the average inclination of the Littleton Spoil Heap ( $22^\circ$ ), it is obvious that it is unstable, as was shown by the 1970 failure (albeit a probable re-activation).

The use of residual shear strength as a guide to stability may be more valuable in the design of spoil heaps than the use of peak shear strength, especially in tips such as Littleton (West-Midlands) where shear strength values are low. This is due to the fact that failures induced during tipping - especially with a MacLane Tippler which must induce layering - may well cause the material to pass its peak strength, and proceed by progressive failure to residual shear strength, or until failure occurs.

## CHAPTER IV

### CHEMISTRY

Major element chemical analyses were carried out on all the samples collected at Littleton Colliery except the Eight Feet Roof. The aim of the experiments was to correlate sample chemistry with sample mineralogy (Chap. II), and to reveal the presence of phenomena such as leaching which may affect shear strength characteristics.

(IV.1)

#### CHEMICAL TECHNIQUES

As in the mineralogical analyses, the samples used were sub-samples of those collected in bulk at Littleton Colliery. Major element analysis was carried out using X-ray fluorescence techniques and wet chemical methods.

Chemical analyses of these types are generally of high precision, especially the X-ray fluorescence technique. However, it must be pointed out that variations in quantitative clay mineralogy can involve an error of up to 11.3% (Table II.2). Chemical analyses perform a very useful function in verifying quantitative mineralogical analyses.

(IV.1.a) X-RAY FLUORESCENCE TECHNIQUES The analyses were carried out using a Philips PW 1212 Automatic Sequential Analyser. This allowed the determination of the following elements and oxides:  $\text{SiO}_2$ ,  $\text{Al}_2\text{O}_3$ ,  $\text{Fe}_2\text{O}_3$  (as total Fe),  $\text{MgO}$ ,  $\text{CaO}$ ,  $\text{Na}_2\text{O}$ ,  $\text{K}_2\text{O}$ ,  $\text{TiO}_2$ ,  $\text{MnO}$ , S, and  $\text{P}_2\text{O}_5$ .

The samples used in the analyses were made up from 10 to 15 gm of the dried and milled material used in the mineralogical experiments (without the addition of boehmite). This powder was mixed thoroughly with a binding substance (Mowoil) before being pelletized under a pressure of  $77.2 \text{ N/mm}^2$  (5 tonf/in<sup>2</sup>). The samples were placed in the Philips Analyser, where they were irradiated with a monochromatic X-ray beam.

On irradiation, the elements fluoresced at characteristic wavelengths, and the intensity of these wavelengths allowed elemental

concentrations to be calculated against 32 pre-existing sedimentary standards. These standards had been previously analysed by wet chemical methods: 29 of them are Coal Measures shales.

The data output from the analyser was in the form of a punched tape. This data was fed into an IBM 360 computer, programmed to reduce the wavelength intensity data to elemental concentration values.

(IV.1. b) WET CHEMICAL TECHNIQUES Carbon cannot be determined by X-ray fluorescence techniques, because of its low atomic mass. Therefore carbon and carbon dioxide were determined by the traditional absorption method (Groves, 1951).

This involved the decomposition of any carbonate in the sample by orthophosphoric acid. Carbon dioxide given off during the reaction was dried and then absorbed by self-indicating Sofnolite. The change in weight of the Sofnolite due to  $\text{CO}_2$  absorption was directly related to the amount of carbonate in the sample.

Organic carbon (coal) was then oxidized to  $\text{CO}_2$  by orthophosphoric and chromic acids, the  $\text{CO}_2$  again being absorbed by Sofnolite. The change in weight of the Sofnolite was related to the organic carbon content of the sample.

#### (IV.2) CHEMICAL RESULTS

The results gained from the analyses carried out on the Littleton samples are shown in Table IV.1. Table IV.2 shows these results with carbon,  $\text{CO}_2$  and total water subtracted, and then normalized to 100% totals. Normalization eliminated the effect of artificially introduced coal (Chap. II. 4. e). The ratios listed in Table IV.3 are taken from the results in Table IV.2. Normalization was carried out to facilitate comparison of materials which had different analytical totals. Because of their high accuracy, the chemical analyses allowed the mineralogical results to be checked. Features such as leaching could be detected from chemical analyses alone.

Sample	SiO <sub>2</sub> (free)	SiO <sub>2</sub> (comb)	Al <sub>2</sub> O <sub>3</sub>	Fe <sub>2</sub> O <sub>3</sub>	MgO	CaO	Na <sub>2</sub> O	K <sub>2</sub> O	TiO <sub>2</sub>	MnO	S	P <sub>2</sub> O <sub>5</sub>	CO <sub>2</sub>	C	Total**
ROOF															
BNCH	34.30	26.22	20.57	4.12	1.71	0.21	0.77	3.66	0.97	0.05	0.00	0.08	0.07	0.41	93.0
BR	21.90	34.05	23.40	4.44	1.73	0.23	0.65	4.60	0.98	0.05	0.00	0.10	0.16	0.92	93.0
FLOOR															
8FF	18.50	34.85	22.69	7.36	1.51	0.52	0.53	3.91	0.83	0.14	0.21	0.06	3.42	4.54	99.0
PF	3.00	49.02	28.61	2.35	1.42	0.23	0.81	4.74	1.06	0.01	0.02	0.06	0.00	3.40	94.7
DF	51.40	16.25	19.48	1.00	0.65	0.14	0.78	1.47	1.27	0.00	0.00	0.01	0.00	1.25	93.6
TIP															
TTO	29.40	27.55	20.46	6.70	1.72	0.43	0.66	3.69	0.94	0.11	0.15	0.12	2.02	4.01	97.9
TTC	26.30	31.49	21.73	4.67	1.74	0.31	0.74	3.90	0.95	0.06	0.08	0.10	0.39	3.53	96.0
TSL	25.00	30.52	19.47	9.04	1.73	0.54	0.51	3.53	0.92	0.14	0.13	0.11	2.71	5.04	98.3
TFB	34.60	23.02	20.44	5.03	1.71	0.34	0.71	3.72	0.97	0.07	0.13	0.11	0.56	3.80	95.2
TIP 1	31.60	20.67	20.29	6.27	1.72	0.41	0.51	3.72	0.94	0.10	0.14	0.11	1.34	4.98	96.8
U 4	30.90	25.38	20.52	5.33	1.65	0.34	0.41	3.76	0.96	0.16	0.11	0.10	0.11	1.95	93.6
M. 1	20.20	37.16	21.15	4.75	1.82	0.48	0.40	3.93	1.00	0.10	0.13	0.09	2.20	1.84	95.2
M. 2	22.00	32.46	20.45	5.41	1.41	0.44	0.46	3.70	0.91	0.08	0.51	0.19	0.00	6.82	94.9
M. 3	22.50	33.14	21.16	6.26	1.55	0.45	0.51	3.54	0.94	0.10	0.50	0.18	0.35	4.20	95.3

LITTLETON MAJOR ELEMENT CHEMICAL ANALYSIS

TABLE IV. 1.

\* Taylor and Hardy (1971)

\*\* Total % = 100% - (H<sub>2</sub>O<sup>+</sup> + H<sub>2</sub>O<sup>-</sup>)%

Sample	SiO <sub>2</sub> (free)	SiO <sub>2</sub> (comb)	Al <sub>2</sub> O <sub>3</sub>	Fe <sub>2</sub> O <sub>3</sub>	MgO	CaO	Na <sub>2</sub> O	K <sub>2</sub> O	TiO <sub>2</sub>	MnO	S	P <sub>2</sub> O <sub>5</sub>
BNCH	38.31	29.29	20.97	4.04	1.67	0.19	0.77	3.73	0.96	0.05	0.00	0.08
ROOF BR	24.32	37.81	24.74	4.57	1.75	0.21	0.68	4.79	1.02	0.05	0.00	0.11
8FF	20.36	38.35	25.51	7.62	1.62	0.55	0.59	4.11	0.86	0.14	0.23	0.07
FLOOR PF	3.33	54.35	30.66	2.57	1.50	0.23	0.86	5.22	1.18	0.01	0.01	0.07
DF	58.12	18.38	18.44	0.93	0.63	0.10	0.75	1.48	1.23	0.00	0.00	0.01
TTO	32.59	30.47	22.11	6.65	1.75	0.44	0.72	3.78	0.93	0.11	0.15	0.12
TTC	29.32	34.87	22.73	4.77	1.78	0.31	0.84	4.01	0.96	0.06	0.08	0.11
TSL	28.43	32.74	21.95	9.01	1.84	0.56	0.57	3.60	0.92	0.13	0.14	0.12
TFB	38.78	25.80	22.11	5.18	1.77	0.34	0.76	3.92	1.00	0.07	0.15	0.12
TIP 1	36.87	26.00	22.54	6.49	1.82	0.43	0.56	3.94	0.98	0.10	0.15	0.12
U 4	34.48	28.46	22.94	6.26	1.77	0.34	0.42	4.04	0.98	0.11	0.07	0.13
M <sub>s</sub> 1	22.14	40.73	23.18	5.21	1.99	0.53	0.44	4.31	1.10	0.11	0.14	0.10
TIP* M <sub>c</sub> 2	24.97	36.85	23.29	6.14	1.60	0.50	0.52	4.20	1.03	0.09	0.58	0.22
M <sub>c</sub> 3	24.78	36.50	23.31	6.89	1.71	0.50	0.56	3.90	1.04	0.11	0.55	0.20

TABLE IV.2. LITTLETON CHEMICAL ANALYSIS: NORMALIZED TO 100%  
WITHOUT CO<sub>2</sub> and H<sub>2</sub>O

\* Taylor and Hardy (1971)

Sample	Total $\frac{\text{SiO}_2}{\text{Al}_2\text{O}_3}$	$\frac{\text{SiO}_2}{\text{Comb. Al}_2\text{O}_3}$	$\frac{\text{Fe}_2\text{O}_3}{\text{Al}_2\text{O}_3}$	$\frac{\text{MgO}}{\text{Al}_2\text{O}_3}$	$\frac{\text{CaO}}{\text{Al}_2\text{O}_3}$	$\frac{\text{Na}_2\text{O}}{\text{Al}_2\text{O}_3}$	$\frac{\text{K}_2\text{O}}{\text{Al}_2\text{O}_3}$	$\frac{\text{SiO}_2(\text{free})}{\text{SiO}_2(\text{comb})}$
ROOF								
BNCH	2.94	1.27	0.20	0.08	0.01	0.04	0.18	1.31
BR	2.39	1.46	0.19	0.07	0.01	0.03	0.20	0.64
8FF	2.35	1.54	0.32	0.07	0.02	0.02	0.17	0.53
FLOOR PF	1.82	1.71	0.08	0.05	0.01	0.03	0.17	0.06
DF	3.47	0.83	0.05	0.03	0.01	0.04	0.08	3.16
TTO	2.77	1.34	0.32	0.08	0.02	0.03	0.18	1.07
TTC	2.65	1.44	0.22	0.08	0.01	0.04	0.18	0.84
TSL	2.85	1.53	0.46	0.09	0.03	0.03	0.18	0.87
TFB	2.82	1.13	0.25	0.08	0.02	0.04	0.19	1.50
TIP 1	2.77	1.15	0.31	0.08	0.02	0.02	0.18	1.42
U 4	2.69	1.22	0.29	0.08	0.02	0.02	0.18	1.21
M. 1	2.71	1.78	0.22	0.09	0.02	0.02	0.19	0.54
M. 2	2.65	1.58	0.26	0.07	0.02	0.02	0.17	0.68
M. 3	2.63	1.57	0.30	0.07	0.02	0.02	0.18	0.68

TABLE IV. 3. LITTLETON CHEMICAL RATIOS CALCULATED FROM  
NORMALIZED RESULTS

(IV.2. a) CHEMICAL ANALYSES: TABLE IV.1 and TABLE IV.2. The percentages listed in Table IV.1 and Table IV.2 are weight percentages of the elements and oxides. Inferences drawn from the concentrations of elements in the samples concerned the sample mineralogy and gave an indication of the veracity of mineralogical analyses.

The elements determined were silicon, aluminium, iron (as  $\text{Fe}_2\text{O}_3$ ), magnesium, calcium, sodium, potassium, titanium, manganese, sulphur, phosphorus and carbon.

The alumina ( $\text{Al}_2\text{O}_3$ ) was almost entirely contained in the clay minerals which were determined by X-ray diffraction. Similarly, the potassium and sodium ions could largely be attributed to clay minerals (especially the 10-Å illitic and mixed-layer minerals), since other  $\text{K}^+$  and  $\text{Na}^+$  bearing minerals such as sulphates and feldspars were either absent or else present in very small quantities.

Some of the  $\text{Fe}_2\text{O}_3$ ,  $\text{MgO}$ ,  $\text{CaO}$  and  $\text{MnO}$  will be contained in the clay minerals, occupying structural sites, but other minerals, especially carbonates, will account for some of these elements.  $\text{CO}_2$  determinations showed that all but three of the samples contained carbonates (PF, DF and M2). Mineralogical analyses agreed with these results, showing no carbonates in the same samples. The samples which contained carbonates showed that ankerite, siderite and calcite were all present, so that  $\text{CO}_2$  was accounted for, as well as some of the  $\text{Fe}_2\text{O}_3$ ,  $\text{MgO}$ ,  $\text{CaO}$  and  $\text{MnO}$ .

$\text{TiO}_2$  in the samples was due to rutile, which was probably present as needles in the clay minerals. Taylor (1971a) has reported their presence in the clay matrix of a non-marine shaly mudstone from the Mansfield Marine Band Cyclothem. He quotes the percentage distribution of  $\text{TiO}_2$  as : marine, mean = 1.05, S.D.  $\pm$  0.13; non-marine, mean = 1.01, S.D. =  $\pm$  0.09. The Littleton  $\text{TiO}_2$  concentrations are closer to the non-marine concentration determined; the Littleton roofs and floors are, in fact, non-marine.

$\text{P}_2\text{O}_5$ , with some of the  $\text{CaO}$  content, was assigned to apatite, and was ubiquitous in the Littleton samples.



Organic carbon was present in varying concentrations.

The provenance of the carbon in the spoil heap has already been discussed (Chap. II. 4. e), but underground it must be pointed out that it was more common in the floor measures than in the roof measures. The  $P_2O_5$  can also be of organic origin, being derived from fossil debris.

(IV.2.b) COMBINED SILICA/ $Al_2O_3$  RATIO: TABLE IV.3 The  $Al_2O_3$ , like the combined silica, was derived from the clay minerals illite, kaolinite and chlorite, and was representative of the clay mineral composition. This ratio, unlike the free silica/combined silica ratio (Chap. IV.2.c) was not related to grain size and could be used to compare different minerals. For example, the standard Fittrian illite (which contains mixed-layer clay) has a ratio of 1.98, whilst theoretical and empirical ratios for kaolinite are about 1.18. Hence samples with high illite and mixed-layer clay have high ratios; those with abundant kaolinite have low ratios.

The variation in the Littleton samples was between 0.83 (DF) and 1.78 (M1; Taylor and Hardy, 1971). The spoil heap samples showed a range 1.13 (TFB) to 1.78 (M1); the underground range was 0.83 (DF) to 1.71 (PF). The Deep Floor showed a significantly lower ratio than any other, the next lowest being 1.13 (TFB), inferring a low concentration of illite. From Table II.2 it can be seen that this is true. However, care had to be exercised when considering the normal relationship of combined silica/ $Al_2O_3$  to clay mineral concentration. The two tip samples with the lowest ratio (TFB and TIP1) had high illite contents relative to the other clay minerals. Tip 1 had the highest kaolinite content however, and this was reflected by its low combined  $SiO_2/Al_2O_3$  ratio. The same could not be said for sample TFB (Table IV.4). The difficulty was one of reconciling

SAMPLE	$\frac{SiO_2(C)}{Al_2O_3}$	ILLITE %	KAOLINITE %	CHLORITE %
TFB	1.13	45.1	7.6	3.6
TIP 1	1.15	59.0	14.9	3.8

TABLE IV.4. RELATIONSHIP OF  $\frac{SiO_2(C)}{Al_2O_3}$  TO MINERALOGY

mineralogy and chemistry. Because of variations in crystallinity quantitative clay mineral assessments will always show some variation - see totals (Table II.2) which give some indication of the errors involved. Similarly, small errors in quartz determinations may result in large differences in combined  $\text{SiO}_2/\text{Al}_2\text{O}_3$  ratios. Combined silica was obtained from total silica minus free silica (Quartz) (Table IV.1 and Table II.2). The X-ray method for quartz estimation was surprisingly accurate (Taylor, 1973). Possibly the best way in which to consider this ratio was in terms of large mineralogical variations like the Deep Floor. Similarly, the Park Floor, which had the highest clay mineral concentration (82%) and was rich in illite, had the second highest ratio (1.71). Trace Feldspars would also have a minor masking effect because the same ratio applies to them as applies to clay minerals.

(IV.2.c) FREE SILICA/COMBINED SILICA RATIO As mentioned above, this ratio is largely dependent upon grain size. This is because the free silica occurs as quartz (generally large grains), and the combined silica occurs in clay minerals (small grains). Hence grain size depends upon mineralogy, and so the ratio could also be used to show mineralogical variations.

The variations found at Littleton showed a range overall of 0.06 (Park Floor) to 3.16 (Deep Floor). Particle size has been discussed (Chap. III.7), and it was pointed out that the Deep Floor showed a larger fundamental particle size than any other material, and that the Park Floor was susceptible to breakdown (high clay content shown by low ratio).

Again, the ratio depended upon quartz determinations and so is always open to some criticism.

(IV.2.d)  $\text{K}_2\text{O}/\text{Al}_2\text{O}_3$  RATIO The  $\text{K}_2\text{O}$  was contained chiefly in the clay minerals, especially the illite and mixed-layer components. On exposure to weathering, micaceous minerals are subject to leaching. The cations are affected by leaching, and the  $\text{K}_2\text{O}/\text{Al}_2\text{O}_3$  ratio could be used to investigate the effect of leaching on the spoil heap material.

The range of values shown by the Littleton samples lay between 0.08 (DF) and 0.20 (BR). The low ratio for the Deep Floor was a reflection of the low illite content; the other ratios all lay between 0.17 and 0.19. The major variations all lay in the underground material, the range of the spoil heap ratios was between 0.17 and 0.19, with six values of 0.18. This reflected the similarity of the spoil heap mineralogies, yet one would have expected a reduction in the Tip Surface Layer ratio, due to leaching. This sample was collected with exactly this in mind. It represented the surface 20mm of spoil, and therefore would have been subjected to weathering processes. The identification of any leaching of the spoil which could lead to alterations in shear strength is important when dumping material on old slopes during re-shaping of a spoil heap. However, TSL showed a ratio of 0.18 and so leaching is unlikely to be an important phenomenon at Littleton.

#### (IV.2. e) COMPARISON OF CHEMISTRY AND MINERALOGY OF SPOIL HEAP

SAMPLES A high total  $\text{SiO}_2/\text{Al}_2\text{O}_3$  ratio is an expression of high quartz content and, possibly high illite content. Of the samples from the spoil heap, TSL, TFB and TIP 1 all fell in this category. However, TSL was ambiguous in that it had not a high quartz content (Table II.2), and illite was low. TIP 1 had a fairly high quartz content and a low combined  $\text{SiO}_2/\text{Al}_2\text{O}_3$  ratio; this indicated a high kaolinite content, which is confirmed in Table II.2. The  $\text{Na}_2\text{O}/\text{Al}_2\text{O}_3$  ratio for (TTC) was high, which may imply a more Na-rich mica. TTO, TTC and U 4 had a constant  $\text{K}_2\text{O}/\text{Al}_2\text{O}_3$  value of 0.18; their combined  $\text{SiO}_2/\text{Al}_2\text{O}_3$  ratios increased in the order U 4, TTO, TTC, which implied an increasing kaolinite content. The mineralogical data confirmed this.

The other oxides  $\text{Fe}_2\text{O}_3$ ,  $\text{MgO}$ ,  $\text{CaO}$  and  $\text{MnO}$  were contained in clay minerals, but it must be realized that carbonates were also responsible for their concentrations. TSL had a high siderite content and the highest  $\text{Fe}_2\text{O}_3/\text{Al}_2\text{O}_3$  ratio.  $\text{CaO}/\text{Al}_2\text{O}_3$  was marginally higher, as was the  $\text{MgO}/\text{Al}_2\text{O}_3$  ratio. This pointed to the carbonates in TSL being

ankerite rather than pure siderite. It also illustrated that the carbonate had not been leached out in this surface sample, which confirmed the inference drawn from  $K_2O/Al_2O_3$  ratios (Chap. IV.2. d).

The chlorite content was always less than 7% and the  $MgO/Al_2O_3$  ratio was fairly constant and no real inference could be gained from this.

(IV.2. f) COMPARISON OF CHEMISTRY AND MINERALOGY OF UNDERGROUND

SAMPLES The Park Floor was very low in free silica (quartz), and had a low total  $SiO_2/Al_2O_3$  ratio which confirmed the mineralogical observation. The Deep Floor had a very high free silica content, and a correspondingly high total  $SiO_2/Al_2O_3$  ratio. The combined  $SiO_2/Al_2O_3$  ratio for the Deep Floor was less than 1.0, which was less than the kaolinite ratio, therefore it must have been rich in quartz.

These unweathered underground samples should not have been affected by leaching and hence any variation in the  $K_2O/Al_2O_3$  ratio could be used as a rough indicator of micaceous mineral variation, as measured by X-ray diffraction  $10\text{-}\overset{\circ}{A}$  peak area/ $7\text{-}\overset{\circ}{A}$  peak area (Table IV.5)

SAMPLE	DF	8FF	PF	BNCH	BR
$10\text{-}\overset{\circ}{A}/7\text{-}\overset{\circ}{A}$	3.19	4.12	6.12	5.59	6.40
$K_2O/Al_2O_3$	0.08	0.17	0.17	0.18	0.20

TABLE IV.5. COMPARISON OF  $K_2O/Al_2O_3$  and  $10\text{-}\overset{\circ}{A}/7\text{-}\overset{\circ}{A}$  RATIOS

This table shows that the  $K_2O/Al_2O_3$  ratio does in fact vary with illite/kaolinite ratio, though the Park Floor  $10\text{-}\overset{\circ}{A}/7\text{-}\overset{\circ}{A}$  was high, and the Benches Roof value a little low. Previous remarks concerning crystallinity will obviously have a bearing on the  $10\text{-}\overset{\circ}{A}/7\text{-}\overset{\circ}{A}$  areas.

(IV.3) STATISTICAL COMPARISON OF CHEMICAL RESULTS

Using the "Student's t" method, as outlined in Chapter II.4. f, the results of the chemical analyses were compared with other sets of data.

OXIDE OR ELEMENT	YORKS' MAIN MEAN	LITTLETON MEAN	t	"Student's" t Test	CONFIDENCE LEVEL
Free SiO <sub>2</sub>	12.89	27.19	7.1252	Highly significantly different	99.9% confidence level
Comb. SiO <sub>2</sub>	27.59	29.22	0.9111	Not significantly different	
Al <sub>2</sub> O <sub>3</sub>	20.96	20.69	0.4937	Not significantly different	
Fe <sub>2</sub> O <sub>3</sub>	6.22	6.03	0.3153	Not significantly different	
MgO	1.34	1.68	5.0488	Highly significantly different	99.9% confidence level
CaO	2.14	0.42	6.3624	Highly significantly different	99.9% confidence level
Na <sub>2</sub> O	0.55	0.55	0.0305	Not significantly different	
K <sub>2</sub> O	3.57	3.75	1.9886	Not significantly different	
TiO <sub>2</sub>	0.81	0.95	5.6944	Highly significantly different	99.9% confidence level
MnO	0.10	0.10	0.7326	Not significantly different	
S	2.70	0.20	4.6556	Highly significantly different	99.9% confidence level
P <sub>2</sub> O <sub>5</sub>	0.15	0.13	0.5254	Not significantly different	
CO <sub>2</sub>	3.42	1.08	3.4156	Definitely significantly different	99.0% confidence level
C	10.99	4.02	6.1020	Highly significantly different	99.9% confidence level

TABLE IV.6. STATISTICAL COMPARISON OF YORKSHIRE MAIN AND LITTLETON SPOIL HEAP CHEMISTRY INCLUDING C and CO<sub>2</sub>

OXIDE OR ELEMENT	YORKS' MAIN LITTLETON		t	"Student's" t Test	CONFIDENCE LEVEL
	MEAN	MEAN			
Free SiO <sub>2</sub>	15.83	30.26	5.9861	Highly significantly different	99.9% confidence level
Comb. SiO <sub>2</sub>	33.68	32.49	0.5543	Not significantly different	
Al <sub>2</sub> O <sub>3</sub>	27.24	22.68	11.0256	Highly significantly different	99.9% confidence level
Fe <sub>2</sub> O <sub>3</sub>	8.43	6.29	2.3637	Probably significantly different	95% confidence level
MgO	1.72	1.78	0.8611	Not significantly different	
CaO	2.88	0.44	6.5829	Highly significantly different	99.9% confidence level
Na <sub>2</sub> O	0.71	0.60	1.9311	Not significantly different	
K <sub>2</sub> O	4.57	3.97	4.2436	Highly significantly different	99.9% confidence level
TiO <sub>2</sub>	1.06	0.99	1.6718	Not significantly different	
MnO	0.15	0.10	3.0901	Significantly different	99% confidence level
S	3.40	0.22	4.7458	Highly significantly different	99.9% confidence level
P <sub>2</sub> O <sub>5</sub>	0.18	0.14	0.9386	Not significantly different	

TABLE IV.7. STATISTICAL COMPARISON OF YORKSHIRE MAIN AND LITTLETON SPOIL HEAPS,  
NORMALIZED WITHOUT C and CO<sub>2</sub>

OXIDE OR ELEMENT	UNDERGROUND MEAN	SPOIL HEAP MEAN	t	"Student's" t Test	CONFIDENCE LEVEL
Total SiO <sub>2</sub>	57.90	56.71	0.4585	Not significantly different	
Free SiO <sub>2</sub>	25.82	30.00	0.5578	Not significantly different	
Comb. SiO <sub>2</sub>	32.08	26.71	1.0503	Not significantly different	
Al <sub>2</sub> O <sub>3</sub>	22.95	20.57	1.6263	Not significantly different	
Fe <sub>2</sub> O <sub>3</sub>	3.85	6.31	2.0657	Not significantly different	
MgO	1.41	1.72	1.7767	Not significantly different	
CaO	0.27	0.40	1.8307	Not significantly different	
Na <sub>2</sub> O	0.71	0.60	1.2778	Not significantly different	
K <sub>2</sub> O	3.68	3.77	0.1616	Not significantly different	
TiO <sub>2</sub>	1.02	0.95	1.0860	Not significantly different	
MnO	0.05	0.10	1.8651	Not significantly different	
S	0.04	0.12	1.7391	Not significantly different	
P <sub>2</sub> O <sub>5</sub>	0.06	0.11	3.5084	Definitely significantly different	99% confidence level
CO <sub>2</sub>	0.73	1.19	0.6007	Not significantly different	
C	2.10	3.89	2.0221	Not significantly different	

TABLE IV. 8.

STATISTICAL COMPARISON OF UNDERGROUND MEASURES  
AND SPOIL HEAP AT LITTLETON

Using analyses from Yorkshire Main Spoil heap (Taylor, 1971b), the spoil heap results from Littleton were compared with those from another geographical area. Given regional variations in clay mineralogy, this should bring out differences in the chemistry of the spoil heap materials. Two sets of data were compared for Yorkshire Main and Littleton; one set included C and CO<sub>2</sub> in the data, the second set excluded C and CO<sub>2</sub> in an attempt to compare uncontaminated spoil with a chemistry close to that of the parent horizons. The third comparison was between the underground measures and spoil heap material of Littleton Spoil Heap No. 1.

(IV.3. a) COMPARISONS OF YORKSHIRE MAIN AND LITTLETON Table IV.6

and Table IV.7 show the "Student's" t Test results for Yorkshire Main compared with Littleton spoil heaps. Table IV.6 contains data for C and CO<sub>2</sub>, which are removed in Table IV.7. Table IV.6 is an expression of chemistry after contamination of the spoil by the addition of coal and associated cleat carbonate (Chap. II. 4. b). Consequently it was not useful for comparison of parent materials, only for the direct comparison of the two spoil heaps.

Table IV.6 shows that free SiO<sub>2</sub>, MgO, CaO, TiO<sub>2</sub>, S, CO<sub>2</sub> and C were all different in the two localities. Free SiO<sub>2</sub> in Littleton was higher than in Yorkshire Main, an indication of the high quartz content of Littleton. Al<sub>2</sub>O<sub>3</sub> was lower in Littleton: the inference being that the clay content of Yorkshire Main was higher, which one would expect as the quartz concentration is lower in Yorkshire Main.

The lower CO<sub>2</sub> and C values in Littleton indicated a good 'picking' of coal out of the spoil in this unwashed spoil heap. Yorkshire Main is a washed spoil heap and contains pyrite (Spears, Taylor and Till, 1970).

Table IV.7 is more conclusive on the differences between the materials. Free SiO<sub>2</sub> and Al<sub>2</sub>O<sub>3</sub> showed the same relationships as in Table IV.6; Fe<sub>2</sub>O<sub>3</sub>, CaO, K<sub>2</sub>O, MnO and S were all lower in Littleton. All except S were indicative of a lower clay mineral concentration in Littleton,



and S was a function of the non-appearance of pyrite in Littleton.

(IV.3.b) COMPARISON OF UNDERGROUND MATERIAL AND SPOIL HEAP

AT LITTLETON Table IV.8 shows the "Student's" t Test results for a chemical comparison of Littleton spoil heap with the contributing underground measures. While the correlation was obviously excellent (only  $P_2O_5$  shows any significant difference), the statistical analysis did not take into account the proportions of different materials which are contained in the spoil heap. Hence, all the underground materials were assumed to contribute equal percentages of the spoil heap, whereas in fact this is not the case. However, the results showed an excellent correlation of the chemical analyses, and pointed to similarity between the spoil heap and contributing horizons.

(IV.4) CHEMISTRY CONCLUSIONS

The chemical analyses are somewhat limited in the conclusions which may be drawn from them. However, used in conjunction with quantitative mineralogical analyses they are important data. Chemical analysis has a much higher precision than quantitative mineralogical analysis. Consequently, chemical analysis is most useful in verifying mineralogy, through independent uses, such as the detection of leaching, are important.

The high quartz content of Littleton spoil heap was confirmed by the high free  $SiO_2$  ratios.  $Al_2O_3$  figures showed that clay minerals formed a lower percentage of Littleton spoil heap than of Yorkshire Main, and both the  $SiO_2$  and  $Al_2O_3$  values for the Littleton spoil heap showed a similarity with the analyses of the underground contributors. The alkali concentrations again showed the low clay content of Littleton, and  $K_2O$  showed a constancy of concentration in the spoil heap which leads one to doubt the presence of leaching effects. The absence of leaching was also borne out by the  $CO_2$  determinations. Carbon percentages in the spoil heap were higher than those for the underground measures, which could be accounted for by the contamination of the spoil by coal during extraction. However, the C percentage was much lower than that for Yorkshire Main and indicated good 'picking' of coal at Littleton.

The features shown by the chemistry analyses were: (1) the chemistry of the underground material was similar to that of the spoil heap, (2) the chemistry of Littleton spoil heap differed radically from that of Yorkshire Main, (3) chemistry correlated broadly with mineralogy in the samples analysed, (4) leaching was not an important feature of the spoil heap material.

## CHAPTER V

### SLOPE STABILITY ANALYSIS

The 1970 slip failure of Littleton Spoil Heap No. 1 had instigated this research project and consequently it was necessary to analyse the slope stability of the spoil heap in the light of the mineralogical, chemical and shear strength information which emerged during this research project. A preliminary report on the 1970 failure (Taylor and Hardy, 1971) had already been produced, and the tentative conclusions as to the nature and genesis of the failure contained therein were pursued further.

All the slope stability analyses were carried out on a section through the 1970 slip area (Fig. II. 1) for which a detailed topographic survey was available. The section was analysed using the Bishop Simplified Method (Bishop, 1955), for which a computer program had been developed in Durham University (Roberts, 1969), and the Janbu Method (Janbu et al., 1956).

The aim of the analyses was primarily to determine the stability of the spoil heap using the shear strength parameters determined during this research and also those determined for the 1970 shear plane sample tested by Taylor and Hardy (1971). Using the results of the stability analysis, conclusions could be drawn concerning the nature and genesis of the 1970 failure. Analyses were also carried out with the aim of determining the effect on the spoil heap stability of variations in the physical properties of the spoil heap material and of the subgrade material.

(V.1)

#### TAYLOR AND HARDY (1971) SLOPE STABILITY ANALYSIS

The slope stability of the 1970 failure was investigated by Taylor and Hardy. They performed direct shear-box tests on a sample cut from the shear plane of the 1970 failure;  $\phi'_r$  was found to be  $20.5^\circ$ ,  $c'_r$  was found to be  $2.76 \text{ kN/m}^2$  ( $57.6 \text{ lbf/ft}^2$ ). Using the Bishop Simplified Method these values of  $\phi'_r$  and  $c'_r$ , together with a density of  $1.874 \text{ Mg/m}^3$  ( $117 \text{ lb/ft}^3$ ), gave a minimum factor of safety for the spoil heap of 1.183.

The slip circle for which this factor of safety was generated is shown in Fig. V. 1. The same values of  $c'_r$  and  $\phi'_r$  with a density of  $1.602 \text{ Mg/m}^3$  ( $100 \text{ lb/ft}^3$ ) increased the minimum factor of safety to 1.193 along the same slip circle.

Since the slope had already failed it would be reasonable to expect the factor of safety to be nearer to unity. However, the values of  $c'_r$  and  $\phi'_r$  used in the 1971 analyses differ slightly from those found for the bulk samples during this project. In view of this it was decided to investigate the effect on factor of safety of alteration in shear strength parameters. Taylor and Hardy concluded that the 1970 failure may well have been the re-activation of an ancient slip and consequently  $c'_r$  and  $\phi'_r$  were used in the calculation of safety factors. Littleton Spoil Heap No. 1 was placed by the MacLane Tippler method which necessarily produces layering of the dumped material running parallel to the tip surface. This increases the danger of slipping during the tip's early history. In an old spoil heap, such as Littleton, these ancient slips may be re-activated by a rising water-table. This factor was also investigated for the Littleton spoil heap.

## (V.2) EFFECT OF WATER-TABLE ON STABILITY

To test the effect of the introduction of a water-table into the slope stability analyses, a series of programs was run in which the water-table was raised through the section. The first set of results set the water-table below the failure circle generated by the line investigated. The second was tangential to this line. As expected no variation in safety factor was noted.

The water-table was then raised in horizontal planes, in 3.048m (10 ft) intervals. The factor of safety was found to drop from 1.541 to 1.522 for a rise in the water-table of 9.144m (30 ft). This was due to the effective reduction in effective normal stress below the water-table, so enhancing the overturning effect of the unsaturated material higher up within the slip circle.

Varying  $c'_r$  and  $\phi'_r$  with a constant water-table showed that an

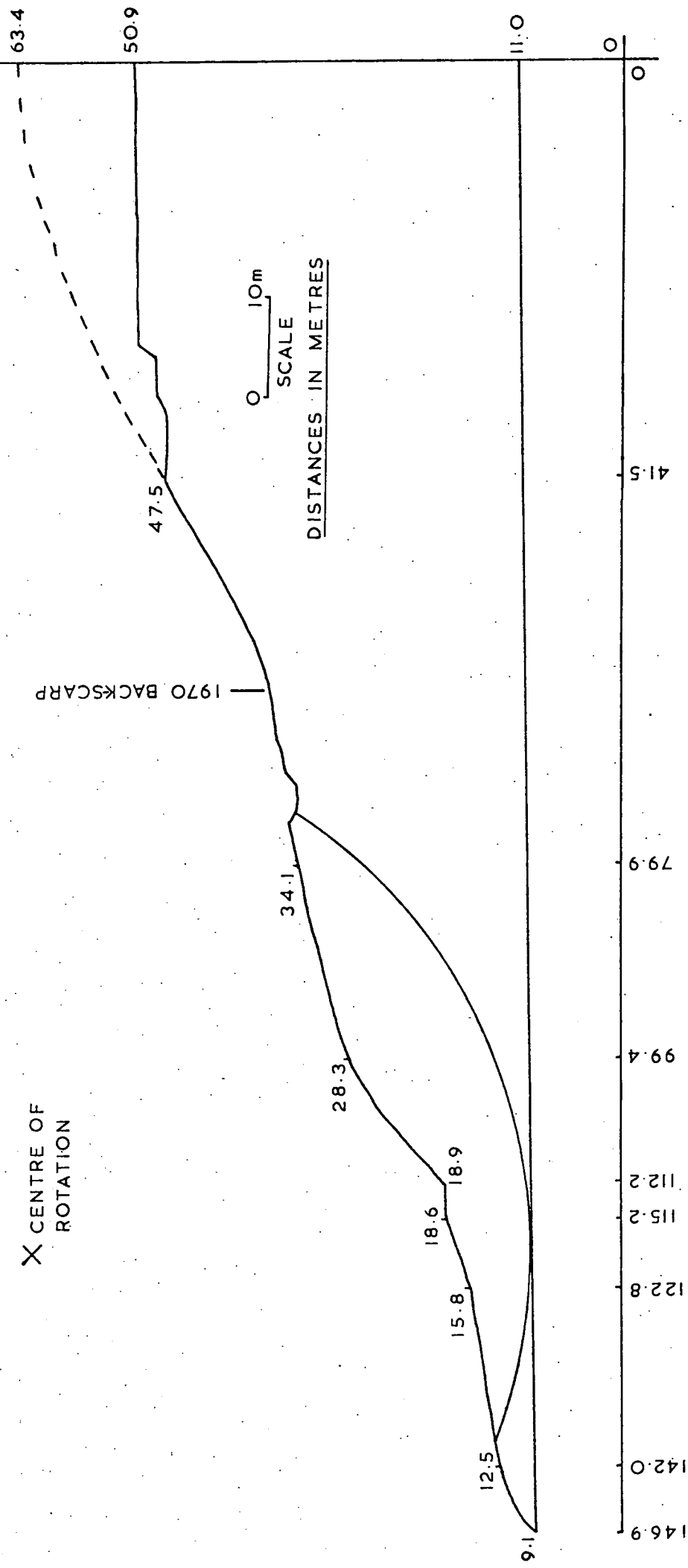


Fig. V.1. Slip circle analysed for the 1970 failure at Littleton (Taylor and Hardy, 1971).

increase in either parameter gave an increase in safety factor, although not so pronounced an increase as that obtained when water is excluded, (Table V.1 and Fig. V.2).

Table V.1 shows that without a water-table, factor of safety drops by 0.274 when  $\phi'_r$  is varied from  $18^\circ$  to  $10^\circ$ ; with a water-table, the decrease is 0.202. Therefore, the presence of a water-table reduces stability, but masks the effects of material properties.

	RUN 1	RUN 2	RUN 1-RUN 2
$c'_r$	33.52 kN/m <sup>2</sup>	33.52 kN/m <sup>2</sup>	-
$\phi'_r$	$18^\circ$	$10^\circ$	$8^\circ$
F.S. (without a water-table)	1.625	1.351	0.274
	RUN 3	RUN 4	RUN 3-RUN 4
$c'_r$	33.52 kN/m <sup>2</sup>	33.52 kN/m <sup>2</sup>	-
$\phi'_r$	$18^\circ$	$10^\circ$	$8^\circ$
F.S. (with a water-table)	1.464	1.262	0.202

TABLE V.1. EFFECT OF WATER-TABLE ON SAFETY FACTOR CHANGE WITH VARYING  $\phi'_r$ .

(V.3)

### EFFECT OF SUBGRADE DATA ALTERATION

The original theory on the Littleton slip held that the surface of failure was deep-seated (Taylor and Hardy, 1971). Consequently the effect of varying the shear strength parameters and density of the underlying boulder-clay was investigated. Naturally, no effect on safety factor was observed until the failure surface passed into the subgrade. New data was needed for the boulder-clay parameters, and this was obtained from Courchee (1970). Variations in factor of safety for variations in the physical parameters of the subgrade are shown in Table V.2.

X CENTRE OF ROTATION

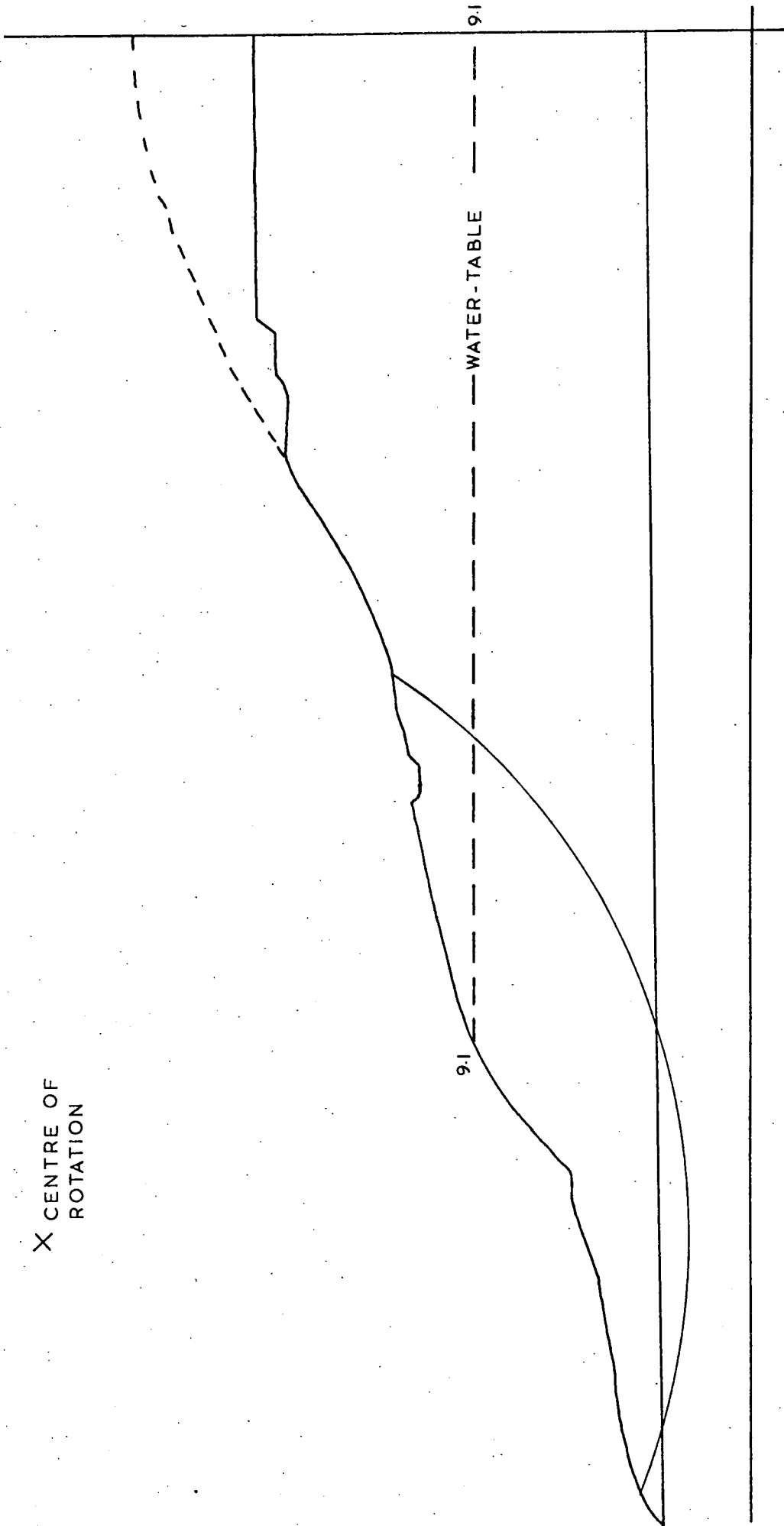


Fig. V.2. Slip circle and water-table used in the calculation of Table V. 1.

Cohesion kN/m <sup>2</sup>	$\phi'$ radians	Density Mg/m <sup>3</sup>	Parameter Varied	Variation %	Safety Factor	Variation %
6.90	0.5498	2.12	(Standard)	-	1.766	-
6.90	0.5498	1.60	$\gamma$	24%	1.712	3.05%
0.00	0.5498	2.12	$c'$	100%	1.708	3.27%
6.90	0.4590	2.12	$\phi'$	17%	1.569	11.15%

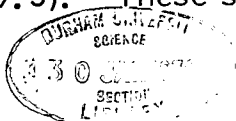
TABLE V.2. RELATIONSHIP OF PHYSICAL PROPERTIES TO SAFETY FACTOR.

The results in Table V.2 show that alteration of density ( $\gamma$ ) has little effect on the stability, varying cohesion has an even smaller effect, but that  $\phi'$  is a sensitive parameter. The slip circle chosen for these determinations is, of course, the same one in each case.

Here, the shear plane was deep-seated. However, rootlets within the old shear plane and vertical cracks in the slipped mass infer that it may be shallow, even planar. This restricts the location of the failure surface to within the spoil heap itself. Therefore the effect of variation in spoil heap material properties on factor of safety was investigated.

#### (V.4) EFFECT OF SPOIL HEAP DATA ALTERATION

To find the sensitivity of spoil heap stability to shear strength properties, variations of  $\phi'_r$  and  $c'_r$  were made, and the results are shown in Fig. V.3. The circle used to calculate the values shown in Fig. V.3 was that shown in Fig. V.4, and the standard parameters quoted for the subgrade in Table V.2 were used. The three values of  $c'_r$  used were 0.00 kN/m<sup>2</sup>, 19.15 kN/m<sup>2</sup> and 33.52 kN/m<sup>2</sup> (0.0 lbf/ft<sup>2</sup>, 40 lbf/ft<sup>2</sup> and 70 lbf/ft<sup>2</sup>) and the three values of  $\phi'_r$  were taken as 5°, 10° and 18°. Figure V.3 shows a linear relationship between factor of safety and  $\phi'_r$  for all three values of  $c'_r$ , (as would be expected), and the relationship between safety factor and  $c'_r$  is also linear since the three lines are parallel. The relationship between  $c'_r$  and safety factor was obtained by linear regression analyses of the points (Fig. V.3). These showed that the three lines all had the same slope.





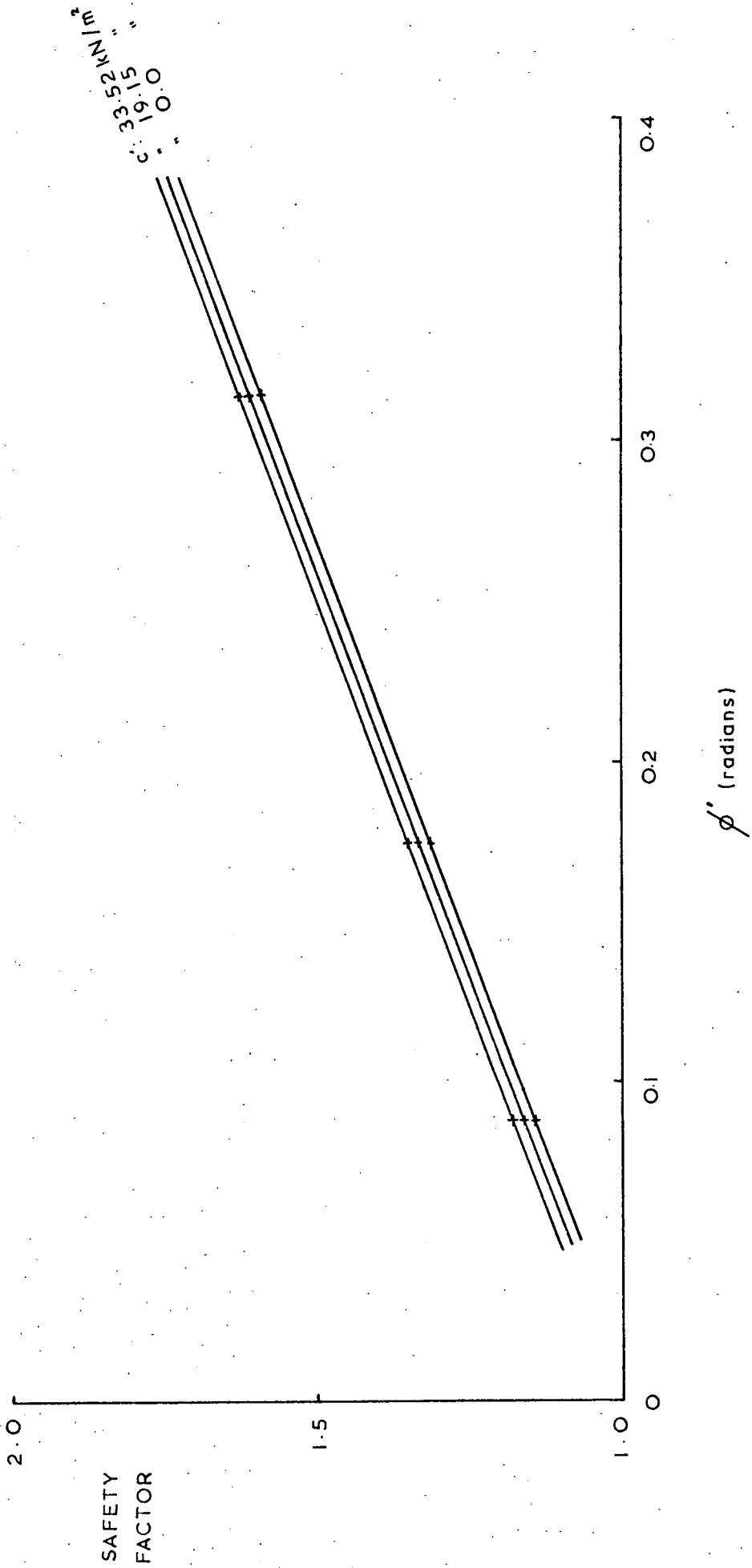


Fig.V.3. Safety factor v  $\phi'$  graphs for the slip circle shown in Fig. V.4.

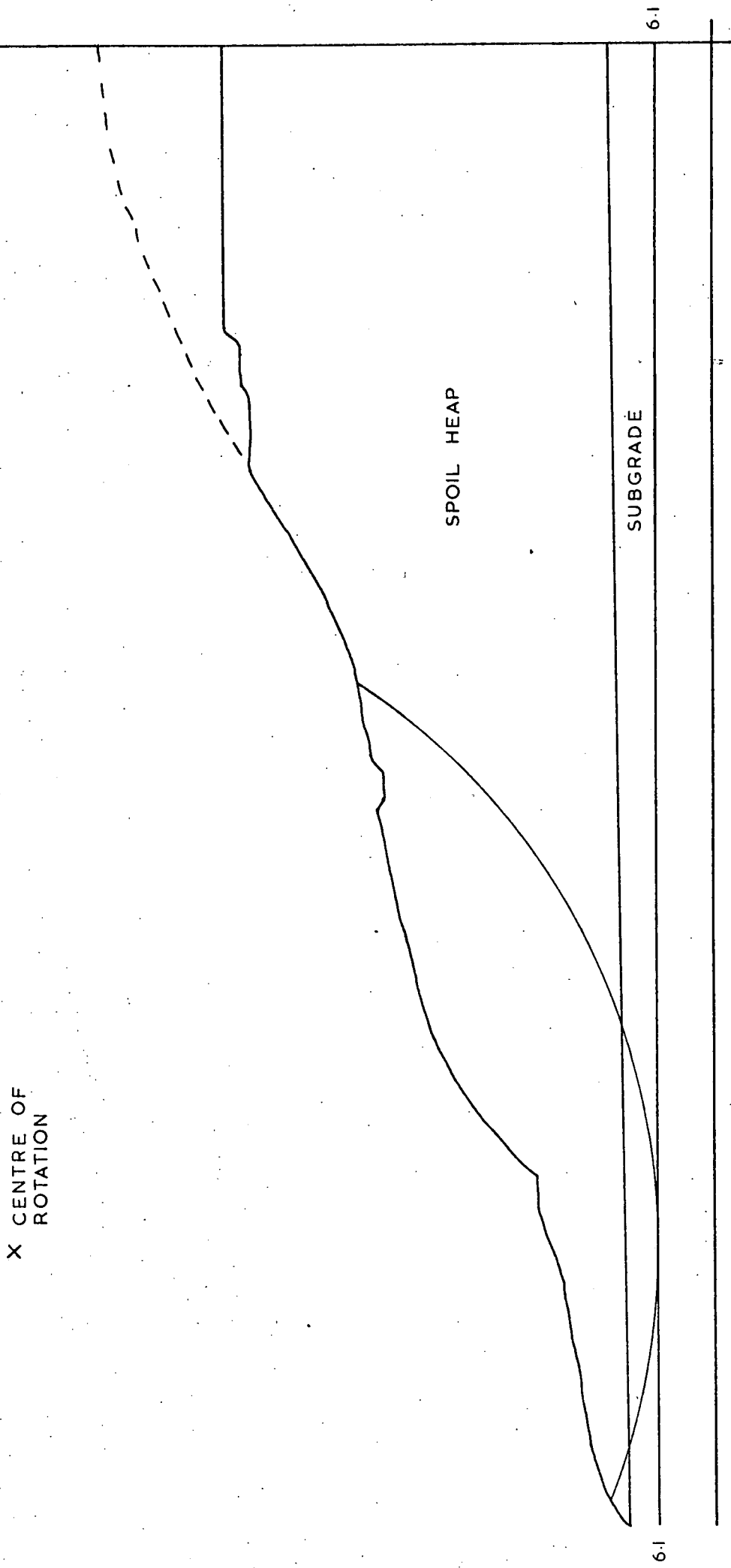


Fig. V.4. Slip circle analysed for the results shown in Fig. V.3.

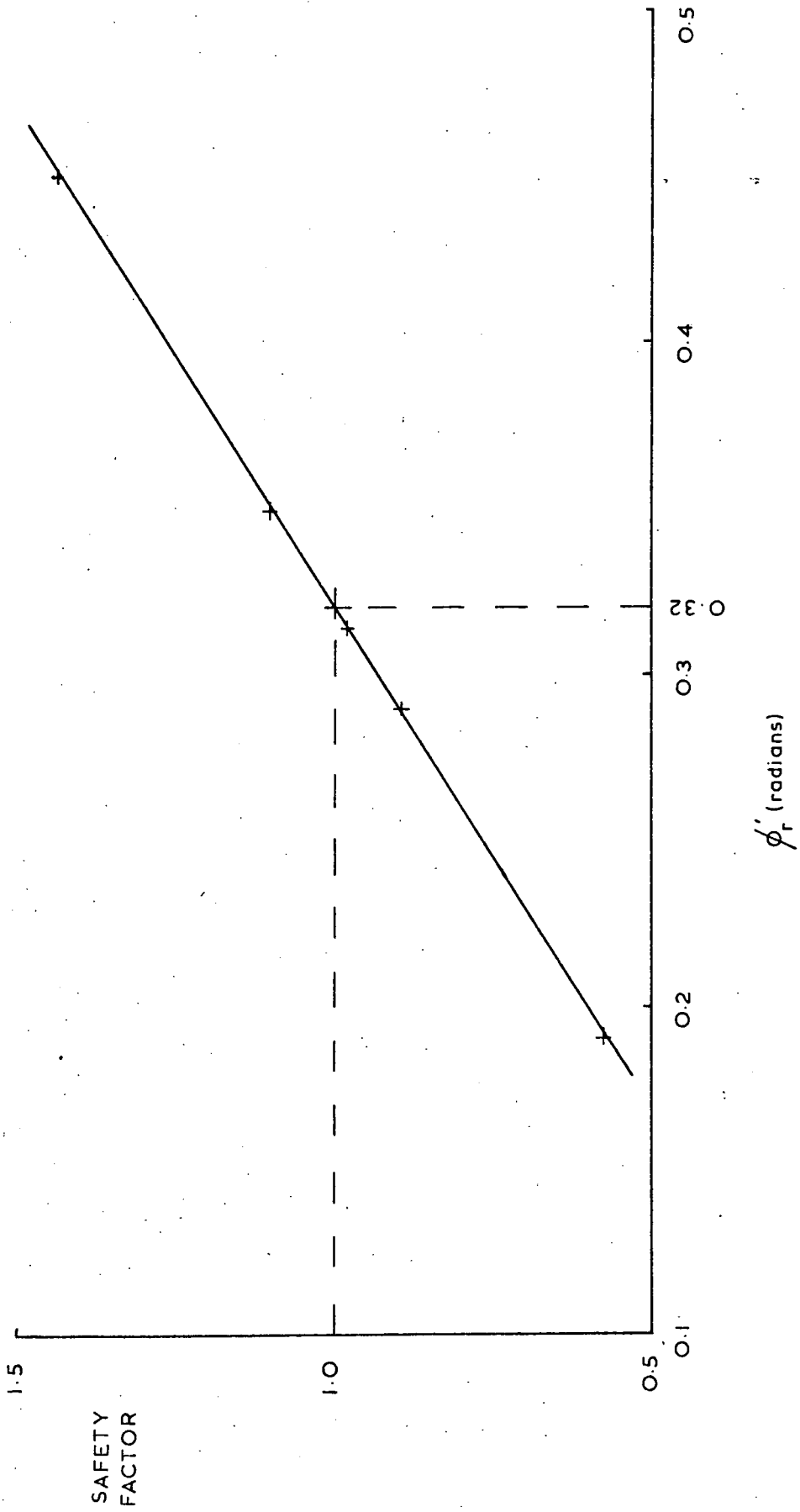


Fig. V.5. Safety factor v  $\phi_r$  graph for the back-analysis of safety factor = unity using the slip circle shown in Fig. V.1.

Taking the slip circle shown in Fig. V. 1 as the most logical possibility of failure, the value of  $\phi'_{cr}$  required to produce a safety factor of unity was investigated. Taking  $c'_{cr}$  as  $0.0 \text{ kN/m}^2$  ( $0.0 \text{ lbf/ft}^2$ ), and density of the spoil heap material as  $1.602 \text{ Mg/m}^3$  ( $100 \text{ lb/ft}^3$ ) the value of  $\phi'_{cr}$  was varied. Figure V. 5 shows the relationship found between  $\phi'_{cr}$  and safety factor. From the graph, a value of  $0.32$  radians ( $18.3^\circ$ ) for  $\phi'_{cr}$  gives a safety factor of unity. The value of  $\phi'_{cr}$  found by Taylor and Hardy was  $20.5^\circ$  and the values of  $\phi'_{er}$  found during this project (Appendix B) were  $20.0^\circ$  and  $17.5^\circ$  for the bulk samples of tip material.

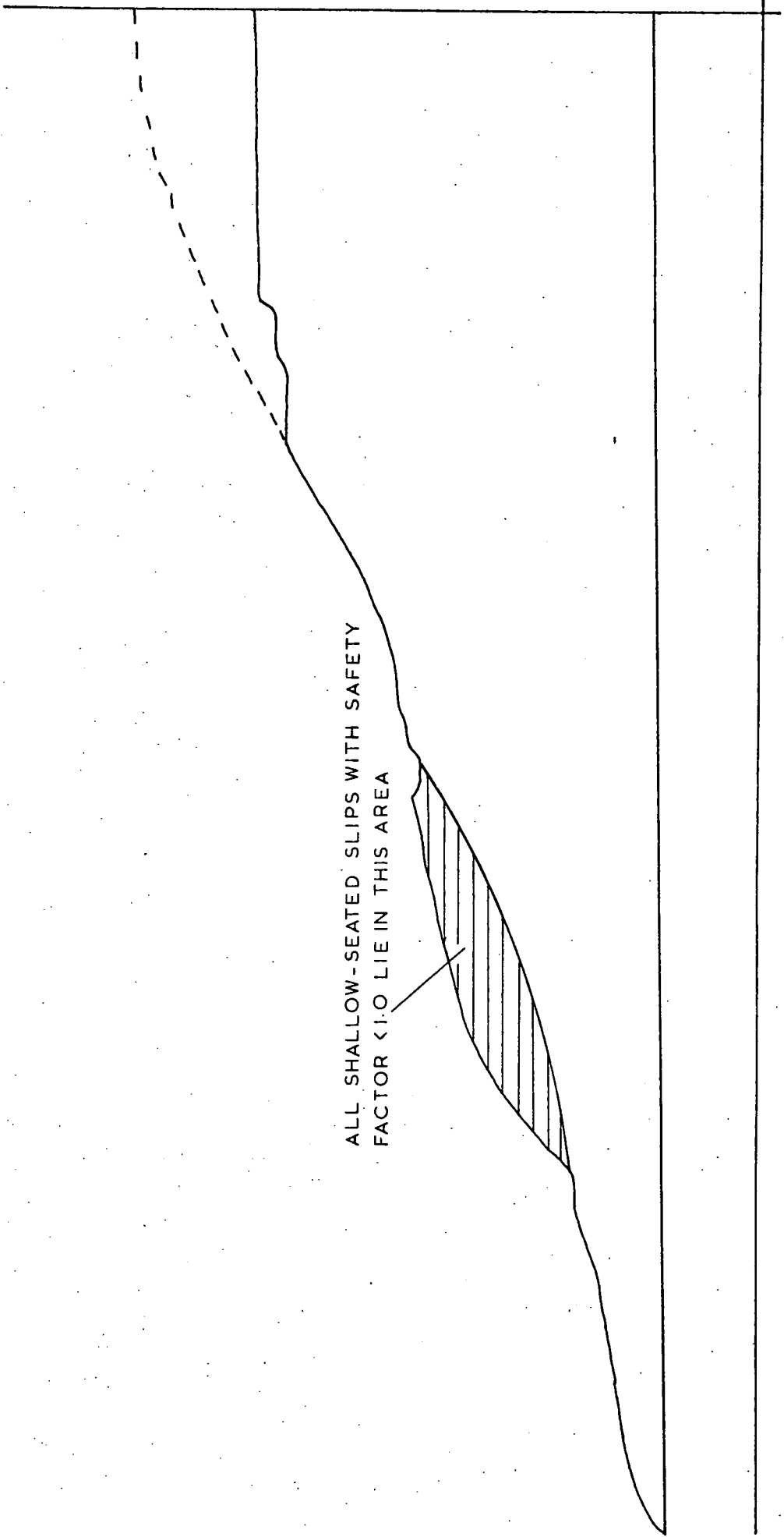
(V. 5)

### SHALLOW SLIP ANALYSIS

In view of the evidence outlined in Chapter V. 3, which pointed to a shallow-seated slip, it was decided to determine safety factors for slips of this type. In analysing the deep-seated slips, Taylor and Hardy (1971) obtained safety factors down to 1.183, using the data listed in Chapter V. 1. However, this result was derived from a circle of failure which did not pass through the most logical upper "slip-scarp" of the 1970 failure. Using a circle passing through this feature, they obtained a relatively high safety factor of 1.356, implying that the tip should be stable. In order to produce instability in their model, a water-table was invoked (i. e. a water-table was necessary to reduce the factor of safety to unity) (Chap. V. 4).

When shallow-seated slips were investigated, it was found that a factor of safety of unity or below could be generated. However, these circles have their toes in the roadway running along the side of the tip (Fig. V. 6) and any movement would have been noted by Board officials; but this was not the case. In fact, the best "fix" for a critical circle is the back-scarp observed by the Area Civil Engineer (Fig. V. 1), which was used in deep-seated circle analyses.

The next approach was to radically increase the radius of the circle of failure to approximate to a planar slide. However, all the solutions which gave a factor of safety of unity and less were again found to be inconsistent with the area of failure designated by the Area Civil Engineer. Once again, the toes of possible slips were grouped around



ALL SHALLOW-SEATED SLIPS WITH SAFETY  
FACTOR < 1.0 LIE IN THIS AREA

Fig. V. 6. Shallow-seated slip circles analysed.

the roadway into the tip, and no such failures were observed.

A deep-seated slip could well produce a boot at the toe. This was not apparent during site investigation at Littleton, but regrading had taken place by then. Before the regrading, local N.C.B. officials had not noticed undue ground heave. However, deep-seated slips are possible at Littleton and have been recorded. On the side of the spoil heap facing Cocksparrow Lane (Fig. I. 1), there is a well-defined incipient deep-seated failure which has not, as yet, failed catastrophically. It exhibits a boot which has displaced the kerb of the road quite noticeably and it is of very large extent, at least 100m across at the toe. The 1970 slip could be of the same type, if a water-table exists in the tip.

During regrading, in 1971, the height of the tip was lowered, but no water-table was exposed. However, the tip itself has well-defined weeping points from which appreciable volumes of water issue. These are most likely to be perched water-tables, formed by discontinuities in the spoil heap. No doubt these contribute to the instability of Littleton tip (Chap. V. 2).

Therefore, deep-seated slips are possible at Littleton, but the evidence of recent rootlets in the shear plane and vertical cracks in the slipped mass would tend to suggest the equally possible explanation of a shallow, planar slip. In an attempt to resolve this problem, a true planar analysis was applied to Littleton.

(V. 6)

#### JANBU METHOD

The Janbu Method allows safety factors to be calculated for any shape of failure surface. In this case, a simple planar slide was analysed at the inclination of  $20^{\circ}$  to the horizontal, and without a water-table (Fig. V. 7). This analysis gave a value of 1.293 for the safety factor - a little lower than the Bishop Simplified Method values for circles in the same area. In assuming no water-table, the best performance of the material is again assumed. As mentioned above, water-tables may be present and can easily lower the factor of safety, as demonstrated in Chapter V.2.

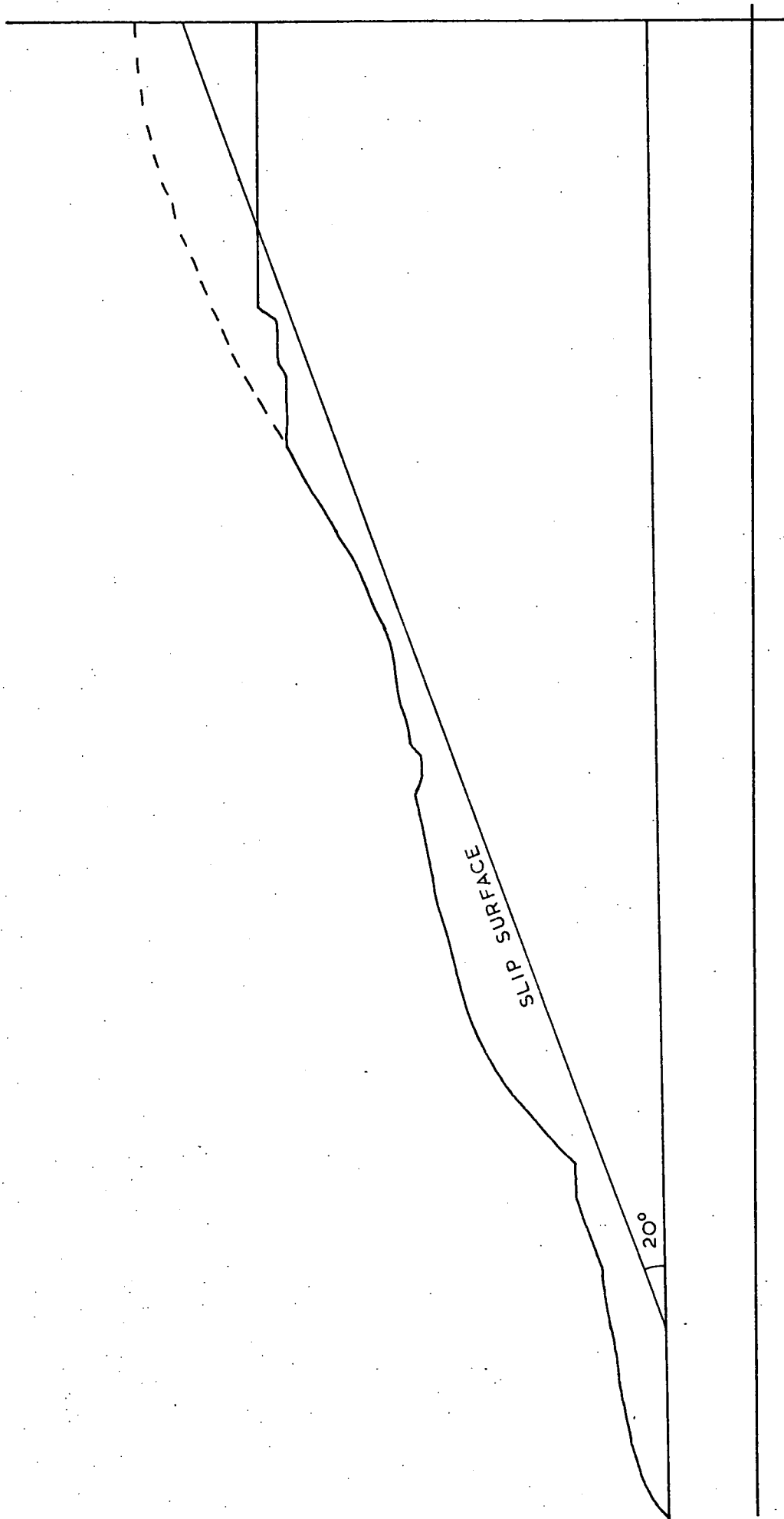


Fig. V.7. Planar slip analysed by the Janbu Method.

The analyses of Littleton Spoil Heap No. 1 show the relationships between  $c'_r$ ,  $\phi'_r$  and safety factor. Values of  $\phi'_r$  have been shown to have a linear relationship with safety factor, as has  $c'_r$ , although  $c'_r$  has a smaller effect on values of safety factor. The relationship between safety factor and water-table has shown that an increase in water-table elevation leads to a decrease in stability. Furthermore, the presence of a water-table masks the effects of changes in  $\phi'_r$  and  $c'_r$ .

Field evidence indicates that the 1970 failure is most likely to be shall<sup>ow</sup>-seated, but the rootlets observed cannot be taken as conclusive of a low depth of burial in view of the method of construction of the tip. More impressive are the conclusions drawn from the deep-seated slip analyses. These show that a slip would be possible in this material if  $\phi'_r$  was  $18.3^\circ$ . The experimental values of  $\phi'_e$  peak lie between  $27.5^\circ$  and  $27.2^\circ$ , indicating that previously undisturbed material is unlikely to be unstable; however, the  $\phi'_{er}$  values of  $20.0^\circ$  and  $17.5^\circ$  show that re-activation of a pre-existing slip is quite possible. Ancient slips are quite possibly present in view of the placement of the tip by Maclane Tippler, and re-activation of one of these may have led to the 1970 failure. These values of  $\phi'_{er}$  indicate that Taylor and Hardy's value of  $20.9^\circ$  for  $\phi'_{er}$  may be marginally high (Appendix B).

The presence of a perched water-table was invoked by Taylor and Hardy (1971) to decrease the calculated factor of safety, and evidence for a perched water-table was observed during site investigation at Littleton. Consequently, the value of  $20.9^\circ$  for  $\phi'_{er}$  may be an average  $\phi'$  value with a perched water-table accounting for  $2.6^\circ$  of  $\phi'$ .

Therefore, the instability of Littleton Spoil Heap No. 1 may be ascribed to the presence of ancient slip planes and a perched water-table which have resulted in a deep-seated circular failure.



## CHAPTER VI

### CONCLUSIONS

The main aim of this research project was to elucidate the compositional and shear strength characteristics of Spoil Heap No. 1 at Littleton Colliery, Staffordshire. This chapter summarizes the main conclusions detailed in previous chapters, and places them in a regional context.

(VI. 1)

#### THE SPOIL HEAP AS A MIXTURE OF THE UNDERGROUND MATERIALS

The mineralogical and chemical analyses confirm that Spoil Heap No. 1 is composed of the underground materials listed by Phillips. The original estimate listed by Bygott from the limited evidence available has been shown to be inadequate in that it did not indicate the high percentages of the Deep Floor and Eight Feet Roof which have been found to be present in the spoil heap. The anomaly due to the presence of the Eight Feet Roof was first noticed during the investigation of illite shape factors of the samples collected (Chap. II. 3. b), and was later confirmed by the  $P_2O_5$  chemical determinations (Table IV. 8) which showed mean values of 0.11% in the tip and 0.06% in the underground materials; the higher  $P_2O_5$  percentage in the tip being attributed to fossil debris in the canneloid shale of the Eight Feet Roof. The detection of the presence of the Eight Feet Roof is a good example of the use of mineralogical and chemical data in the elucidation of the history of ancient tips.

The parentage of the spoil heap is best illustrated by the "Student's-t" test carried out on the spoil heap and underground chemical analyses (Table IV. 8). The high precision of such analyses coupled with good correlation, shown statistically, is strong evidence that the spoil heap is derived from the underground materials listed by Phillips.

The strongest mineralogical evidence is given in Fig. II. 2 which shows the (quartz/total clay) v (10-Å/7-Å clay) graph for the Littleton samples. This graph shows the compositions of the tip samples to lie in

an "average" region of the compositional range shown by the underground samples. The tip samples show some constancy of composition, indicating a good mixing of the materials contributing to the tip.

The high mean percentage of quartz in the tip (29.63%) as against the mean in the underground materials (25.80%) tends to confirm the high proportion of quartz-rich Deep Floor in the tip, as postulated by Phillips. The high kaolinite and chlorite percentages in the tip as compared with the underground materials analysed show the absence of the Eight Feet Roof, which is rich in these minerals. The higher carbon content of the tip is due to contamination of the spoil by coal during the extraction processes; yet the "picking" of coal must have been good since the absence of pyrite in the samples indicates a low coal content. In his survey of spoil heaps in England and Wales, Taylor (1975) gives a mean organic carbon (coal) content of 13.3%, well above the mean Littleton figure of 3.87%.

Broadly, the chemical analyses correlate well with the mineralogical analyses.

(VI.2)

#### SHEAR STRENGTH RELATIONSHIPS

The shear strengths of the tip samples lie within the range of values shown by the underground materials. This tends to reconfirm that the tip is a mixture of the underground materials tested, though this evidence is not as conclusive as the results of the chemical and mineralogical analyses.

The extremes shown by the underground materials are reflected by their mineralogical and chemical analyses. The high  $\phi'_e$  of the Deep Floor (31.7°) and the low  $\phi'_{er}$  of the Park Floor (13.0°) are reflected by their respectively high (51.4%) and low (3.0%) quartz contents. In materials of this type, the quartz concentration varies inversely with clay mineral concentration (Taylor, 1975), and the shear strengths also reflect the high (PF 92.0%) and low (DF 38.2%) clay mineral contents of these extreme samples. The  $\phi'_e$  values of the Eight Feet Floor (23.3°) and Park

Floor (23.8°) are very similar, but their  $\phi'_{er}$  values reflect the higher quartz and lower clay mineral composition of the Eight Feet Floor (8FF, quartz 18.5%,  $\phi'_{er}$  18.7°; PF, 3.0%, 13.0°).

The constancy of composition shown by the spoil heap samples is reflected by their similarity in shear strength (Appendix B).

Taylor (1975) has presented a statistical analysis of shear strength and compositional data for 68 specimens from English and Welsh spoil heaps. Dealing only with peak shear strengths, he found a mean  $\phi'$  of 35° and a lowest value of 26°. On this evidence Littleton must be considered as having a low shear strength in a regional context. Taylor found a significant negative correlation between  $\phi'$  and element oxides of the "clay minerals group" - SiO<sub>2</sub>, Al<sub>2</sub>O<sub>3</sub>, MgO, K<sub>2</sub>O and Na<sub>2</sub>O, and it seems that the low shear strengths of Littleton samples are a reflection of this relationship (Table VI.1).

Element Oxide	Littleton Tip (Table IV.8)	English and Welsh Tips (Taylor, 1975)
SiO <sub>2</sub> (total)	57.90	46.23
Al <sub>2</sub> O <sub>3</sub>	22.95	19.74
MgO	1.41	1.01
K <sub>2</sub> O	3.68	3.40
Na <sub>2</sub> O	0.71	0.41

TABLE VI.1. TABLE OF "CLAY MINERAL GROUP" ELEMENT OXIDE MEAN PERCENTAGES

It should be noted that attempts to follow this argument into mineralogical compositions are rendered ineffective by the relative inaccuracy of the quantitative mineralogical techniques.

Taylor also found a strong positive correlation between organic carbon (coal) content and  $\phi'$ . The mean value determined for Littleton spoil heap materials was 3.87%, while that for the 74 English and Welsh specimens was 13.3%; this agrees with the low  $\phi'_e$  determined for the Littleton spoil heap samples.

(VI.3)

### WEATHERING AND LEACHING

Bishop et al. (1969) suggested that chemical weathering may have played a part in the attainment of residual shear strength and consequent failure at Aberfan. In view of this, the identification of any weathering and associated leaching was considered of prime importance at Littleton, where a back-calculation of  $\phi^i$  for the 1970 failure had shown the required value ( $18.3^\circ$ ) to be close to that of the residual shear strength ( $20.5^\circ$ ) (Taylor and Hardy, 1971). The  $K_2O$  and  $CO_2$  determinations have shown that leaching has not taken place in the spoil heap. Previous research (Spears, Taylor and Till, 1970; Taylor and Spears, 1972) has also concluded that there is little evidence of chemical degradation or weathering once unburnt spoil is buried in a spoil heap. In fact, even the surface skin of the Littleton spoil heap (TSL) showed neither chemical (Chap. IV.2. d) nor physical (Chap. III.7. d) leaching or weathering effects.

(VI.4)

### SLOPE STABILITY

The stability analyses carried out on the 1970 slip indicated that the value of  $\phi^i$  necessary to give a factor of safety of unity was  $18.3^\circ$ . On testing a sample cut from the shear plane of that slip, the value of  $\phi^i_r$  was found to be  $20.5^\circ$  ( $\phi^i_{er} = 20.9^\circ$ ). Peak shear strength values ( $\phi^i_e$ ) for the tip material were found to be  $27.2^\circ$  (TIP 1) and  $27.5^\circ$  (TTO), with residual ( $\phi^i_{er}$ ) values of  $20.0^\circ$  (TIP 1) and  $17.5^\circ$  (TTO). This indicates that residual values of shear strength are liable to be the best design criteria for conical spoil heaps of the Maclane Tippler type. It is interesting to note that current N.C.B. practice is to place colliery discard in horizontal, compacted layers 0.3 m thick (National Coal Board, 1970). This has the dual effect of improving the mechanical properties of the spoil by compaction and removing the weakening effect of layering parallel to the spoil heap surface.

(VI.5)

### GENESIS OF THE 1970 FAILURE

The 1970 slip failure occurred because the tip material had reached a shear strength which approached residual shear strength; this has been shown by back-calculation of  $\phi^i$  for a factor of safety of unity.

The chemical and particle size results have shown that weathering and leaching have not been responsible for this reduction in shear strength. The most likely cause of the reduction is the method of emplacement of the spoil heap. The Maclane Tippler forms a conical heap in which layers of material slide down from the peak of the tip. It is felt that this movement - which takes place over very considerable distances - has produced layers of spoil in which the shear strength has been reduced to, or close to, the residual shear strength. Consequently,  $\phi'_r$  is the best design criterion for such spoil heaps.

It will be noted that the values of  $\phi'_{er}$  are marginally high when compared with the value of  $\phi'$  required to induce failure. This may be due to experimental errors in determination of the residual shear strength. However, the evidence of the presence of a perched water-table in the spoil heap leads one to suspect that the values determined are correct and that the effect of the water-table - which has been shown to reduce stability - is sufficient to account for the necessary drop in  $\phi'$ , inducing a deep-seated failure.

## BIBLIOGRAPHY

- AGARWAL, K.B. 1967. The influence of size and orientation of sample on the undrained strength of London Clay. Ph.D. Thesis: London.
- AKROYD, T.N.W. 1964. Laboratory testing in soils engineering. Geotechnical Monograph 1. London: Soil Mechanics Ltd.
- BISHOP, A.W. 1955. The use of the slip circle in the stability analysis of slopes. *Geotechnique* 5, 7-17.
- BISHOP, A.W., HUTCHINSON, J.N., PENMAN, A.D.M & EVANS, H.E. 1969. Geotechnical investigations into the causes and circumstances of the disaster of 21st October 1966. A selection of technical reports submitted to the Aberfan Tribunal, Welsh Office. London: H.M.S.O.
- BISHOP, A.W., GREEN, G.E., GANGA, V.K., ANDRESEN, A. & BROWN, J.D. 1971. A new ring shear apparatus and its application to the measurement of residual shear strength. *Geotechnique* 21, 273-328.
- BISHOP, A.W. & HENKEL, D.J. 1972 ed. The measurement of soil properties in the triaxial test. London: Edward Arnold.
- BRITISH STANDARDS INSTITUTION. 1967. Methods of testing soils for civil engineering purposes. BS 1377.
- CHANDLER, R.J. 1969. The effect of weathering on the shear strength properties of Keuper Marl. *Geotechnique* 19, 321-334.
- COURCHEE, J. 1970. Properties of boulder-clay slopes and their influence on coastal erosion at Robin Hood's Bay, Yorkshire. M.Sc. dissertation: Durham.
- CRAIG, R.F. 1974. Soil Mechanics. London: Van Nostrand Reinhold Ltd.
- GIBBS, R.J. 1967. Quantitative X-ray diffraction analysis using clay mineral standards extracted from the samples to be analysed. *Clay Minerals* 7, 79-90.
- GILLOTT, J.E. 1968. Clay in Engineering Geology. Amsterdam: Elsevier.
- GRIFFIN, O.G. 1954. A new internal standard for the quantitative X-ray analysis of shales and mine dusts. Safety in Mines Research Establishment. Ministry of Fuel and Power.
- GRIM, R.E. 1968 ed. Clay Mineralogy. New York: McGraw-Hill.
- GRIM R.E., JOHNS, W.D. & BRADLEY, W.F. 1954. Quantitative estimations of clay minerals by diffraction methods. *Journ. Sed. Pet.* 24, 242-251.
- GROVES, A.W. 1951. Silicate Analysis. London: Allen and Unwin.
- HOLLAND, J.G. & BRINDLE, D.W. 1966. A self-consistent mass absorption correction for silicate analysis by X-ray fluorescence. *Spectrochim. Acta* 22, 2083-2093.
- JANBU, N., BJERRUM, L. & KJAERNSLI, B. 1956. Soil mechanics applied to some engineering problems. Norwegian Geotechnical Inst., Publ. No. 16.

- KENNEY, T.C. 1967. The influence of mineralogical compositions on the residual strength of natural soils. Proc. Geotech. Conf., Oslo 1, 123.
- KLUG, H.P. & ALEXANDER, L.E. 1954. X-ray diffraction procedure for polycrystalline and amorphous materials. New York: Wiley.
- McKECHNIE THOMPSON, G. & RODIN, S. 1972. Colliery spoil tips - after Aberfan. Institution of Civil Engineers, London, Paper 7522.
- McKECHNIE THOMPSON, G. & RODIN, S. 1973. Colliery spoil tips - after Aberfan. Proc. Inst. Civ. Eng. 55, 677-712.
- MORONEY, M.J. 1970. Facts from Figures. Harmondsworth, Middlesex: Penguin Books.
- NATIONAL COAL BOARD. 1970. Spoil Heaps and Lagoons. National Coal Board; London, 2nd draft (Technical Handbook).
- NATIONAL COAL BOARD. 1971. Technical memorandum relating to BS 1377: 1967. National Coal Board; London.
- NATIONAL COAL BOARD. 1972. Review on Research on Properties of Spoil Tip Materials. National Coal Board; London.
- PERRIN, R.M.S. 1971. The clay mineralogy of British Sediments. Mineralogical Soc. (Clay Minerals Group): London.
- REEVES, M.J. 1971. Geochemistry - mineralogy of British Carboniferous seatearths from northern coalfields. Ph.D. Thesis: Durham.
- ROBERTS, R.G. 1969. Stability analysis of colliery spoil heaps. B.Sc. Project: Durham.
- SKEMPTON, A.W. 1964. Long-term stability of clay slopes. 4th Rankine Lecture. Geotechnique 14, 77-102.
- SKEMPTON, A.W. & HUTCHINSON, J.N. 1969. Stability of natural slopes and embankment foundations. Proc. 7th Int. Conf. Soil Mech., (Mexico), State-of-the-Art, 291-340.
- SPEARS, D.A. 1964. The major element geochemistry of the Mansfield Marine Band in the Westphalian of Yorkshire. Geochim. Cosmochim. Acta 28, 1679-1696.
- SPEARS, D.A., TAYLOR, R.K. & TILL, R. 1971. A mineralogical investigation of a spoil heap at Yorkshire Main Colliery. Q. Jl. Engng Geol. 3, 239-252.
- TAYLOR, R.K. 1971a. The petrography of the Mansfield Marine Band cyclothem at Tinsley Park, Sheffield. Proc. Yorks. Geol. Soc. 38, 299-328.
- TAYLOR, R.K. 1971b. Deformational and physico-chemical properties of certain sediments, with particular reference to colliery spoil. Ph.D. Thesis: Durham.
- TAYLOR, R.K. 1973. Composition and geotechnical characteristics of a 100-year-old colliery spoil heap. Trans. Inst. Min. Metall., Sect. A (Mining Industry), 82 (A1-14); (A145-147).

- TAYLOR, R.K. 1975. English and Welsh colliery spoil heaps - mineralogical and mechanical interrelationships. *Engng. Geol.* 9, 39-52.
- TAYLOR, R.K. & HARDY, R.G. 1971. A preliminary report on the 1970 failure at Littleton Colliery, Staffs. National Coal Board report.
- TAYLOR, R.K. & SPEARS, D.A. 1970. The breakdown of British Coal Measure rocks. *Int. J. Rock Mech. Min. Sci.* 7, 481-501.
- TAYLOR, R.K. & SPEARS, D.A. 1972. The geotechnical characteristics of a spoil heap at Yorkshire Main Colliery. *Q. Jl Engng Geol.* 5, 243-263.



## APPENDIX A

### COMPUTER PRINT-OUT OF SHEAR-BOX RESULTS

This Appendix contains the computer program developed to process the direct shear-box results produced during the shear strength investigation. Examples of the graphs produced are also presented. The x-axis shows total shear displacement in metres, and the y-axis shows  $D/E$ , i. e. shear stress/vertical stress.

```

PAGE 1 DES97                                DES97
// JOB
LOG DRIVE CART SPEC CART AVAIL PHY DRIVE
0000 000A 000A 0000
VZ M09 ACTUAL 8K CONFIG 32K
// FOR
*IOCS11403PRINTER,2501READER,PLNTEP)
*LIST ALL
C
C PROGRAM TO PLOT RESULTS FROM SHEAR BOX TESTS
C
C SET UP THE SCALE AND GRID LINES
CALL SCALE(39.4,10,0,0,0,0)
CALL FGRID(0,0,0,0,0,0,12)
CALL FGRID(1,0,0,0,0,1,10)
CALL FCHAR(0,50,-0.05,0.1,0,1,0,0)
WRITE(7,2)
2 FORMAT('DISPLACEMENT IN M(CPES)')
CALL FCHAR(-0.02,0.8,0.1,0.1,1,571)
WRITE(7,11)
11 FORMAT('D/A/E')
DO 9 I=5,60,5
AA=I*0.01
CALL FCHAR(AA,-6.02,0.1,0.1,0,0)
9 WRITE(7,3) AA
3 FORMAT('P=2')
DO 10 J=1,10
AA=0.1*I
CALL FCHAR(-0.01,AA,0.1,0.1,0,0)
10 WRITE(7,4) AA
4 FORMAT('F3.1')
CALL FCHAR(0.20,0.9,0.2,0.2,0,0)
WRITE(7,12)
12 FORMAT('SAMPLE PFI, 12 IN. SHEAR BOX.')
```

READ IN THE NO. OF SETS TO BE DRAWN THIS RUN

```

PEARL,5) N
5 FORMAT(I3)
DO 50 I=1,N
```

READ IN THE DATA WHICH IS CONSTANT FOR ONE SET

```

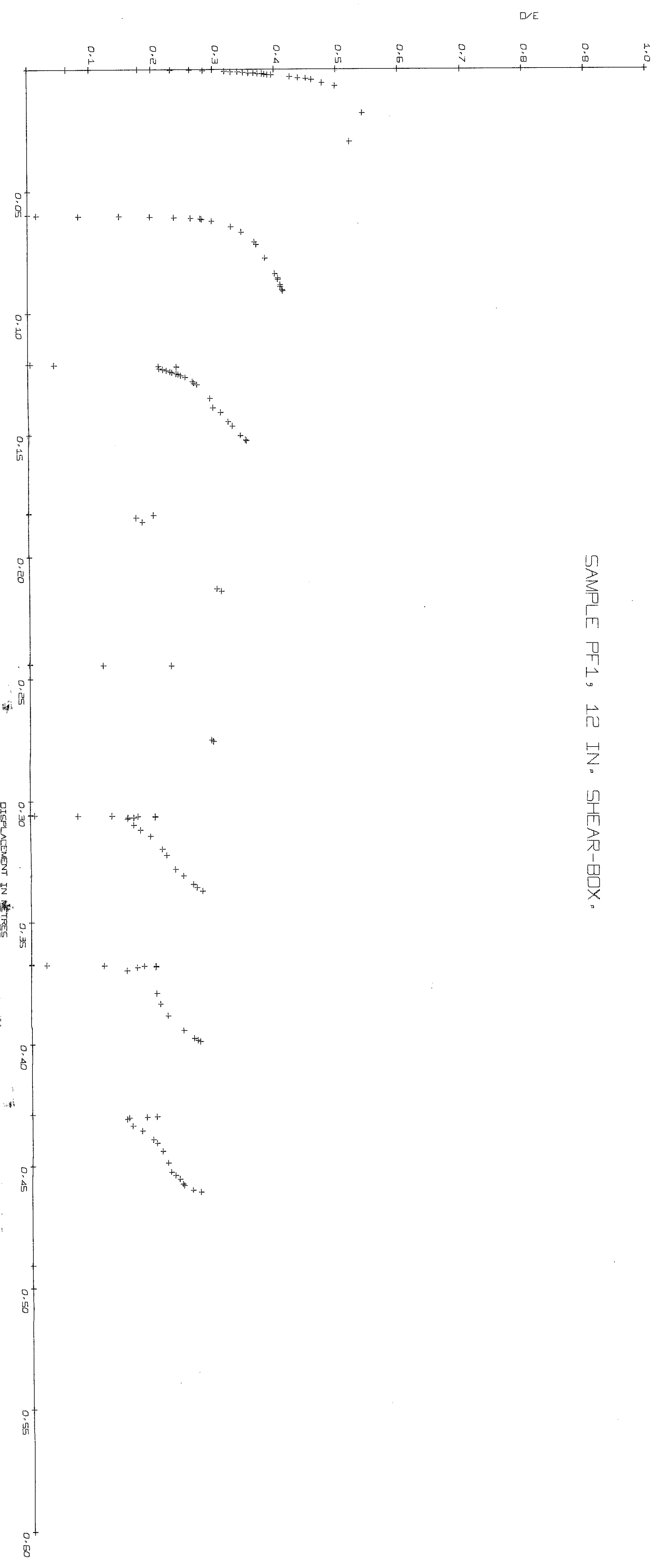
READR,5) DSMP,DSSE,DWR,M
N IS THE NO. OF POINTS IN THIS PARTICULAR SET
6 FORMAT(3F5.1,13)
-----HAVING GOT THE INITIAL DATA, PROCEED WITH THE
POINT CALCULATIONS AND PLOTTING
DO 51 J=1,M
READR,7) SSP,SSP
7 FORMAT(F8.1,F7.1)
SNR=STRATY, SSP*STRESS -----DIAL READINGS
A=(SNR-DSNF)*I, E=05
R=(0.3049-A)*0.3740
C=(SSR-DSSE)*11.77
D=C*0.00447/B
E=0V5*(0.3049*A*2)/A
X=A
Y=0/E
```



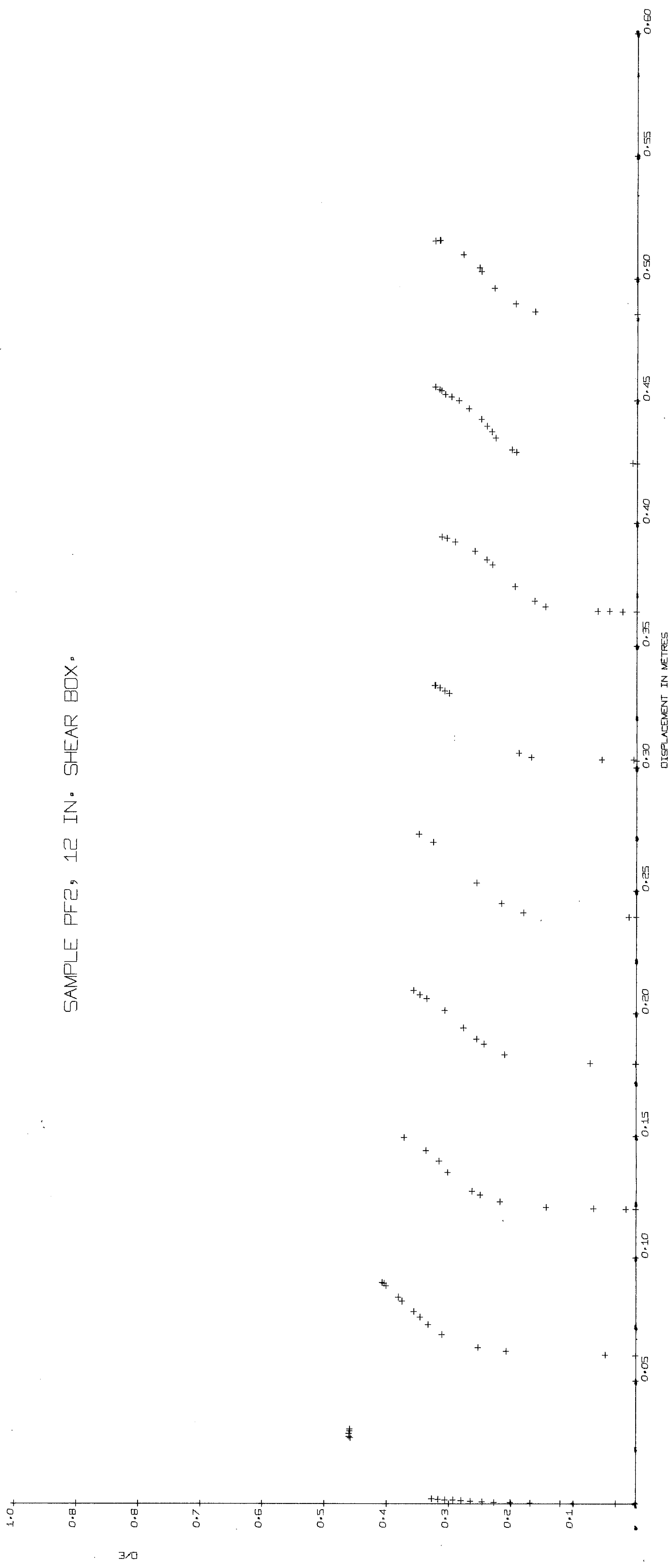
A/E 0.295F-01 D/E 0.327F-01  
A/E 0.30E-00 D/E 0.31E-00  
A/E 0.190F-03 D/E 0.145E-00  
A/E 0.450F-03 D/E 0.322E-01  
A/E 0.561E-03 D/E 0.167E-00  
A/E 0.775E-03 D/E 0.199E-00  
A/E 0.100E-02 D/E 0.237E-00  
A/E 0.123E-02 D/E 0.244E-00  
A/E 0.147E-02 D/E 0.279E-00  
A/E 0.170E-02 D/E 0.292E-00  
A/E 0.245E-02 D/E 0.297E-00  
A/E 0.470E-02 D/E 0.325E-00  
A/E 0.697E-02 D/E 0.365E-00  
A/E 0.110F-01 D/E 0.349E-00  
A/E 0.120E-01 D/E 0.370E-00  
A/E 0.176E-01 D/E 0.394E-00  
A/E 0.241E-01 D/E 0.399E-00  
A/E 0.299F-01 D/E 0.694E-00  
A/E 0.264E-01 D/E 0.455E-00  
A/E 0.236E-01 D/E 0.473E-00  
A/E 0.294E-01 D/E 0.609F-00  
A/E 0.307E-01 D/E 0.412E-00  
A/E 0.310E-01 D/E 0.413E-00  
A/E 0.600F-00 D/E 0.600E-00  
A/E 0.000E-00 D/E 0.391E-02  
A/E 0.162E-03 D/E 0.421E-01  
A/E 0.632E-03 D/E 0.210E-00  
A/E 0.800E-03 D/E 0.240E-00  
A/E 0.104E-02 D/E 0.240E-00  
A/E 0.161E-02 D/E 0.212E-00  
A/E 0.254E-02 D/E 0.217E-00  
A/E 0.251E-02 D/E 0.224E-00  
A/E 0.202E-02 D/E 0.237E-00  
A/E 0.333E-02 D/E 0.233F-00  
A/E 0.373E-02 D/E 0.239F-00  
A/E 0.413E-02 D/E 0.241E-00  
A/E 0.453E-02 D/E 0.244E-00  
A/E 0.533E-02 D/E 0.243E-00  
A/E 0.713E-02 D/E 0.245E-00  
A/E 0.762E-02 D/E 0.248E-00  
A/E 0.900E-02 D/E 0.273F-00  
A/E 0.134E-01 D/E 0.294E-00  
A/E 0.177E-01 D/E 0.299E-00  
A/E 0.195E-01 D/E 0.311E-00  
A/E 0.235E-01 D/E 0.323E-00  
A/E 0.253F-01 D/E 0.329E-00  
A/E 0.293E-01 D/E 0.342E-00  
A/E 0.311E-01 D/E 0.351E-00  
A/E 0.213E-01 D/E 0.352E-00  
A/E 0.500E-00 D/E 0.600E-00  
A/E 0.170E-03 D/E 0.600E-00  
A/E 0.795F-03 D/E 0.211E-00  
A/E 0.172F-02 D/E 0.173E-00  
A/E 0.350E-02 D/E 0.184E-00  
A/E 0.302F-01 D/E 0.202E-00  
A/E 0.319E-01 D/E 0.210E-00  
A/E 0.600F-00 D/E 0.600E-00  
A/E 0.236E-03 D/E 0.300E-00  
A/E 0.450E-03 D/E 0.118E-00  
A/E 0.611E-03 D/E 0.228E-00  
A/E 0.311E-01 D/E 0.207E-00  
A/E 0.315E-01 D/E 0.256E-00  
A/E 0.000E-00 D/E 0.000E-00  
A/E 0.200E-03 D/E 0.000E-00  
A/E 0.250E-03 D/E 0.000E-00  
A/E 0.250E-03 D/E 0.000E-00

A= 0.485E-03 D/E= 0.132E 00  
A= 0.630E-03 D/E= 0.172E 00  
A= 0.790E-03 D/E= 0.211E 00  
A= 0.940E-03 D/E= 0.252E 00  
A= 0.114E-02 D/E= 0.165E 00  
A= 0.131E-02 D/E= 0.158E 00  
A= 0.179E-02 D/E= 0.154E 00  
A= 0.428E-02 D/E= 0.163E 00  
A= 0.631E-02 D/E= 0.174E 00  
A= 0.879E-02 D/E= 0.193E 00  
A= 0.141E-01 D/E= 0.218E 00  
A= 0.166E-01 D/E= 0.219E 00  
A= 0.226E-01 D/E= 0.233E 00  
A= 0.253E-01 D/E= 0.246E 00  
A= 0.288E-01 D/E= 0.262E 00  
A= 0.301E-01 D/E= 0.259E 00  
A= 0.315E-01 D/E= 0.277E 00  
A= 0.500E-00 D/E= 0.000E 00  
A= 0.130E-02 D/E= 0.000E 00  
A= 0.230E-03 D/E= 0.245E-01  
A= 0.410E-03 D/E= 0.118E-00  
A= 0.620E-03 D/E= 0.143E 00  
A= 0.770E-03 D/E= 0.231E 00  
A= 0.850E-02 D/E= 0.202E 00  
A= 0.115E-02 D/E= 0.172E 00  
A= 0.249E-02 D/E= 0.165E 00  
A= 0.118E-01 D/E= 0.203E 00  
A= 0.161E-01 D/E= 0.221E 00  
A= 0.209E-01 D/E= 0.221E 00  
A= 0.270E-01 D/E= 0.245E 00  
A= 0.303E-01 D/E= 0.263E 00  
A= 0.311E-01 D/E= 0.269E 00  
A= 0.316E-01 D/E= 0.272E 00  
A= 0.320E-00 D/E= 0.000E 00  
A= 0.710E-03 D/E= 0.201E 00  
A= 0.950E-03 D/E= 0.185E 00  
A= 0.121E-02 D/E= 0.166E 00  
A= 0.141E-02 D/E= 0.153E 00  
A= 0.450E-02 D/E= 0.177E 00  
A= 0.454E-02 D/E= 0.177E 00  
A= 0.101E-01 D/E= 0.196E 00  
A= 0.115E-01 D/E= 0.201E 00  
A= 0.150E-01 D/E= 0.210E 00  
A= 0.167E-01 D/E= 0.219E 00  
A= 0.235E-01 D/E= 0.274E 00  
A= 0.249E-01 D/E= 0.231E 00  
A= 0.264E-01 D/E= 0.239E 00  
A= 0.242E-01 D/E= 0.243E 00  
A= 0.287E-01 D/E= 0.245E 00  
A= 0.310E-01 D/E= 0.269E 00  
A= 0.315E-01 D/E= 0.272E 00

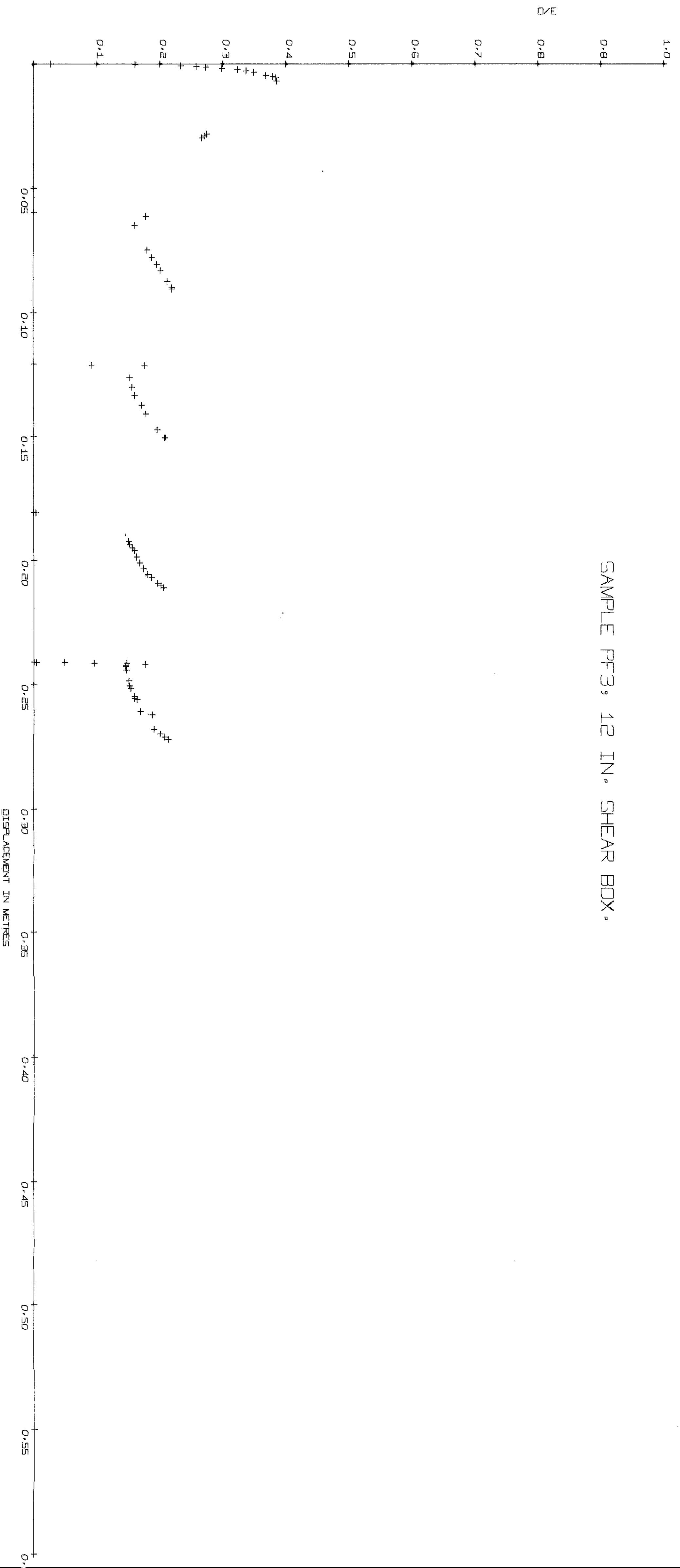
SAMPLE PF1, 12 IN. SHEAR-BOX.



SAMPLE PF2, 12 IN. SHEAR BOX.

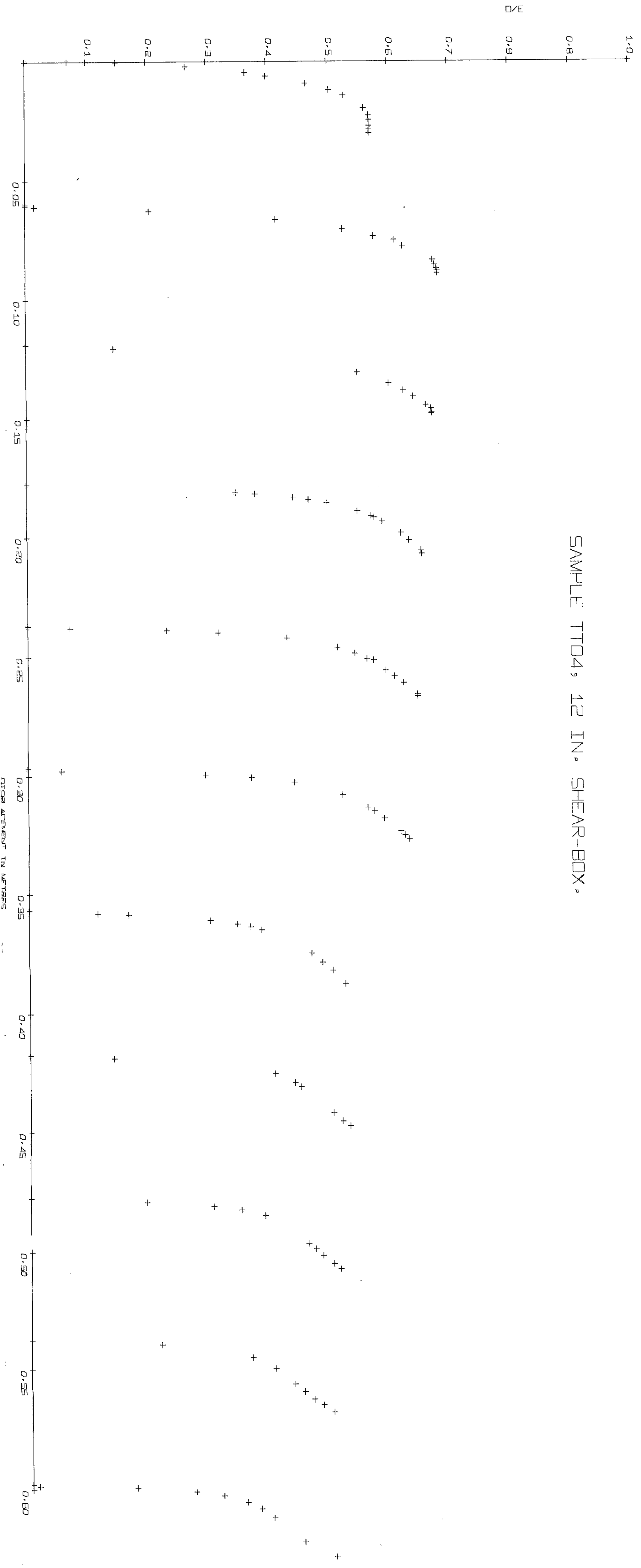


SAMPLE PF3, 12 IN. SHEAR BOX.





SAMPLE T104, 12 IN. SHEAR-BOX



APPENDIX B

SHEAR STRENGTH TEST RESULTS

TIP 1:

Triaxial Tests (Peak):

$\frac{(\sigma'_1 + \sigma'_3)}{2}$ (kN/m <sup>2</sup> )	$\frac{(\sigma'_1 - \sigma'_3)}{2}$ (kN/m <sup>2</sup> )
168.0	88.0
268.5	128.5
408.5	188.5

Shear-Box Tests (Residual):

$\tau$ (kN/m <sup>2</sup> )	$\sigma_h$ (kN/m <sup>2</sup> )
53.9	89.5
72.8	147.0
96.1	236.1

TIP TOP OUTER:

Shear-Box Tests (Peak):

$\tau$ (kN/m <sup>2</sup> )	$\sigma_h$ (kN/m <sup>2</sup> )
128.0	229.9
80.6	147.5
61.0	88.7

Shear-Box Tests (Residual):

$\tau$ (kN/m <sup>2</sup> )	$\sigma_h$ (kN/m <sup>2</sup> )
24.1	89.2
48.7	149.3
73.6	232.8

EIGHT FEET FLOOR:

Triaxial Tests (Peak):

$\frac{(\sigma'_1 + \sigma'_3)}{2} \text{ (kN/m}^2\text{)}$	$\frac{(\sigma'_1 - \sigma'_3)}{2} \text{ (kN/m}^2\text{)}$
352.5	142.5
223.5	83.5
131.5	51.5

Shear-Box Tests (Residual):

$\tau \text{ (kN/m}^2\text{)}$	$\sigma_h \text{ (kN/m}^2\text{)}$
81.2	225.6
66.6	145.3
39.9	86.7

PARK FLOOR:

Shear-Box Tests (Peak):

$\tau \text{ (kN/m}^2\text{)}$	$\sigma_h \text{ (kN/m}^2\text{)}$
108.0	234.8
52.5	136.8
46.3	85.3

Shear-Box Tests (Residual):

$\tau \text{ (kN/m}^2\text{)}$	$\sigma_h \text{ (kN/m}^2\text{)}$
57.7	228.0
24.3	143.1
18.8	85.9

DEEP FLOOR:

Shear-Box Tests (Peak):

$\tau \text{ (kN/m}^2\text{)}$	$\sigma_h \text{ (kN/m}^2\text{)}$
135.5	207.5
100.1	139.0
63.5	81.0

SAMPLE	PEAK		RESIDUAL	
	$\phi^i$	$c^i(\text{kN/m}^2)$	$\phi^i_r$	$c^i_r(\text{kN/m}^2)$
TIP 1	24.7°	18.8	16.0°	29.3
TTO	25.4°	16.3	17.5°	0.0
8FF	23.3°	0.0	16.0°	18.0
PF	23.3°	3.4	13.0°	0.0
DF	29.3°	20.0	-	-
1970 Slip Plane	-	-	20.5°	2.8
				$\phi^i_{er}$
				20.0°
				17.5°
				18.7°
				13.0°
				-
				20.9°

Table B.1. Shear strength parameters of the Littleton samples, calculated from the shear-box and triaxial tests results using the 'least squares' regression method. The presence of cohesion in the residual samples may be a result of failure envelope curvature. Consequently, the McKechnie Thompson and Rodin  $\phi^i_e$  construction (Chap. III.4) has been used on both peak and residual results to represent the shear strength over the normal stress range applicable to high tips (Taylor, 1975).